2013-12-04

Towards On-site Detection of Nucleic Acids for Pathogen Monitoring

Daohong Zhang
University of Miami, daohongzhang@hotmail.com

UNIVERSITY OF MIAMI

TOWARDS ON-SITE DETECTION OF NUCLEIC ACIDS FOR PATHOGEN MONITORING

By

Daohong Zhang

A DISSERTATION

Submitted to the Faculty
of the University of Miami
in partial fulfillment of the requirements for
the degree of Doctor of Philosophy

Coral Gables, Florida

December 2013

UNIVERSITY OF MIAMI

A dissertation submitted in partial fulfillment of
the requirements for the degree of
Doctor of Philosophy

TOWARDS ON-SITE DETECTION OF NUCLEIC ACIDS FOR PATHOGEN MONITORING

Daohong Zhang

Approved:

_____ Sapna Deo, Ph.D. Professor of Biochemistry	_____ Roger LeBlanc, Ph.D. Professor of Chemistry
_____ James Wilson, Ph.D. Professor of Chemistry	_____ M. Brian Blake, Ph.D. Dean of the Graduate School
_____ Yanbin Zhang, Ph.D. Professor of Biochemistry	

ZHANG, DAOHONG (Ph.D., Chemistry)
Towards On-site Detection of Nucleic Acids for Pathogen Monitoring (December 2013)

Abstract of a dissertation at the University of Miami.

Dissertation supervised by Professor Sapna Deo.
No. of pages in text. (124)

As a leading cause of death in developing countries and a persistent problem elsewhere, pathogenic organisms are as ubiquitous as they are dangerous. Significant worldwide resources are directed toward their detection and eradication, leading to a broad coalition of government agencies, healthcare providers, academic researchers, and food manufacturers dedicated to providing the best-available prevention strategies for mitigating exposure risk. At the forefront of this effort is the field of pathogen detection. Our work directly addresses the current lack of simple, rapid, sensitive, and selective pathogen detection methods needed for frontline intervention in the most at-risk populations. To begin, we focused on the common food- and water-borne contaminant, *E. coli*. Using a resonance energy transfer system incorporating a bioluminescent protein and quantum dots, we demonstrated that adjacent hybridization of sequence-specific, labeled probes could detect *E. coli* 16s rRNA at concentrations as low as 2.1 nM in only 5 minutes. Continuing, we developed a paper-based platform for Epstein-Barr virus (EBV) detection using a target-bridged capture scheme in which EBER-1 RNA from EBV linked a tethered probe to a fluorescent reporter probe for a low nanomolar detection limit. Finally, we

developed a novel tuberculosis (TB) biosensor in both microtiter plate and paper-based microfluidic platforms that utilized zinc finger proteins as selective capture reagents for the detection of two different TB DNA biomarkers. The dual-platform design afforded either quantitative (microtiter plate, 1.0-20.0 nM) or qualitative (paper microfluidic) detection. While divergent in design and target, these assays achieve the aims of current pathogen detection research while providing cost-effective options for deployment in resource-poor environments.

ACKNOWLEDGEMENT

I would like to express my sincere appreciation to Dr. Sapna Deo, as she is not only my thesis mentor, but also a friend who has always guided me with tremendous patience. Also, I want to thank Dr. Vineet Gupta for his support and helpful suggestions.

I also want to thank my committee members, Dr. Roger LeBlanc and Dr. James Wilson, for their insightful advice and encouragement. Likewise, I wish to thank Dr. Yanbin Zhang for agreeing to be the external examiner for my defense.

I thank everyone in the Deo lab, the Daunert lab, and the Bachas lab, for their omnipresent support and informative conversation. They are always patient to listen to my complaints, give suggestions, and grow my passion. Especially, I owe a thank you to David Broyles, who helped me as an English teacher during the past five years and arranged all the pieces of my work into one picture. I also need to specifically thank Eric Hunt, my twin brother, who was always willing to listen and guide my curiosity toward productive answers. I wish to thank Dr. Manoj Kumar, who trained me when I was a new graduate student. His challenge and encouragement gave me the confidence to meet my goals.

Finally, I would like to thank my family and all my friends in China. I could not have completed my graduate work without their help.

TABLE OF CONTENTS

LIST OF FIGURES

CHAPTER 1

CHAPTER 2

CHAPTER 3

CHATPER 4

LIST OF TABLES

CHAPTER 1: INTRODUCTION

1.1 Overview of pathogen detection

The detection of pathogens is a major issue in the fields of clinical diagnostics, food preparation and processing, environmental control, and bioterrorism prevention [1-5]. Infectious disease is the leading cause of death in low-income countries, and the major diseases including lower respiratory infections, HIV/AIDS, diarrheal diseases, and malaria are responsible for 45% of these deaths [6]. Meanwhile, infectious disease caused two-thirds of deaths in children younger than five years old [7]. Early diagnosis plays an important role in interrupting transmission of infectious diseases. High quality diagnostic tools are available for some infectious diseases. However, due to the lack of technical infrastructure and highly-skilled personnel, they are usually unaffordable or inaccessible to people in developing countries. Meanwhile, most of the widely-used, inexpensive diagnosis tests cannot provide accurate and adequate results [8]. Therefore, pathogen detection for point-of-care (POC) testing in resource-poor settings is still in high demand [9]. As requested by the World Health Organization (WHO), these detection methods should meet the ASSURED criteria: affordable, sensitive, specific, user-friendly, rapid and robust, equipment-free, and deliverable to end users [9].

1.2 Principles of pathogen detection methods

1.2.1 Culture and colony count

Culture and colony count is the gold standard of bacterial detection and usually provides a conclusive result. Meanwhile, it can provide information such as drug-susceptibility, which is one of the major issues in infectious disease treatment. Low-cost, culture-based tests for drug-susceptibility of *Mycobacterium tuberculosis* are recommended by the WHO [8]. However, culture and colony count is time-consuming (typically weeks), needs highly skilled personnel, and can still be subject to misinterpretation [10, 11].

1.2.2 Enzyme-linked immunosorbent assay (ELISA)

Immunology-based assays utilize antibodies that bind specific antigens and report using a secondary, enzyme-labeled antibody [12-14]. The detection target for ELISA is usually protein, and a test can be performed in as few as several hours. However, the binding affinity and specificity of antibodies varies significantly [15]. Also, antibodies have short shelf life, batch-to-batch variation, and cannot withstand harsh environmental conditions. Furthermore, in some occasions such as infant HIV detection, antibody-based assays are not suitable because maternal anti-HIV antibodies may persist in infant blood up to 18-months [9].

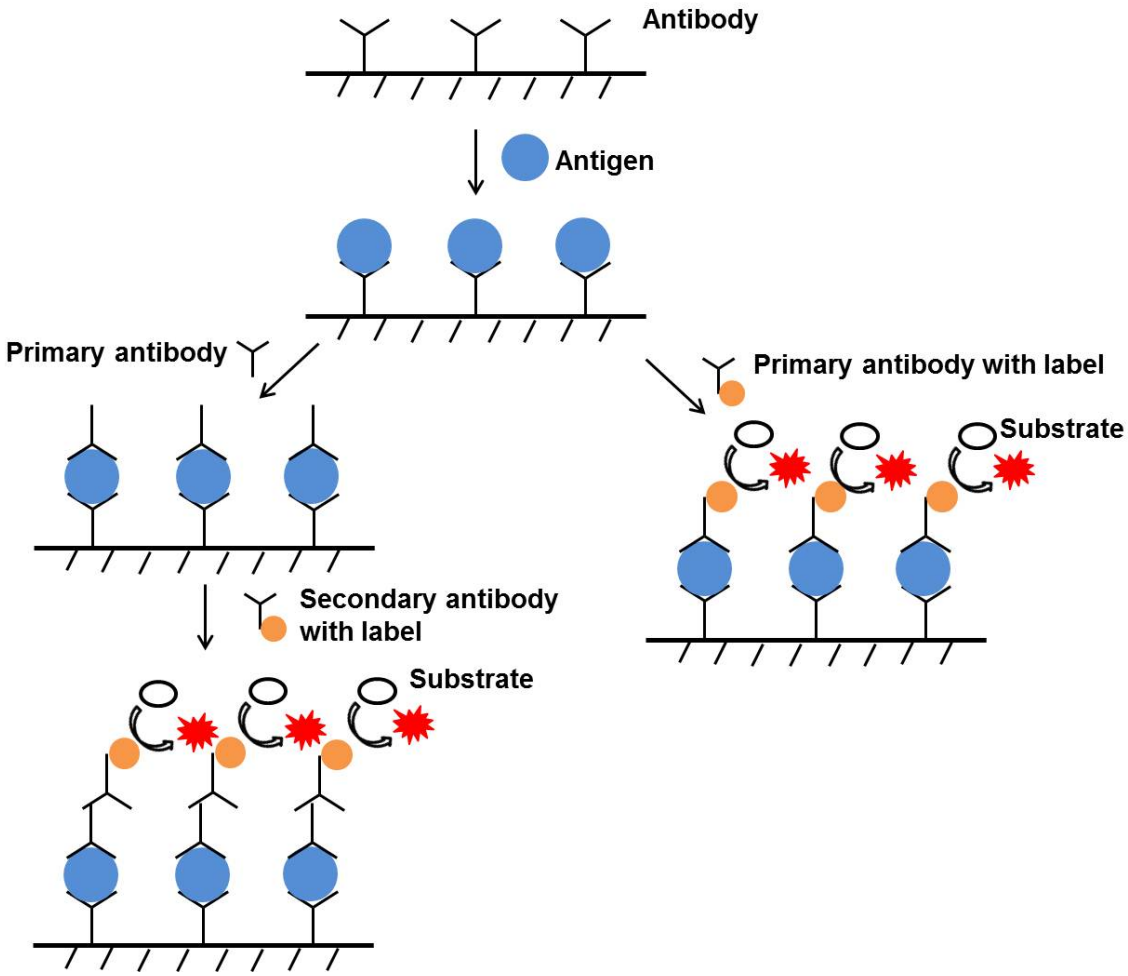

Figure 1.1 Scheme of ELISA detection platform. Antigen is captured by immobilized antibody. The antigen can be detected with either labeled primary antibody, or primary antibody with an enzyme-labeled secondary antibody.

1.2.3 Nucleic acids hybridization

Instead of proteins, nucleic acids can also serve as target for pathogen detection. Each organism has its own specific nucleic acid code, which enables differentiation based solely on sequence. Nucleic acid hybridization employs

oligonucleotides (oligos) with complementary sequence to a target strand for capture or detection due to the highly-specific base pairing of A-T(U) and C-G in a unique sequence. The simplest configuration of a nucleic acid hybridization platform includes three steps: immobilization of target on a surface, hybridization of a labeled probe, and detection after a thorough wash step.

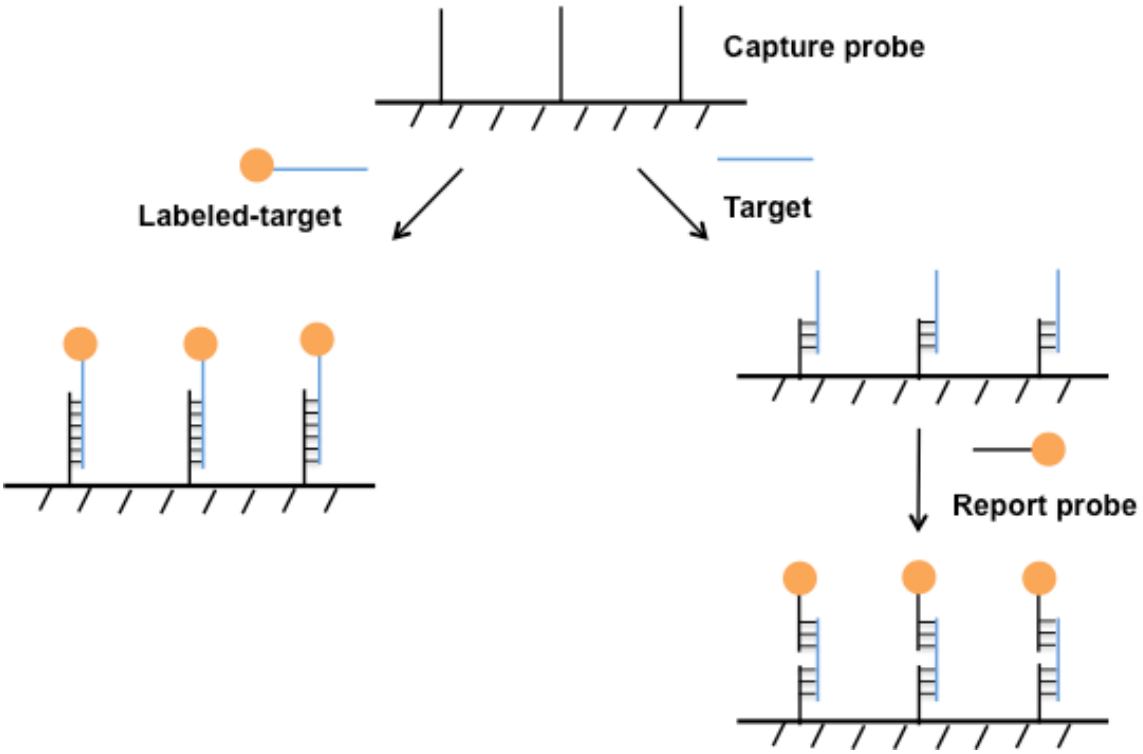

Figure 1.2 Scheme of nucleic acid hybridization. The capture probe is immobilized on surface and hybridizes to a labeled target. A non-labeled target can also be detected through a bridge format in which the target hybridizes to both the capture and reporter probes.

Compared to antibody production, oligonucleotide synthesis is less expensive, and the final product can be stored at 4 °C for up to 6 months in a broad range of concentrations (1 μM-5 mM) [16]. Additionally, nucleic acid

samples are very stable: plasmid storage on a filter paper is a prevalent way for shipping plasmid, and nucleic acids detection in dried blood spots is a well-developed technology [17, 18]. Thus, nucleic acid-based detection methods are suitable for low-cost POC testing.

1.2.4 Polymerase chain reaction (PCR)

Polymerase Chain Reaction (PCR), currently the most prevalent nucleic acids amplification method, was developed in 1987 by Kary Mullis [19] and enabled him to enrich specific nucleic acid sequences by a factor of 10^6 [20]. Nucleic acid sequences are often difficult to detect in clinical samples as a result of matrix effects, limited sample volume, low concentrations, and instability [20]. Before the development of PCR, a cell or tissue culture step was typically performed to increase cell or organism number, thereby enriching target nucleic acids [21]. PCR dramatically reduced the time (2-3 hours) necessary to amplify specific nucleic acid regions with high accuracy.

The inherent value of PCR stems from its simplicity. A PCR mixture is composed of template DNA, two single-stranded oligonucleotide primers, a thermostable DNA polymerase, deoxynucleotide triphosphates (dNTPs, including dATP, dTTP, dCTP, and dGTP), $MgCl_2$, and reaction buffer. To initiate the process, double-stranded DNA (template) is denatured under high temperature (usually 95 °C). Then, two antisense primers are allowed to anneal at opposite ends of the desired amplification region when the reaction temperature is decreased below the melting temperature (T_m) of both primers. The annealed

primers can be extended using the free dNTPs with the aid of *Taq* polymerase, a temperature-stable DNA polymerase isolated from the thermophilic bacterium *Thermus aquaticus*. By repeating these three steps (typically 20-40 cycles), a specific nucleic acid region can be selectively amplified. If the template is RNA, a reverse transcription process (usually with Avian myeloblastosis virus (AMV) or Moloney murine leukemia virus (M-MLV) reverse transcriptases) can generate a single-stranded cDNA (complementary DNA) strand, which is complementary to the RNA sequence and acts as a stable template for amplifying a DNA copy of the RNA sequence.

PCR is advantageous in that it is much faster and less complicated than cell or tissue culture. The two primers confine the amplification region, which guarantees the efficient amplification of a specific region. The amplified product from one cycle serves as a new template in the following cycle so that the amount of product approximately doubles with every cycle. This leads to an exponential increase of the desired DNA fragment and allows high-sensitivity detection. *Taq* polymerase is utilized because it can withstand the high temperature during the denaturation step. However, PCR has some drawbacks. It may give false-positives, and some nucleic acid sequence information is required in order to design primers. Also, *Taq* polymerase lacks a $3' \rightarrow 5'$ proofreading activity, leading to low replication fidelity (1 error per 5×10^5 [22] nucleic acids).

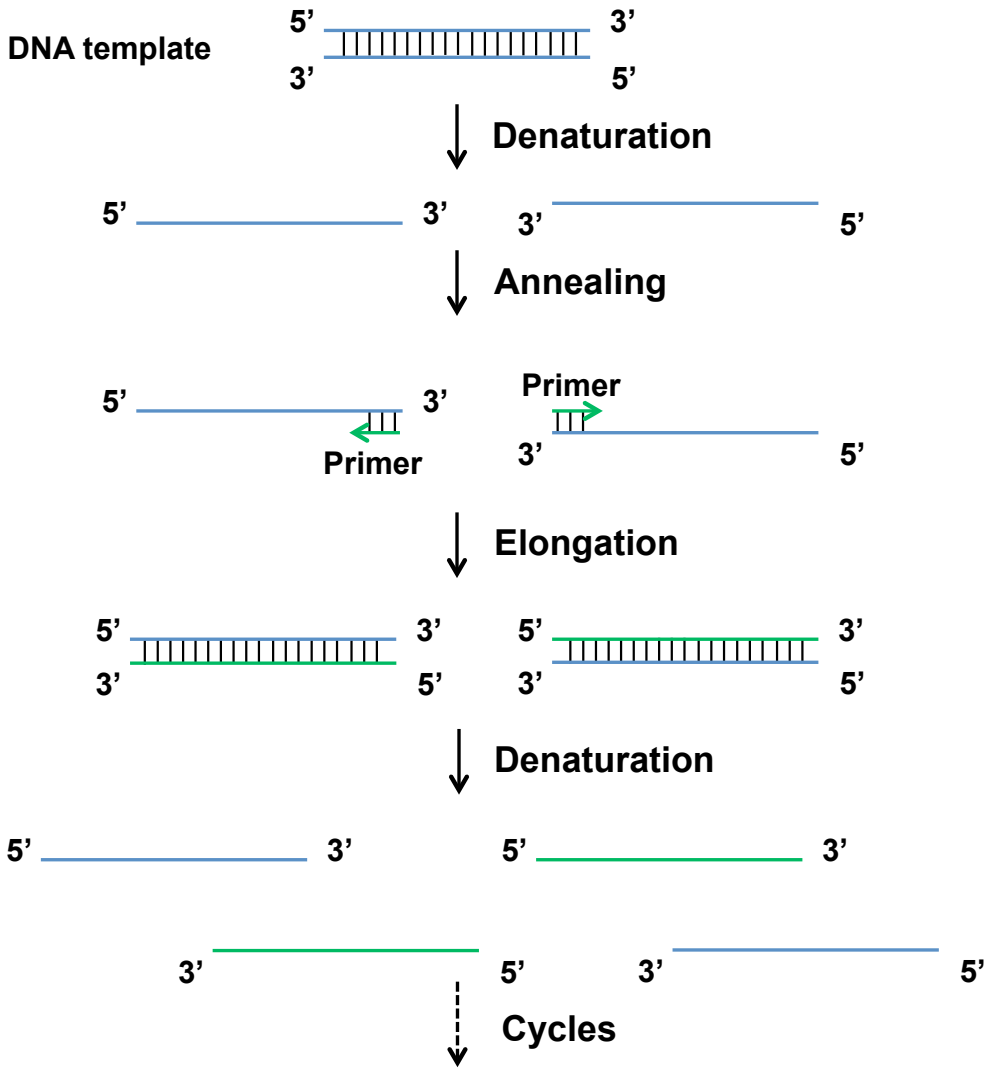

Figure 1.3 Scheme of PCR amplification. The double-stranded template is denatured using high temperature, and then the primers are annealed at a lower temperature. In the presence of DNA polymerase, the primers are extended, resulting in double-stranded DNA. The specific nucleic acid region is amplified by repeating these three steps.

Various techniques are utilized for increasing PCR quality. Higher annealing temperatures and Mg^{2+} concentration will increase PCR stringency [22]. Furthermore, several methods have been developed to limit non-specific

binding, such as nested PCR, hot start PCR, and touchdown PCR. Nested PCR employs an additional primer set which allows amplification of a long region of DNA containing the target DNA sequence that can be used as template for a second PCR to generate the desired DNA product [23-25]. The two-round amplification increases the efficiency of specific amplification because of complete denaturation of the smaller template (1st round PCR product). While nested PCR can amplify long DNA fragments from complex DNA template (such as genomic DNA), it requires more sequence information. Hot start PCR involves heating the mixture without polymerase to denaturation temperature followed by addition of polymerase in order to reduce non-specific amplification during initial setup [26, 27]. In touchdown PCR, the annealing temperature of the initial cycle is 3-5 degrees higher than the T_m of primers and is gradually decreased to 3-5 degrees lower than the T_m in the later cycles [28]. The high annealing temperature increases PCR stringency, while the lower annealing temperature in subsequent cycles ensures efficient amplification. Several other DNA polymerases which do incorporate 3´→ 5´ exonuclease activity have also been employed to eliminate amplification errors common to *Taq* polymerase. These polymerases were either discovered from other organisms or designed through protein engineering. Nowadays, commercially-available, high-fidelity DNA polymerases include *Pyrococcus furiosu*s (*Pfu*) DNA polymerase (1.6 x 10^{-6} errors per nucleotide (nt) [29]), Phusion® High-Fidelity DNA polymerase (4.4 x 10^{-7} errors per nt), and Q5® High-Fidelity DNA polymerase (error rate is 12-fold lower than that of *pfu*).

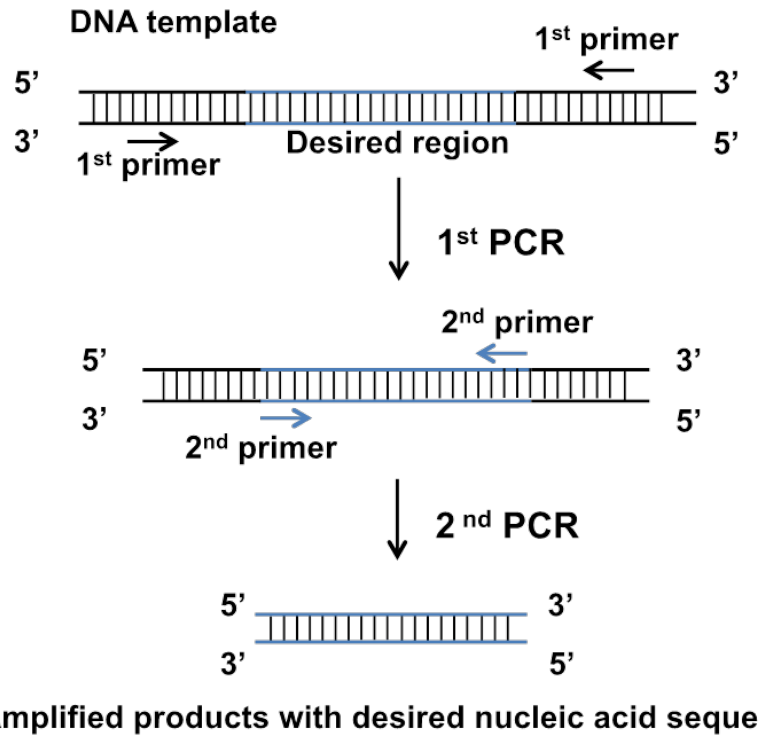

Figure 1.4 Scheme of nested PCR. Two sets of PCR primers are employed in nested PCR (black and blue). First, PCR products amplified with the 1st primer set are generated, which contain the desired nucleic acid region. Those PCR products are employed as template for 2nd PCR amplification. With the 2nd set of primers, the target nucleic acid region is amplified as the final PCR product.

1.3 Signal detection methods

1.3.1 Optical detection methods

Optical detection methods consist of fluorescence, bioluminescence, chemiluminescence, and absorbance. The first three methods utilize specific labels to generate signal, and though most absorbance assays still employ labels, absorbance techniques can be performed in a label-free format. Typically, the detection limits of bioluminescence and chemiluminescence assays

are higher than fluorescence platforms, which are more comparable to absorbance assays. However, because the signal output of certain absorbance methods such as colorimetric assays can be observed visually, absorbance is more useful in point-of-care (POC) detection. Since the major difference between fluorescence, bioluminescence, and chemiluminescence assays is the labeling reagent, fluorescence and absorbance techniques will be discussed in detail, while bioluminescence and chemiluminescence methods will be mentioned briefly.

The simplest detection method for nucleic acids amplification is gel electrophoresis. DNA fragments of different size and/or charge can be separated on a gel (usually made of agarose) in an external electrical field. The result is typically visualized with UV-excited fluorescent intercalating dyes such as ethidium bromide, propidium iodide, and SYBR green. Gel electrophoresis is quite simple and has been reported to detect pathogenic bacteria following PCR amplification [30-32]. However, it is a qualitative method, providing only information about DNA size, and does not have the ability to differentiate specific amplification products from non-specific products.

The need to quantify PCR products during the amplification process led to the development of real-time PCR (qPCR). Two quantitative labels are employed in qPCR: intercalating dyes (usually SYBR green) [33, 34] and fluorophore-labeled, antisense oligos [35-37]. While the same intercalating dye is also used in gel-electrophoresis, its non-specific nature precludes sequence identity, providing information only about the quantity of amplification product. By

combining the ability to determine product quantity with labeled, sequence-specific DNA probes, qPCR enables the direct quantitation of up to several PCR products in real-time. Probes are designed using a stem-loop approach, where a fluorophore and quencher are appended to opposite ends of each sequence. In the absence of target, probe fluorescence is quenched due to the proximity of the fluorophore to the quencher dye following hybridization of the stem region. The increase in product concentration during amplification promotes hybridization of a complementary sequence in the loop region to the amplified product, thereby producing a fluorescence signal that is directly proportional to the product concentration. A significant drawback to this method is the expense of the stem-loop probes, and the specialized thermocycler required for detection further limits the utilization of qPCR to well-equipped laboratories.

DNA hybridization is accurate and specific because of the uniform structure of DNA. The simplest configuration of a fluorescence-based DNA detection platform includes three steps: immobilization of target on a surface, hybridization of a fluorophore-labeled probe, and detection after a thorough wash step. This format is widely used for DNA microarrays (DNA chip), which can screen thousands of DNA sequences with high sensitivity and selectivity [38]. The limit of detection (LOD) is 10^7 molecules/cm^2 [39] and includes the ability to distinguish single-nucleotide polymorphisms (SNPs) [40]. However, the high sensitivity of DNA microarrays results from a combination of elaborate procedures, sophisticated instrumentation, and precise computational and statistical analysis. Because microarray assays are so time-consuming and

expensive, they are best suited for core facilities or commercial applications. For simple fluorophore-labeled DNA hybridization, the LOD is defined by the characteristics of the fluorophore given that there is often significant excitation and emission peak overlap that can contribute to high background. Additionally, fluorescent dyes are susceptible to photo-bleaching. Therefore, several methods have been reported to minimize these limitations in order to increase the LOD.

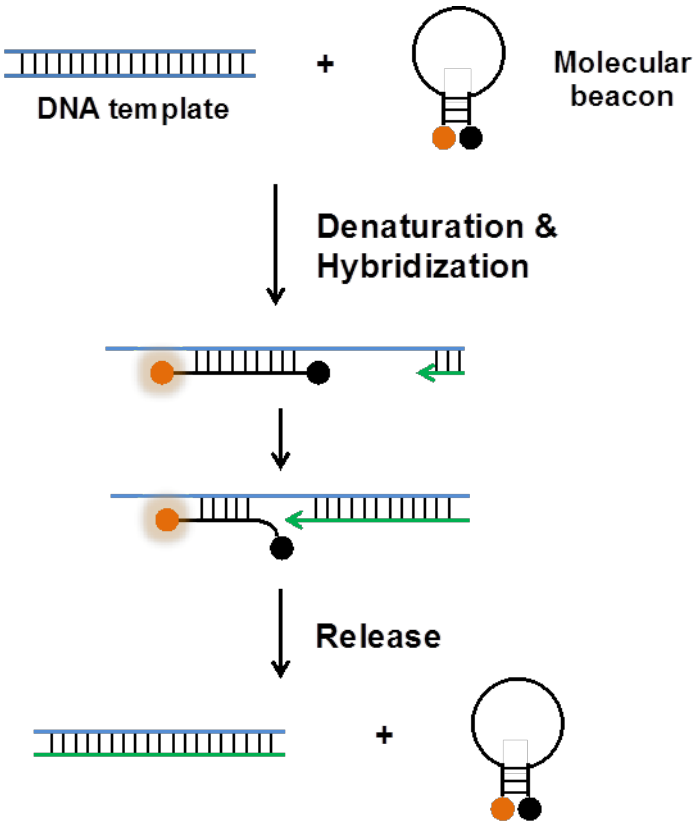

Figure 1.5 Scheme of qPCR detection with stem-loop probe. The stem-loop probe is conjugated with a fluorophore and a quencher. When the loop is closed, the fluorescence is quenched. In presence of target, the loop opens by hybridization to target. During the elongation process, the stem-loop probe is released by DNA polymerase.

One strategy is to utilize fluorescence resonance energy transfer (FRET) to reduce excitation background in fluorescence assays [41]. FRET is the result of long-range, dipole-dipole interactions between a donor (D) molecule in the excited state and an accepter (A) molecule in the ground state. It is distance-dependent as defined by the Förster radius for each donor and acceptor pair and does not involve donor photon emission [42]. Rather, the emission spectrum of the donor and excitation spectrum of the acceptor need to have significant overlap in order to non-radiatively transfer energy from donor to acceptor. The utility of this technique is demonstrated by either the generation of significant peak separation from acceptor emission or signal quenching from acceptor resonance decay. A breakthrough technique based on FRET theory occurred with the development of molecular beacons in 1996 [43]. As introduced above with respect to qPCR, molecular beacons incorporate a fluorophore-quencher D-A pair appended to either end of an oligonucleotide sequence designed with short, terminal complementary regions that, when hybridized, bring the D-A pair within their respective Förster radii for efficient resonance energy transfer. The loop that forms upon hybridization of the complementary “stem” sequences contains a region that is complementary to a target oligonucleotide. In absence of target, donor fluorescence is quenched by the acceptor, while target binding introduces sufficient strain at the stem region to force the loop open and separate the D-A pair. As target concentration increases, fluorescence also increases in a dose-dependent response. By designing the stem sequence appropriately, it is possible to use molecular beacons to efficiently distinguish SNPs [44].

Besides fluorescent dyes, other labels are employed to increase the LOD, including quantum dots (Qds), bioluminescent proteins, and chemiluminescent enzymes. Qds are zero-dimension semiconductor nanoparticles which are characterized by a broad excitation and a narrow emission spectrum that are well-separated compared to organic fluorophores [45, 46]. Additionally, Qds have a high extinction coefficient that efficiently lowers the LOD for Qd-labeled nucleic acid assays to single molecule hybridization [47]. However, Qds are significantly larger and typically more expensive than organic dyes. Bioluminescent protein generates luminescence from a chemical modification of its substrate. Compared to an external excitation source, luminescence is very weak and confined, resulting in greatly reduced background and non-specific signal. Some of the most widely used bioluminescent proteins include aequorin [48-50] and luciferase [51-55]. However, the requirement for substrate addition complicates the operation of bioluminescent protein-based assays.

Enzyme-based signal amplification using chemiluminescence (color change) has been widely used, and ELISA is one of the most developed techniques. Prevalent enzymes include horseradish peroxidase (HRP) and alkaline phosphatase (AP). HRP catalyzes the oxidation of substrate in the presence of hydrogen peroxide with a high turnover rate, resulting in a colorful compound that serves as a dose-dependent signal indicator. AP is the name of a family of enzymes which hydrolyze phosphates from nucleotides and proteins. This enzyme family is activated by divalent cations, and inhibited by cysteine, cyanides, arsenate, inorganic phosphate and divalent cation chelators such as

EDTA [56]. Previous literature reported the utilization of HRP or AP probe to detect viral DNA [57-59] or other target DNA [60, 61] with different substrates. These enzymes have high sensitivity and a long shelf life (compared to antibodies). However, they are much larger than organic fluorophores and require substrate to generate signal.

Another method to increase LOD is to incorporate an amplification step prior to detection. However, because the amplification product is double-stranded, it is still subject to competition between the original amplification product and target sequence as well as the potential for secondary structure formation when amplifying sections of long, single-stranded DNA. To overcome this problem, some researchers have included biotin-labeled primers that enable subsequent capture of the double-stranded PCR products using streptavidin-coated magnetic beads [62]. Following denaturation via a NaOH wash, single-stranded DNA without biotin can be recovered. Also, the Hill group developed a method to block the hybridization of PCR complementary sequences [63]. However, the excessive number of steps and inconvenient operation requires this method to be automated.

To avoid a separation step for double-stranded amplification products, some reports employed rolling circle amplification (RCA) for single-stranded DNA generation, or zinc finger protein (ZFP) binding to specific double-stranded DNA sequences. RCA is an isothermal amplification method that utilizes a circularizable oligonucleotide, called a ‘padlock probe,’ which hybridizes to a single target nucleic acid using both termini. After ligation, the circular template

is amplified with DNA polymerase phage ø29 to generate a long, single-stranded DNA with a repeating sequence. The single-stranded RCA product can be detected with fluorophore-labeled probe [59, 64-67]. The nucleic acid target is employed as a bridge to allow priming (Figure 1.6) of the circular template.

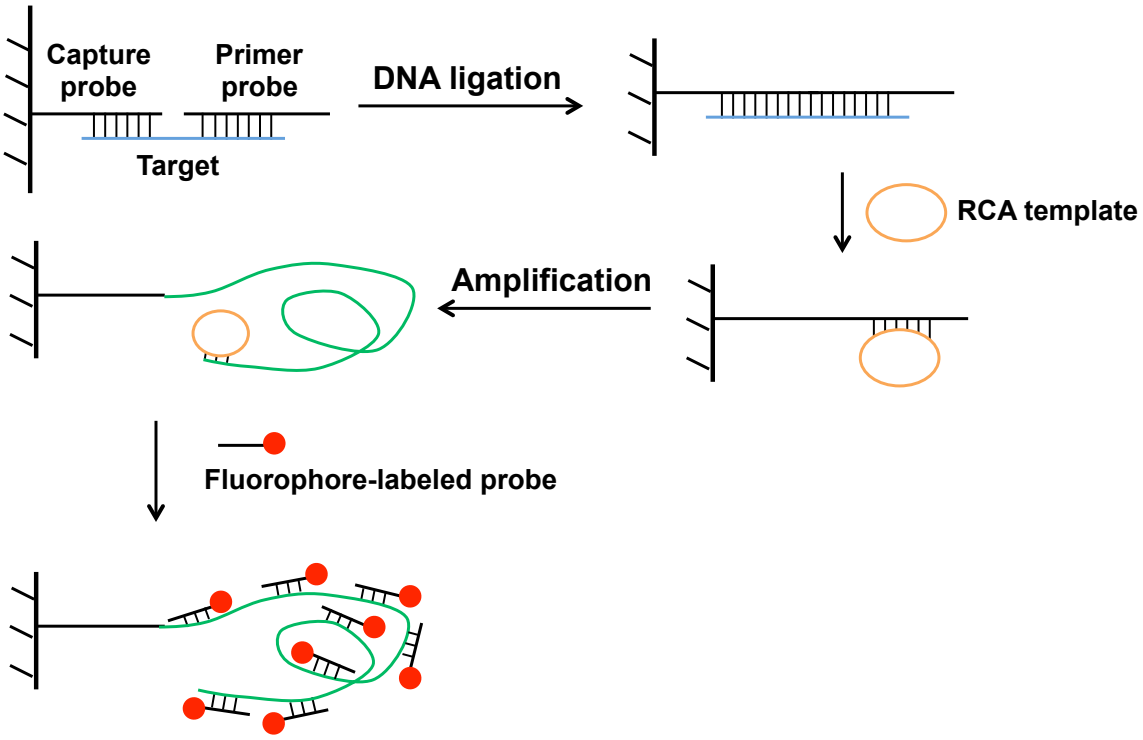

Figure 1.6 Scheme of nucleic acid detection with RCA. In order to start the RCA reaction, the target bridges two probes. After DNA ligation, the circular template is amplified with DNA polymerase. The resulting single-stranded amplification product is detected with fluorophore-labeled probe. These schemes are adapted from literature [67].

If the target is present as double-stranded DNA, ZFPs can be used to capture a specific sequence in the target. Previous literature reported detection of *E. coli* with a bioluminescent protein-ZFP fusion [68, 69]. Another group labeled both halves of a split enzyme using two ZFPs that recognized a target

DNA, resulting in enzyme reassembly for detection [70]. However, these methods required that the ZFP binding sequence be present in the target DNA, which limited their utility.

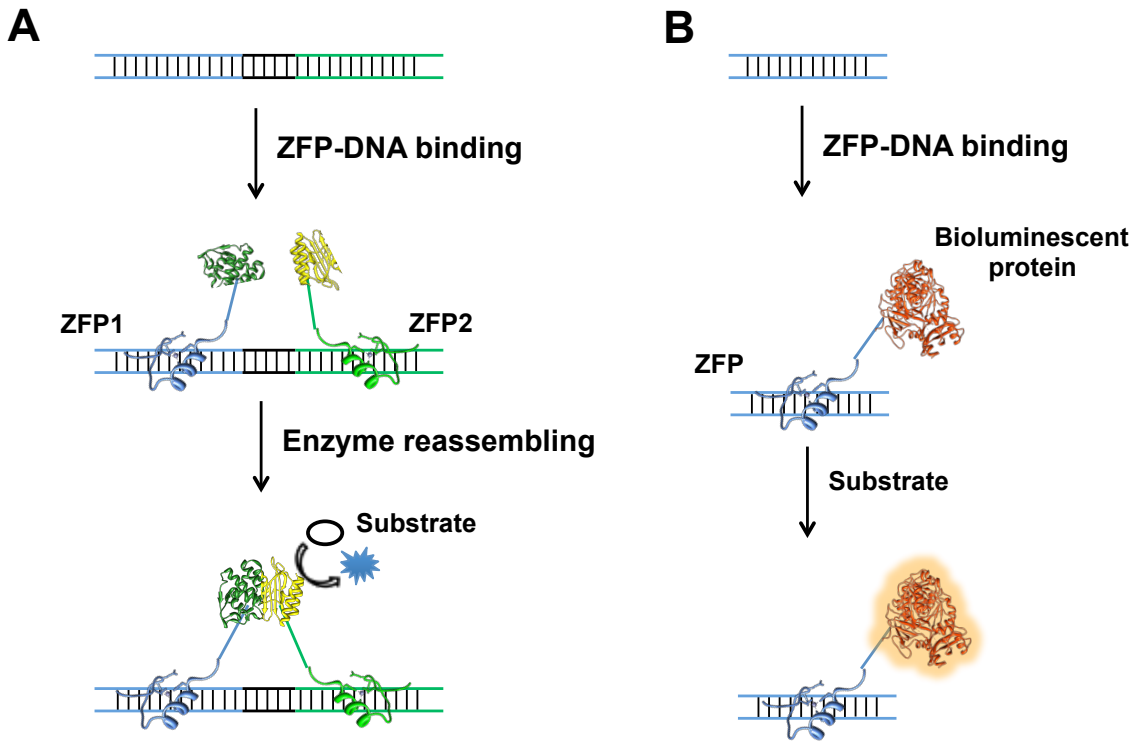

Figure 1.7 Scheme of double-stranded DNA detection with ZFP. **A)** Two ZFPs recognize a specific target region on double-stranded DNA, allowing the reassembly of an enzyme. A color change is measured upon substrate addition. **B)** Double-stranded DNA sequence is recognized and detected with ZFP and bioluminescent protein fusion. These schemes are adapted from literature [69, 70]. The structure of ZFP, bioluminescent protein (firefly luciferase), and TEM1 beta lactamase were obtained from RCSB protein data bank (1SP1, 1LCI, and 1ZG4, respectively).

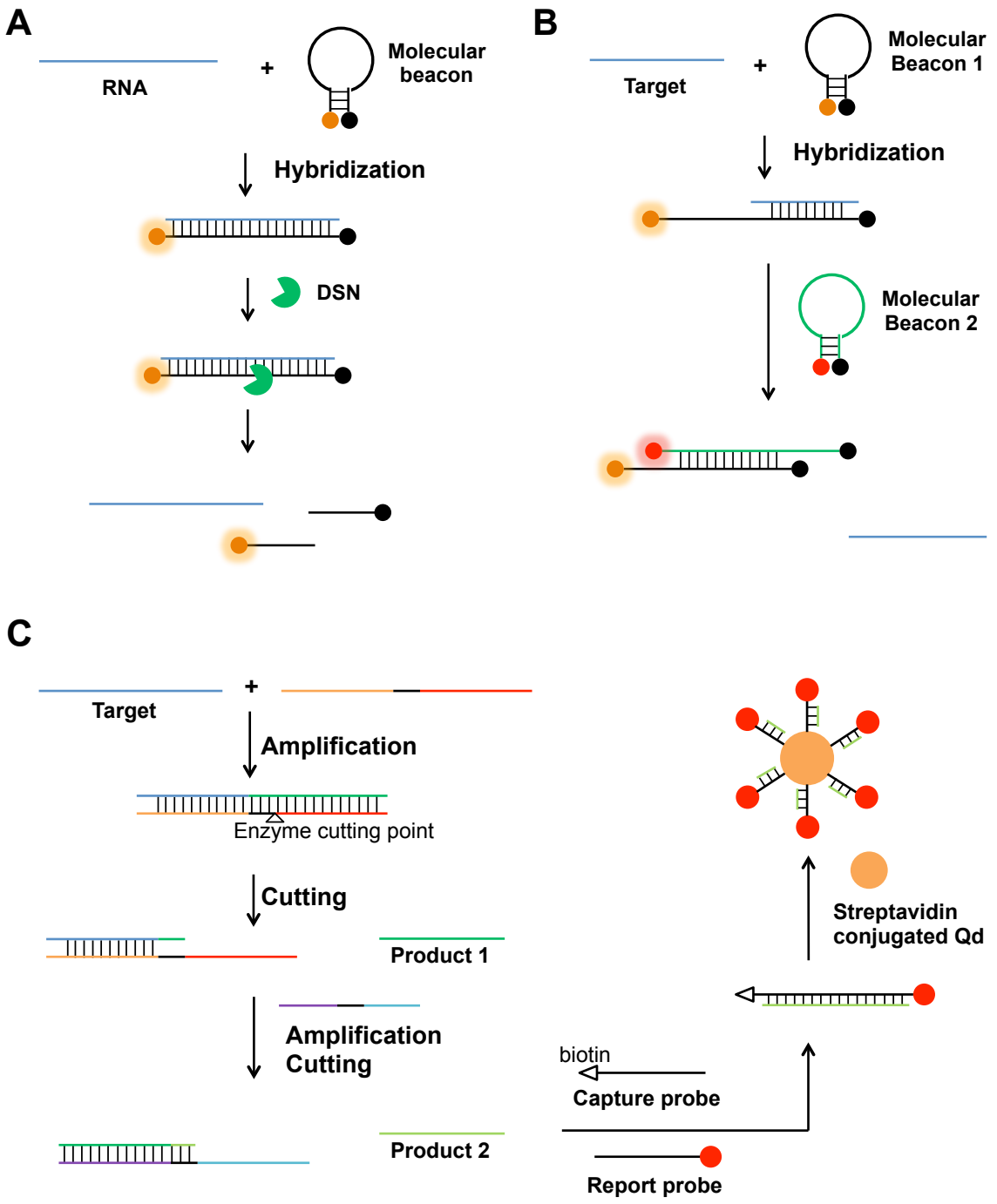

Figure 1.8 Scheme of single-tube amplification and detection. **A)** Molecular beacon is opened through hybridization to RNA target. In presence of duplex-specific nuclease (DSN), the DNA portion of the DNA-RNA hybrid is cut, resulting in released RNA target and separation of fluorophore and quencher probes. **B)** Molecular beacon 1 is hybridized to target first. Then, upon addition of molecular beacon 2, the target is released by strand replacement, leaving a beacon-beacon

hybrid with high fluorescent emission. **C)** Target nucleic acid is employed as primer. After DNA amplification and nicking enzyme cutting, another nucleic acid product 1 is generated. Serving as primer, product 1 can generate product 2 upon amplification with another template and cutting. Product 2 bridges the biotinylated capture probe and fluorophore-labeled reporter probe. The sandwich DNA hybrid is captured by streptavidin-conjugated Qd and detected via FRET between Qd and fluorophore label. These schemes are adapted from literature [71-73].

Some assay designs even incorporate target amplification and detection in one tube. These can include polymerase-based target amplification and enzyme-based target regeneration. The Ye group employed duplex-specific nuclease (DSN) to cut the DNA strand in a DNA-RNA hybrid, resulting in release of RNA target which would be free to hybridize with another DNA probe [71]. The Zhang group utilized nicking enzymes to cut specific regions of the PCR product to force aggregation of single-stranded target, which could then be detected using FRET [73]. Another report demonstrated an enzyme-free signal amplification method with two molecular beacons [72]. The first beacon was hybridized with target, followed by the addition of the second beacon which had a longer complementary sequence to the first beacon than target. Thus, the target was freed due to a strand displacement. The increased target concentration was measured as enhanced fluorescence from the opened beacon.

However, fluorescence-based detection methods such as these cannot be used in the field, and absorbance assays are still the prevalent method for POC detection. More recent literature has begun to amplify target regions using a relatively new technique called loop-mediated isothermal amplification (LAMP) [74-78]. LAMP employs 4-6 primers that synthesize a loop structure using a

Target	Detection	Detection Platform	Can use in resource-poor settings?	Sample Volume	LOD	Reaction Time	Target Amplification Method	Ref
Salmonella, *C. jejuni*, *Shigella*, *V. cholerae*	Fluorescence	PCR chip	Yes		10–100 copies per reaction	30 min	LAMP	[79]
HIV-1, HIV-2, human T-lymphotrophic virus types I and II	Fluorescence	PCR tube	No		10 molecules	2 hrs	real-time PCR	[80]
Salmonella	Fluorescence	PCR tube	Yes	1 μL	9 amol	2 hrs	RCA	[65]
P. falciparum	Bioluminescence	microtiter plate	No	100 μL	0.03 nM	3 hrs	N/A	[48]
Anthrax DNA	Absorbance	microtiter plate	No	100 μL	10 zmol	4-5 hrs	N/A	[58]
Pseudorabies virus	Absorbance	PCR chip	Yes	0.4 μL	10 fg	1 hr	LAMP	[74]
Crimean-Congo hemorrhagic fever virus	Absorbance	microtiter plate	No		600 copies per reaction	3-4 hrs	RCA	[59]
E. coli	Electrochemistry	carbon electrodes	No	1 μL	0.75 amol	40 min	N/A	[81]
C. perfringens, C. tetani, S. pneumonia, P. aeruginosa, E. coli	QCM	chip	No		1.5×10^2 CFU/mL	5 hrs	PCR	[82]
V. vulnificus, Salmonella spp., S. aureus, E. faecalis, N. gonorrhea, S. epidermidis, K. oxytoca	SPR	chip	No	5 μL	50 zmol	6 hrs	PCR	[83]
E. faecium, S. aureus, S. maltophilia, V. vulnificus	SERS	Au nanowire	No	30 μL	10 pM	14 hrs	PCR	[84]
Hepatitis B Virus (HBV)	Cantilever	cantilever	No	100 μL	23.1 fM	6-7 hrs	PCR	[85]

Table 1.1 Some examples of previously reported methods of pathogen detection using various platforms. The reaction time was considered to begin at the time of sample addition and includes the target amplification time.

strand-displacing DNA polymerase, a process that can be detected as turbidity due to the increasing quantity of magnesium pyrophosphate byproduct in solution [77]. The resulting loop is utilized as the template for subsequent amplification [78]. This method, combined with its simple detection technique, is suitable for resource-limited setting usage. However, it cannot detect multiple targets in one amplification reaction.

Gold nanoparticles (AuNPs) are another widely used label for POC detection, especially in paper strip assays, due to their biocompatibility, chemical stability, ease of conjugation, and optical properties. Because of a high affinity for thiols, AuNPs can be linked to thiol-modified oligos or proteins (via cysteine) by simply mixing. Additionally, the adsorption characteristics of AuNPs are highly dependent on particle size. In other words, aggregation of AuNPs can be seen as a color change. This property led to the development of commercial pregnancy kits [86]. Simply, AuNPs separate in the presence of human chorionic gonadotropin, a hormone produced after fertilization. Thus, a positive sample would disrupt aggregation and produce a pink color in the correct window, while a negative sample would show a gray color due to intact aggregate. Some reports also demonstrate the detection of specific nucleic acid sequences based on this characteristic. In these assays, two AuNPs-labeled oligos were allowed to hybridize to target in a sandwich format. Target recognition would produce a color change due to the induced aggregation stimulated by the proximity of the two labeled probes [87]. Another prevalent detection technique using AuNPs employs silver as an enhancer to enlarge a gold colloid via precipitation of the silver, resulting in a colorful signal. Many reports employ this strategy for nucleic acids detection [44, 88], which is capable of detection limits as low as 100 fM [89].

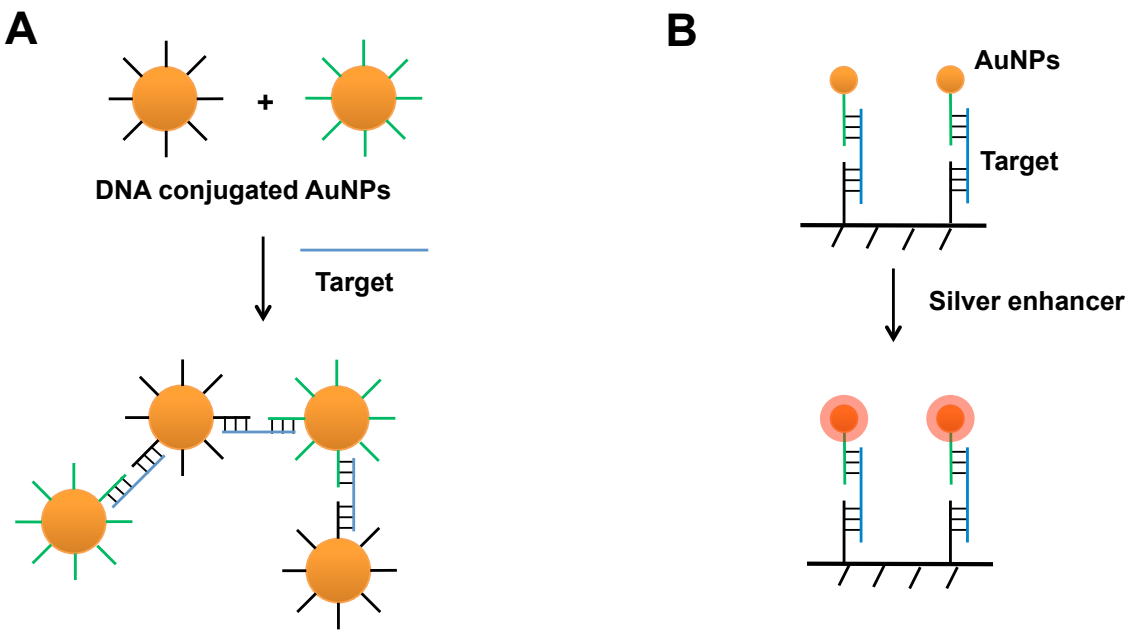

Figure 1.9 Scheme of AuNP-based nucleic acid detection methods. **A)** AuNPs conjugated with oligonucleotides aggregate upon nucleic acid hybridization, resulting in a color change. **B)** AuNP label utilized in nucleic acid sandwich hybridization can be visually detected upon addition of silver enhancer, which aggregates on the AuNPs to increase the nanoparticle size and change the absorption characteristics. These schemes are adapted from literature [87, 88].

1.3.2 Electrochemical detection method

Electrochemical methods enable label-free detection of nucleic acids simply by detecting hybridization events [90, 91]. Label-based detection methods are also employed through the use of electroactive molecules which allow for distinguishing ssDNA verses dsDNA as well as DNA-RNA hybrids [92]. Labels include nanoparticles [93], intercalators (methylene blue) [94-96], and enzymes [97-99] and allow for detection limits in the femtomolar range [100].

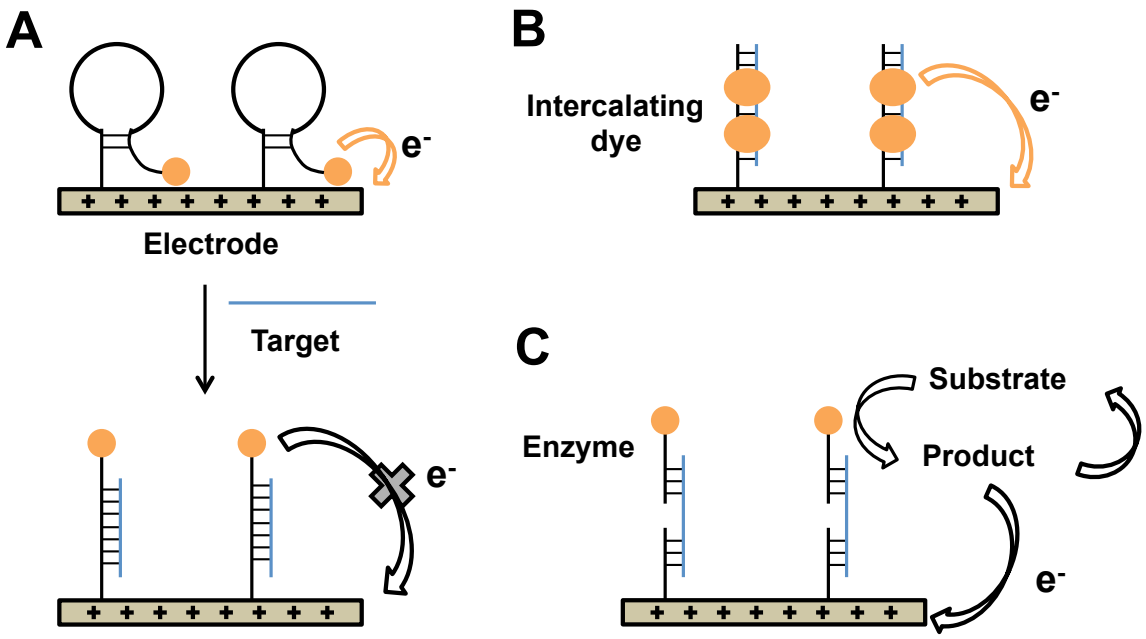

Figure 1.10 Different schemes of electrochemical nucleic acid detection. **A)** Molecular beacon is opened through hybridization with target, which decreases the electron transfer from label to electrode. **B)** Intercalating dyes only bind to double-stranded nucleic acids following hybridization. The dye is detected by increasing electron transfer to the electrode. **C)** Enzyme-labeled nucleic acid sandwich platforms can also be performed using electrochemistry. The enzyme-catalyzed reaction serves as the electron donor to the electrode. For clarity, all schemes show only the anode.

To further increase the detection limit, nanomaterials have been utilized as electrodes [100, 101]. Nanoparticles effectively increase surface area, enhance delivery of amplification agents, and allow precise conjugation to biomolecules [92] to provide an attamolar-range detection limit [102]. Carbon nanomaterials, including nanowires, nanotubes, and graphene, are the most prevalent nanomaterials employed because of their excellent electric conductivity, low cost, and easy implementation [103-105].

Electrochemical detection for nucleic acids is fast, provides low detection limits, and can be label-free, as opposed to luminescence-based methods. However, reports of electrochemical methods in biological samples are limited due to the high background commonly present in complex matrices [92]. Additionally, instrumentation is often delicate and complex, relegating these methods to the laboratory.

1.3.3 Other detection techniques

By immobilizing capture probes to a metal film surface, surface plasmon resonance (SPR) can detect target hybridization by observing a change in the local refractive index of the support matrix [106-108]. Another label-free method, quartz crystal microbalance (QCM), can provide real-time monitoring of target hybridization [109-112]. This method detects a mass change per unit area by measuring frequency perturbations in a harmonically oscillating quartz crystal resonator. Surface acoustic wave (SAW) sensors measure perturbations in a generated mechanical wave when analyte selectively binds to the surface [113, 114]. The cantilever method detects target hybridization by measuring incident angle changes that are reported by laser reflection from the cantilever surface [85]. These label-free detection methods have high LOD, but they are typically laboratory-based because of the precise instrumentation required.

1.4 Multiplex nucleic acids detection

There are two major methods to detect multiple targets at same time: detect individual targets in each reaction and perform several reactions at same time, or detect several targets in one reaction (multiplex). Since multiplex detection is significantly more complex, many reports rely on performing multiple reactions.

Real-time PCR with intercalating dye (or stem-loop probe) is the most prevalent multiplex technique. Probes with chemiluminescent [115] or fluorescent (including microarray) [116, 117] labels have also been utilized for multiplex target detection. Newer methods have employed isothermal amplification, especially LAMP, to detect multiple pathogens [79, 118], or several sequences for one pathogen [119], which is ideal for on-site detection. Some detection techniques like electrochemistry and SERS enable multiplexed target detection using different probes attached to separate areas [84, 120-122]. QCM was utilized to detect several bacterial targets in parallel using different channels [82].

Reporter probes with different labels are employed for multiplex nucleic acid detection. Molecular beacons (MB) labeled with non-overlapping fluorophores have shown detection limits at the picomolar level [80, 123, 124]. Ferrocene (Fc)- and MB-labeled probes have been used to detect two DNA targets electrochemically [125]. Another electrochemical assay employed HRP- and AP-labeled AuNPs for detecting two targets, producing detection limits of 0.1 and 12 pM, respectively [126]. Different color Qds were also employed to detect

DNA hybridization as emission peak shifts [127] or intensity changes to give nanomolar - range detection limits [128-131]. Additionally, Qds have been

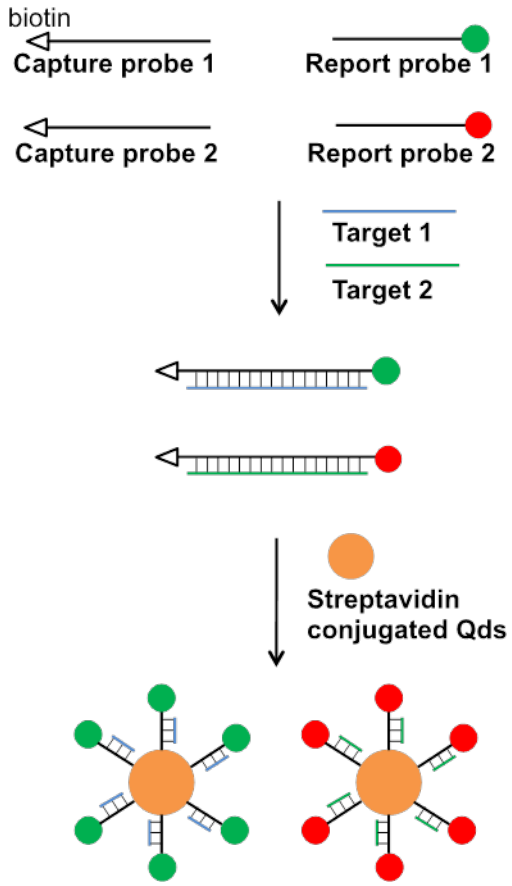

Figure 1.11 Scheme for nucleic acid multiplex detection with FRET. The target is hybridized with a biotinylated capture probe and a fluorophore-labeled reporter probe. The DNA hybrid is captured by streptavidin-conjugated Qd through biotin-streptavidin binding. Based on overlap, the Qd can only transfer energy to Alexa Fluor 647, while Alexa Fluor 488 is excited using the same excitation wavelength as Qd. Therefore, one target is detected via FRET transfer from the Qd to Alexa Fluor 647, while the other target is detected with the emission from Alexa Fluor 488. This scheme is adapted from literature [132].

combined with fluorophores as energy transfer D-A pairs to detect multiplex DNA target with picomolar-range detection limits [132]. As previously mentioned,

DNA/RNA hybrids have been detected using a combined target amplification and regeneration step to increase sensitivity. Target regeneration was performed enzymatically using DSN [71] and nicking enzyme [73]. Multiplex analysis was accomplished by taking advantage of non-overlapping signals from the labels.

CHAPTER 2: RAPID DETECTION OF BACTERIAL NUCLEIC ACIDS USING BRET BETWEEN RLUC AND QDS

2.1 Overview of Study

We developed a bioluminescence resonance energy transfer (BRET)-based sensing system that was able to detect nucleic acid target in 5 min with high sensitivity and selectivity. Upon presence of target, the individual *Renilla* luciferase (Rluc)-labeled and quantum dot (Qd)-labeled oligos formed a head-to-head binding format, which brought Rluc and Qds within proximity for non-radiative energy transfer. Rluc, as the energy donor, is a bioluminescent protein that generates light via substrate cleavage. The energy was transferred to Qds that served as an energy acceptor. A higher target concentration was indicated by decreased emission from Rluc, with a commensurate increase in Qd luminescence. This sensing system could detect target nucleic acid in buffer with a LOD of 2.1 nM after a 5-min incubation. This assay was also tested with *E. coli* 16s rRNA detection in cell lysate.

2.2 Background

Nucleic acid detection has found applications in fields such as medicine, molecular biology, clinical diagnostics, forensics, bioterrorism prevention, and food technology. These applications require very rapid results with high sensitivity and selectivity, leading to many reports that focus on the design of qualified sensing systems [133-136]. The nucleic acids hybridization between a

target strand and a probe with complimentary sequence is commonly utilized in the design of nucleic acid sensing systems. Among many reporters that exist for nucleic acid detection techniques, fluorescence is the most popular reporter due to its high detection sensitivity, multiplexing capability, the accessibility of diverse labels, and the possibility of non-invasive detection [42, 43, 137-149].

Fluorescence-based methods such as fluorescence resonance energy transfer (FRET) have gained wide acceptance as sensitive detection platforms. Bioluminescence resonance energy transfer (BRET) is a highly similar technique that avoids the need for an external excitation source. In BRET, light is produced by cleavage of a specific substrate molecule by a bioluminescent protein. Therefore, inadvertent excitation of the acceptor is prevented, leading to significantly reduced background and improved signal-to-noise ratio. Bioluminescent proteins such as aequorin and luciferase can be easily expressed from *E. coli*. BRET has mainly been employed in the detection of protein–protein [150] or protein–ligand interactions [151-155] because the energy transfer ratio is highly dependent on the distance between donor (D) and acceptor (A) [42]. A few recent reports demonstrated applications of the bioluminescent protein *Renilla* luciferase (Rluc) with green fluorescent protein (GFP) in an on-type assay [156, 157]. These assays are promising, but their LOD could be further improved by utilizing an acceptor with a higher extinction coefficient (ε) and/or a D-A pair with better spectral overlap. For example, a previous nucleic acid detection method from our lab utilized an Rluc-Qd705 D-A pair in a signal-off assay format [51]. This D-A pair was chosen because Rluc

has a broad emission spectrum that favorably overlaps with the Qd705 excitation spectrum, and the extinction coefficient of Qd705 ($\varepsilon = 3\times10^6$ $cm^{-1}M^{-1}$, λ_{ex} = 488 nm) is larger than that of GFP (less than 10^5 $cm^{-1}M^{-1}$) or organic dyes (ex. Alexa Fluor 488, $\varepsilon = 7.3\times10^4$ $cm^{-1}M^{-1}$, λ_{ex} = 495 nm). In order to further increase the detection limit, we tested a similar Rluc-Qd D-A pair in a signal-on assay format. Instead of Qd705, we employed Qd625 due to a similar extinction coefficient ($\varepsilon = 2.7\times10^6$ $cm^{-1}M^{-1}$, λ_{ex} = 488 nm) but higher absorption around 480 nm.

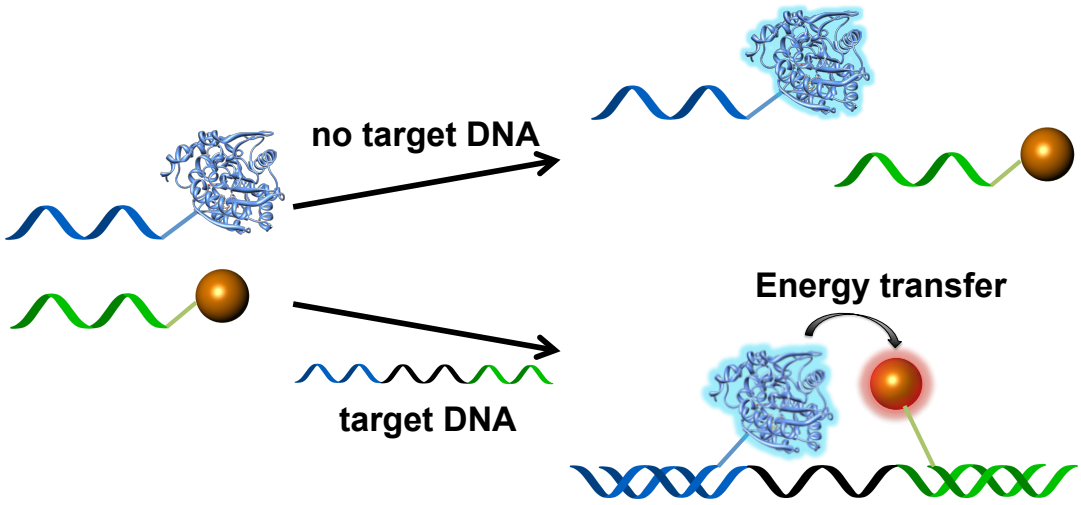

Figure 2.1 Scheme of the BRET-based nucleic acid sensing system. Two probes were employed in this detection platform, Rluc-probe (blue) and Qd625-DAP-probe (green). When no target was present, Rluc would luminesce upon addition of coelenterazine, but Qd625 would not emit due to the lack of an excitation source. In the presence of target, the two probes hybridized to adjacent regions of the target. When coelenterazine was injected, Qd625 accepted and then emitted the transferred energy from coelenterazine oxidation. Increased target concentrations were indicated by increased red emission from Qd625 and decreased blue emission from Rluc in a dose-dependent response. The Rluc8 structure was obtained from RCSB protein data bank (2PSD).

In this design, two oligonucleotide (oligo) probes terminally-labeled with either Rluc or Qd625 were designed to include sequence complementary to adjacent regions of a target oligo (Figure 2.1). This design feature allowed the labeled probes to hybridize with the target in a head-to-head arrangement, promoting efficient energy transfer between Rluc and Qd625. Increasing target concentrations were directly proportional to increased Qd625 emission and decreased Rluc emission, and the detection limit of this assay was found to be 2.1 nM after a 5-min hybridization.

2.3 Materials and Methods

2.3.1 Materials

All purchased chemicals were used without further purification. 1,3-diamino-2-hdroxypropane (DAP) and imidazole were purchased from ACROS (Fair Lawn, NJ). Microcon YM-30 spin columns were from Millipore (Billercia, MA). Zeba desalting spin columns were purchased from Thermo Fisher Scientific (Rockford, IL). Miller Lysogeny Broth (LB), sodium tetraborate decahydrate, ethylenediaminetetraacetic acid (EDTA), sodium phosphate dibasic heptahydrate, and sodium phosphate monobasic anhydrous were from Fisher Scientific (Fairlawn, NJ). Carboxylated-quantum dots (Qd625, CdSe/ZnS) and aldehyde-modified oligonucleotides probes were purchased from Invitrogen (Carlsbad, CA). MP Biomedical (Solon, OH) supplied the agarose, while ampicillin, diethyl pyrocarbonate (DEPC), and Coomassie Brilliant Blue R250 stain were purchased from Sigma-Aldrich (St. Louis, MO). Succinimidyl 6-

hydrazinonicotinate acetone hydrazone (SANH), 96-well microtiter plates, and 1-ethyl- 3-(3-dimethylaminopropyl) carbodiimide (EDC) were obtained from Pierce Thermo Fisher Scientific (Rockford, IL). High performance Ni^{2+}-NTA agarose was purchased from GE Healthcare (Uppsala, Sweden). Native coelenterazine was from Prolume (Pinetop, AZ). All oligonucleotide targets and amine-modified oligonucleotides were obtained from Eurofins MWG Operon (Huntsville, AL).

Buffers that were used in the present study were prepared in the laboratory and their compositions are as follows: binding buffer (20 mM sodium phosphate, 500 mM NaCl, 20 mM imidazole pH 7.0); elution buffer (20 mM sodium phosphate, 500 mM NaCl, 500 mM imidazole pH 7.0); hybridization buffer (100 mM sodium phosphate pH 7.0), borate buffer (10 mM sodium borate pH 7.0); SANH conjugation buffer (100 mM sodium phosphate, 150 mM NaCl pH 7.5); DNA conjugation buffer (100 mM sodium phosphate, 150 mM NaCl pH 5.8). DEPC-treated buffer preparation consisted of adding 0.1% (v/v) DEPC to hybridization buffer, followed by 2-h incubation before autoclaving.

2.3.2 Oligonucleotide sequences

All targets and probes used for this work are listed in Table 2.1. Target oligonucleotides were DNA analogues of a small sequence from *Escherichia coli* 16s rRNA (Genbank NR_024570.1). Two small oligonucleotides (Probe-1 and Probe-2) were employed as detection probes. Probe-1 was an 18-base oligo with a 5′-aldehyde for Rluc conjugation. Probe-2 was a 20-base oligo conjugated to Qd625 using a 3′ linker consisting of a 7-carbon spacer and a terminal amine.

Target oligonucleotides (Tar-1, Tar-2, Tar-3, and Tar-4) were designed to vary the distance between the two complementary sequence regions. The single nucleotide polymorphism (SNP) contained a mismatch within the complementary region for both Probe-1 and Probe-2. The multiple mismatch target (MM-Tar) contained one mismatch in the complementary region for Probe-1 and two mismatches in the region complementary to Probe-2.

Tar-1 (5-nucleotide spacer)	AAC GTC GCA AGA CCA AAG AGC AGC CAC ACT GGA ACT GAG ACA C 43 bases
Tar-2 (10-nucleotide spacer)	AAC GTC GCA AGA CCA AAG AGG GGA CCA GCC ACA CTG GAA CTG AGA CAC 48 bases
Tar-3 (15-nucleotide spacer)	AAC GTC GCA AGA CCA AAG AGG GGG AAT GAC CAG CCA CAC TGG AAC TGA GAC AC 53 bases
Tar-4 (20-nucleotide spacer)	AAC GTC GCA AGA CCA AAG AGG GGG ACC AGG ATG ACC AGC CAC ACT GGA ACT GAG ACA C 58 bases
Probe-1	Aldehyde - CTT TGG TCT TGC GAC GTT 18 bases
Probe-2	GTG TCT CAG TTC CAG TGT GG - C_7 Amine 20 bases
SNP	AAC GTC GCA TGA CCA AAG AGG GGG AAT GAC CAG CCA CAC TGG TAC TGA GAC AC 53 bases
MM-Tar	AAC GTC GCA TGA CGA AAG AGG GGG AAT GAC CAG CCG CAC TGG TAC TGA GAC AC 53 bases
E. coli 16s rRNA	Genbank NR_024570.1

Table 2.1 List of nucleotide sequences for targets and probes (5'-3'). The underlined and double-underlined sequences in targets indicate the complementary regions to Probe-1 and Probe-2, respectively. The mismatched nucleotides in SNP and MM-Tar are shown in red.

2.3.3 Rluc expression and purification

The plasmid containing the gene for Rluc8, a serum-stable mutant (noted as Rluc in this manuscript) was constructed according to previous reports [51]. *E. coli* (strain LMG-194) containing the Rluc-encoding plasmid was cultured in 400 mL LB broth with 100 µg/mL ampicillin at 37 °C. At OD_{600} of 0.6-0.8, Rluc was induced with 0.2% L-arabinose at 37 °C for 5 h. Then, the cells were pelleted at 7,000 RPM for 20 min and resuspended in binding buffer. Following a freeze-thaw cycle (-80 °C to 37 °C, 3X), cells were sonicated (Fisher Scientific, Sonic Dismembrator, Model-500) for 2 min (5 sec on, 20 sec off) to release protein. The protein was separated by centrifuging at 17,000 RPM for 10 min, and the supernatant was passed through a 0.2 µm filter. Approximately 10 mL of the filtered, crude protein was subsequently loaded on fresh Ni^{2+}-NTA beads and incubated while mixing at room temperature for 2 h. The column was washed with three 10 mL aliquots of binding buffer prior to Rluc elution using 5 mL elution buffer. Luminescence activity of the elution was verified before SDS-PAGE analysis. The concentration of the purified protein was determined using a Bradford assay.

2.3.4 Rluc conjugation to aldehyde-modified oligonucleotide

As shown in Figure 2.2, Rluc was covalently attached to the oligonucleotide probe using a previously described method [156]. Briefly, 25 nmol of Rluc was added to 206 µL of SANH conjugation buffer, followed by addition of 10X mole excess of SANH. The mixture was allowed to incubate for 3 h at room

temperature. The reaction was stopped by buffer-exchanging the mixture to the DNA hybridization buffer using a Zeba desalting spin column. The concentration of SANH-modified Rluc was determined using Bradford assay. Then, Probe-1 with 1.5X mole excess of the SANH -modified Rluc was added and reacted

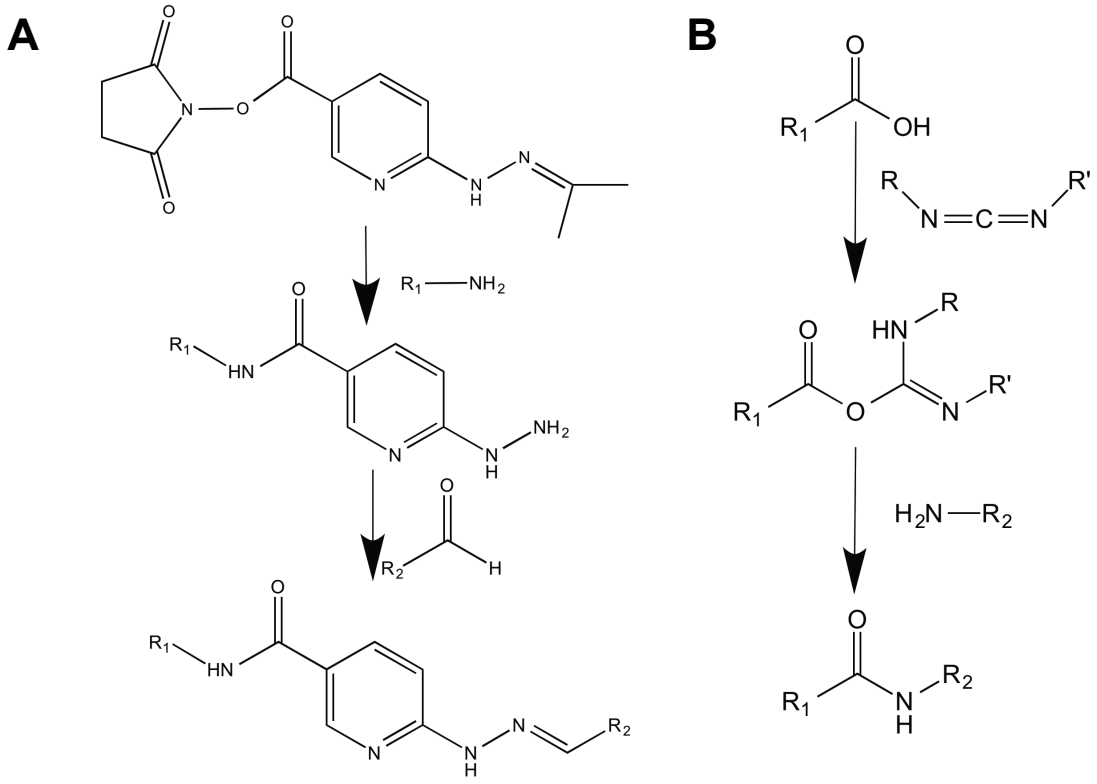

Figure 2.2 Chemical reaction for Rluc-probe **(A)** and Qd625-DAP-probe **(B)** conjugation. **A)** Rluc was conjugated with aldehyde-modified oligonucleotide through SANH. **B)** EDC was employed as crosslinker in Qd625 blocking and conjugation steps. The carboxylated Qd625 was blocked with DAP first, followed by conjugation to amine-modified oligonucleotide.

overnight at room temperature. The resulting Rluc-probe was separated from unreacted reagents by passing through a Zeba desalting column. The

concentration of Rluc-probe was determined using a Bradford assay. The Rluc-probe was stored at 4 °C prior to use.

2.3.5 Conjugation of Qd625 to amine-functionalized oligonucleotide

Probe-2 was conjugated to Qd625 after blocking with DAP. This blocking method was reported previously [158], with some modifications described below. Briefly, carboxyl-coated Qd625 was blocked with DAP using EDC chemistry (Figure 2.2). For this, 0.8 nmol Qd625 was buffer-exchanged to borate buffer using Zeba desalting columns, followed by dilution to a final volume of 2 mL in borate buffer. EDC solution was then added to a final amount of 88.6 µmol. After 5-min incubation, 11.4 µmol DAP was injected into the mixture, and the mixture was incubated for 1 h. Unreacted EDC and DAP were separated by passing the mixture through a YM-30 spin column at 5000 RPM for 6 min. The separated Qd625-DAP was then mixed with 88.6 µmol EDC and 1.5 nmol Probe-2, and reacted for 1 h. The conjugated Qd625-DAP-probe was again separated from excess reactants by passing the mixture through a YM-30 spin-column at 5000 RPM for 6 min. The concentration of Qd625-DAP-probe was determined by measuring the fluorescence intensity (ex: 480/10 nm, em: 630/10 nm) of 2 µL of Qd625-DAP-probe in 148 µL borate buffer in a 96-well microtiter plate using a Varian Cary Eclipse spectrofluorometer (Agilent; Santa Clara, CA). The concentration of Qd625-probe was calculated using a calibration curve generated by measuring the fluorescence intensity of Qd625 standard dilutions. The Qd625-DAP-probe was stored at 4 °C before use. In order to compare

conjugation efficiencies with and without the addition of DAP, Qd625 was covalently conjugated to Probe-2 following the above procedure, with the exception of excluding the blocking step.

2.3.6 BRET D-A pair distance optimization

The spacing between the Rluc-probe and Qd625-DAP-probe hybridized to the target was optimized. Four oligonucleotide targets (Tar-1, Tar-2, Tar-3 and Tar-4) with spacing variations of 5, 10, 15, and 20 nucleotides were tested. In a 100 µL reaction, 1.3 pmol of Qd625-DAP-probe and 1.7 pmol of Rluc-probe were mixed, followed by addition of various volumes of 2 µM target stock solution. The mixture was hybridized for 35 min at room temperature in hybridization buffer. For detection, a 50 µL aliquot of 2.6 nM coelenterazine was injected into each well. Bioluminescence intensity was detected using a PerkinElmer Victor X Light luminometer (PerkinElmer, Model-2030) with 486 ± 10 nm and 630 ± 10 nm filters. All luminescence readings were obtained with a 1-sec integration time. Negative controls were performed concurrently with all assay components except target.

2.3.7 Hybridization time optimization

The hybridization time required for the labeled probes to capture target was optimized to obtain maximum BRET signal. In this experiment, 1.3 pmol of Qd625-DAP-probe and 1.7 pmol of Rluc-probe were mixed with different volumes of 2 µM Tar-3 stock solution (final concentrations ranging from 1 nM to 133 nM)

for a total volume of 100 μL in hybridization buffer. Oligonucleotides were hybridized at room temperature for 1, 5, and 35 min, and the luminescence intensity was measured after injecting a 50 μL aliquot of 2.6 nM coelenterazine. Negative controls (no target) were performed concurrently.

2.3.8 Detection limit and dynamic range determination

To ascertain the sensitivity and range of this sensing platform, a calibration curve was generated by adding from 75 fmol to 4.5 pmol of Tar-3 to a mixture of 1.3 pmol of Qd625-DAP-probe and 1.7 pmol of Rluc-probe in a total reaction volume of 100 μL. Luminescence intensity was measured after 5-min hybridization via injection of a 50 μL aliquot of 2.6 nM coelenterazine. Negative controls (no target) were performed concurrently. Three independent experiments were carried out as validation. Identical conditions were maintained for comparing Qd625-probe to Qd625-DAP-probe.

2.3.9 Selectivity studies

The ability of the sensing system to discriminate between specific target and mismatched targets (SNP and MM-Tar) was tested in DEPC-treated buffer. In a 100 μL reaction solution, Tar-3 and mismatch targets (SNP and MM-Tar) with a concentration range of 2.67 nM to 20 nM were added to a mixture of 1.3 pmol of Qd625-DAP-probe and 1.7 pmol of Rluc-probe. After 5-min incubation, 50 μL of 2.6 nM coelenterazine was injected prior to detection. Negative controls

(no target) were performed concurrently. Three independent experiments were performed to validate reproducibility.

2.3.10 Detection of *E. coli* 16s rRNA

An *E. coli* ER2566 5 ml culture was transferred to 200 mL LB and incubated at 37 °C with shaking at 250 RPM until reaching OD_{600} 0.6-0.8. Cells were harvested by centrifugation at 7,000 RPM for 10 min and resuspended in 35 mL hybridization buffer for sonication. After centrifuging at 17,000 RPM for 1 min, the supernatant was passed through a 0.2 μm filter to eliminate any remaining cellular debris. The filtered cell extract was diluted 100-fold in DEPC-treated buffer before further usage.

In 100 μL of reaction solution, 3-25 μL of diluted *E. coli* cell extract was added to a mixture of 1.3 pmol Qd625-DAP-probe and 1.7 pmol Rluc-probe. After 5-min hybridization, a 50 μL aliquot of 2.6 nM coelenterazine was injected to the mixture prior to luminescence detection. Negative controls (no cell extract) were performed concurrently.

2.4 Results and discussion

For this work, we designed an on-type BRET nucleic acid sensing system around two oligonucleotide probes individually labeled with either Rluc or Qd625 to form an energy D-A pair. Rluc is a bioluminescent protein that generates light (λ_{max} = 488 nm) by catalyzing a chemical reaction of its substrate, coelenterazine. Because of the absence of an external excitation source, bioluminescent proteins

improve the detection limit of an assay by significantly reducing background [159, 160]. Qds are zero-dimensional nanoparticles with wide absorption bands and narrow emission spectrums that incorporate significantly larger extinction coefficients than organic fluorophores. With an extinction coefficient of 2,700,000 cm^{-1} M^{-1} and a large spectral overlap with Rluc (data not shown), Qd625 (Ex: 488 nm, Em: 625 nm) allowed efficient energy transfer from donor to acceptor. Meanwhile, Qds with different λ_{em} can be effectively excited with the same λ_{ex}, which allows the possibility of multiple target detection using different Qd labels. The conjugation method of Probe-1 to Rluc and Probe-2 to Qd625 were reported previously [51, 156] (Figure 2.2). We blocked Qd625 with DAP prior to Probe-2 linkage to reduce non-specific binding between Qd625 and Rluc [158] and increase the electronic stability of conjugated Qd625. The zeta potentials of Qd625 and Qd625-DAP were −39.5 mV and −31.3 mV, respectively. All measurements were carried out at room temperature in phosphate buffer at pH 8.5. To verify the necessity of blocking Qd625, we tested the same assay with Qd625-probe and demonstrated that a higher background existed with the unblocked Qd625 than with the Qd625-DAP-probe (Figure 2.3). Thus, DAP could block the non-specific binding between Qd625 and Rluc for a lower detection limit.

Energy transfer efficiency (E) is highly dependent on the separation distance between donor and acceptor (r) as shown in Equation 2.1. However, Rluc and Qd625 had a minimum separation boundary because steric hindrance could potentially disrupt the hybridization between probe and target. Thus, we

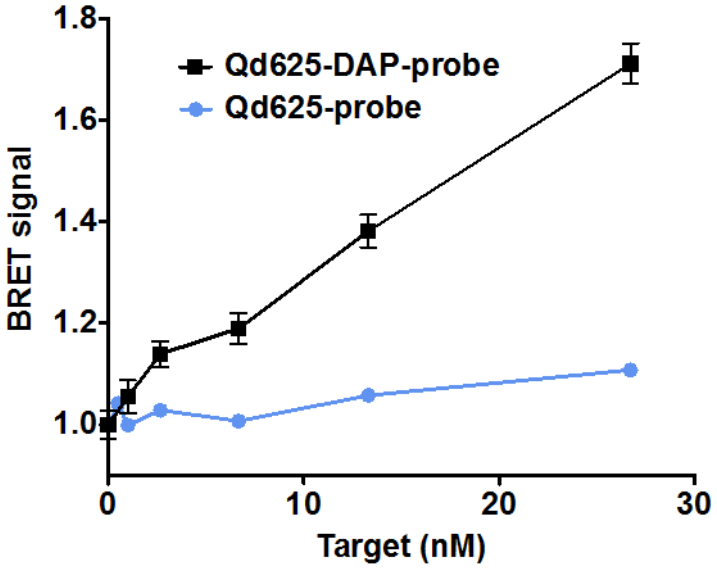

Figure 2.3 The effect of DAP blocking. The DAP-blocked Qd probe (Qd625-DAP-probe, black square) hybridized to the target more efficiently than non-blocked Qd probe (Qd625-probe, blue circle). Thus, DAP effectively prevented non-specific binding between Qds and Rluc.

tested different separation distances within the Förster radius (R_0), as calculated from Equations 2.2 & 2.3. From the normalized emission of Rluc and the absorption of Qd625, we used the refractive index of the medium (n = 1.33), the quantum yield of Rluc (Q=0.07) [161], the orientation factor (κ_p^2 = 0.67), and the extinction coefficient of Qd625 at 488 nm (ε(λ) = 2,700,000 cm^{-1} M^{-1}) to determine an overlap integral J(λ) of 1.53 × 10^{-11} cm^3 M^{-1} using Equation 2.2. A R_0 of 7.6 nm was estimated using Equation 2.3.

$$E = \frac{R_0^6}{R_0^6 + r^6} \qquad \textbf{(Eq. 2.1)}$$

$$\mathrm{J}(\lambda) = \frac{\int f(\lambda)\varepsilon(\lambda)\lambda^4 d\lambda}{\int f(\lambda) d\lambda} \qquad \textbf{(Eq. 2.2)}$$

$$R_0 = \left(\frac{9000(\ln 10)\kappa_p^2 Q J(\lambda)}{128 N_A (\pi)^5 (n)^4}\right)^{1/6} \qquad \textbf{(Eq. 2.3)}$$

Based on the calculated Förster radius, we estimated that effective energy transfer required donor and accepter separation to be less than 7.6 nm. Thus, we tested spacing distances between the two probes ranging from 5 to 20 nucleotides (1.7-6.8 nm). BRET signal was shown to increase as the spacer length increased from 5 to 15 nucleotides and then decreased as the distance extended to 20 nucleotides (data not shown). Steric effects reduced hybridization efficiency between the two probes and the target when the separation distance of two probes was ≤10 nucleotides. If the spacer length was longer than 15 nucleotides, the BRET signal decreased commensurately with an increase in D-A distance. Therefore, a spacer length of 15 nucleotides was employed in the following studies in order to maximize BRET efficiency without destabilizing the hybridization dynamics.

The BRET signal was calculated as the ratio of normalized emission from Qd625 over the normalized emission from Rluc:

$$BRET\ signal = \frac{I_{Rluc}/I_{Rluc,0}}{I_{Qd625}/I_{Qd625,0}} \qquad \textbf{(Eq. 2.4)}$$

where I_{Rluc} and I_{Qd625} are luminescence intensities from Rluc and Qd625, respectively, when target/sample was present, while $I_{Rluc,0}$ and $I_{Qd625,0}$ are the emissions from Rluc and Qd625 in absence of target.

After spacer selection, the time required for a stable hybridization between labeled probes and target was also studied. As shown in Figure 2.4, maximum BRET signal was obtained after incubating for 5 min, which gave a similar response to 35-min hybridization. Meanwhile, energy transfer occurred even after 1-min incubation. However, the BRET signal for 1-min incubation was lower than the corresponding BRET signals for 5-min and 35-min hybridization due to incomplete hybridization.

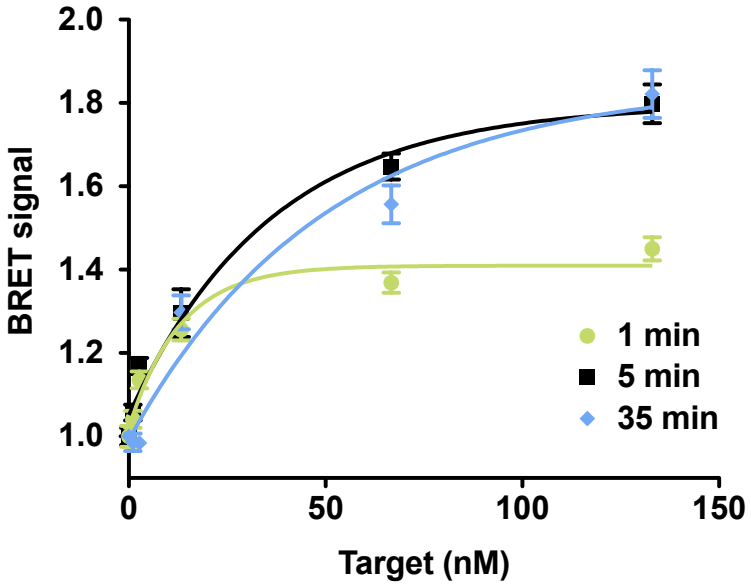

Figure 2.4 Hybridization time optimization. Energy transfer between Rluc and Qd625 could be seen after 1-min incubation (green circle). Maximum BRET signal was obtained after 5-min hybridization (black square), which showed a similar result to 35-min hybridization (blue diamond).

The selectivity of this detection platform was then evaluated using the 5-min incubation timepoint (Figure 2.5), and our sensor demonstrated the capability

of distinguishing mismatched oligonucleotides (SNP and MM-Tar) from perfectly matched target (Tar-3) with high fidelity. Only minimal energy transfer could be seen in SNP and MM-Tar, which resulted from a significantly-reduced energy transfer ratio as labeled probes failed to completely hybridize. The larger standard deviation of mismatched targets also illustrated this hybridization instability.

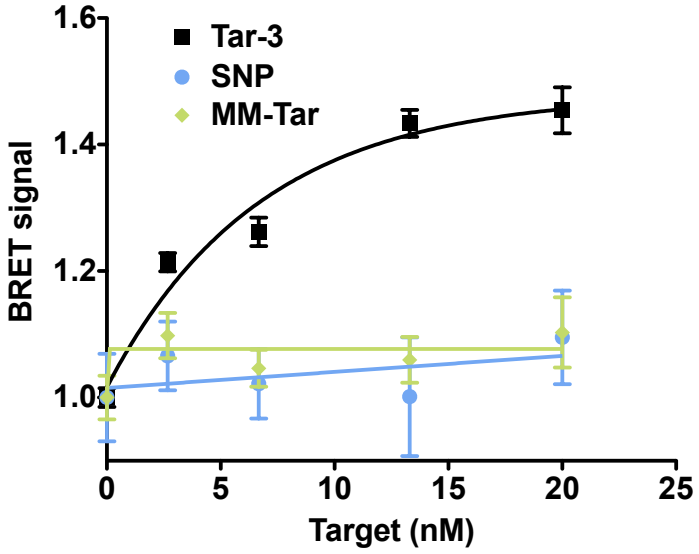

Figure 2.5 Selectivity between perfectly-matched target and mismatched targets. Efficient energy transfer only occurred in the presence of perfectly-matched target (Tar-3, black square). Increasing concentrations of mismatched target produced no substantial increase in BRET signal (SNP (blue circle) and MM-Tar (green diamond)).

As shown in Figure 2.6, a linear calibration curve was generated in a range of 0.5 nM to 26.7 nM (75 fmol to 4 pmol) from three independent assays. The detection limit was calculated as 2.1 nM or 0.32 pmol with blank + 3σ. The

dynamic range of this assay was 0.5 nM to 467 nM (75 fmol to 70 pmol). The linear portion has a limited range because we employed 1.3 pmol of Qd625-DAP-probe and 1.7 pmol of Rluc-probe. Increasing the amount of each probe could compensate for higher target concentrations.

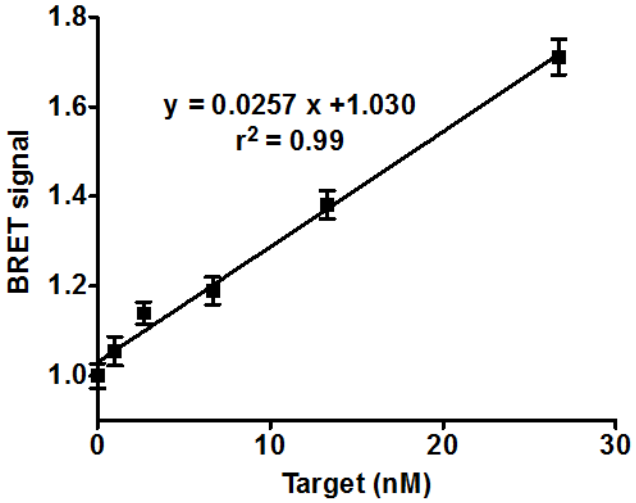

Figure 2.6 Detection of target in DEPC-treated buffer. This detection platform could detect synthesized oligonucleotide with a linear range from 0.5 nM to 26.7 nM. The calibration curve was generated with the data obtained from three independent experiments.

Following synthetic oligonucleotide target detection, we further optimized this system for *E. coli* 16s rRNA detection. The *E. coli* ER2566 cell extract was diluted 100-fold in DEPC-treated buffer in order to prevent RNA degradation. An increasing BRET signal was observed for increasing volumes of *E. coli* cell extract (Figure 2.7).

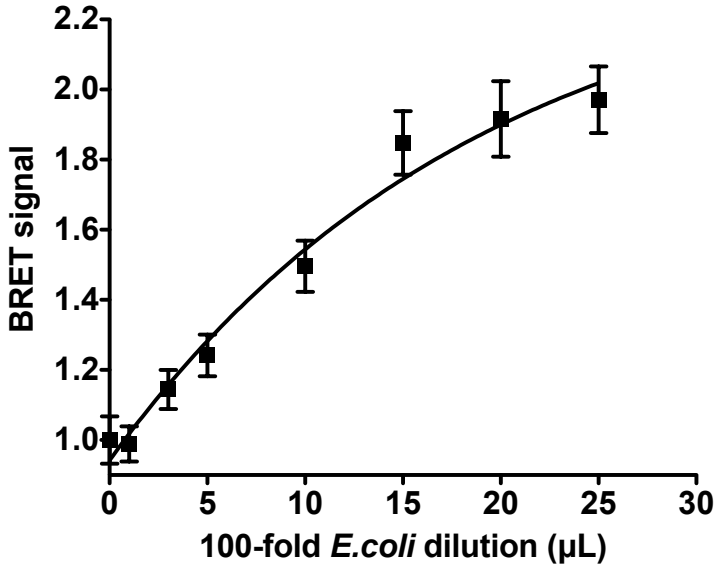

Figure 2.7 Detection of *E. coli* cell extract. The *E. coli* cell extract was diluted 100-fold and detected in DEPC-treated buffer. The BRET signal increased with increasing volumes of *E. coli* extract added.

2.5 Conclusion

We designed an on-type, BRET-based sensing platform which could detect oligonucleotides after a 5-min incubation with a LOD of 2.1 nM. Two probes with sequences complementary to adjacent regions of a target strand were conjugated to either Rluc or Qd625. This format enabled head-to-head proximity of the labels when hybridized to target, allowing energy transfer from Rluc to Qd625. This detection platform demonstrated high selectivity against mismatched targets. It could also successfully detect *E. coli* 16s rRNA. We believe that our method can be applied for target nucleic acid detection in diagnostic, clinical, and environmental applications.

CHAPTER 3: PAPER-BASED VIRAL RNA DETECTION

3.1 Overview of study

Viral detection presents a host of challenges for even the most sensitive analytical techniques, and the complexity of common detection platforms typically preclude portability. With these considerations in mind, we designed a paper-based virus sensing system to detect cDNA reverse-transcribed from total RNA extraction by utilizing a biotinylated capture probe and an Alexa Fluor 647-labeled reporter probe. The biotinylated capture probe was linked to the paper surface via NeutrAvidin® that was physically adsorbed on the paper. After addition of sample and reporter in sequence, the target captured the reporter probe and tethered it to the capture probe using a bridged format. Fluorophore capture was imaged by a Western blot imaging system, and higher target concentration was visible by the increased emission intensity from Alexa Fluor 647. By utilizing paper, this detection setup could also serve as a sample concentration method via evaporation, which could remarkably lower the detection limit. This detection platform was utilized for Epstein-Barr virus (EBV) RNA detection by sensing cDNA resulting from reverse transcription and can be further expanded as a general method for pathogen nucleic acids detection. The assay was accomplished within 2.5 hours including the RNA extraction and reverse transcription steps. Also, this paper-based platform was stored for 3 months without a discernible chance in signal, which is an important criterion for analytical testing tools in resource-poor conditions.

3.2 Background

Rapid virus detection with high sensitivity and selectivity is critical in many fields such as food production, disease diagnosis, and environmental monitoring [1, 2]. As reported by the WHO, infectious disease was the leading cause of death in low-income countries [6]. Also, it was responsible for two-thirds of deaths in children below age 5 worldwide in 2008 [7]. To prevent the transmission of infectious disease, early diagnosis and treatment is very important. However, high-quality diagnosis tests are typically unaffordable or inaccessible to people in underdeveloped countries, and the inexpensive diagnostic methods prevalent in these areas cannot provide enough information [8]. Therefore, a cheap, portable, high-quality virus detection method, which can be used in resource-limited environments, is in high demand.

The targets for virus detection include viral particles, antigens, and nucleic acids. Viral particle detection is based on recognition of antigens on the surface of a virus, and these antigens are detected with enzyme linked immunosorbent assay (ELISA) using labeled antibody [10]. However, the antigen must be at a sufficient concentration above the assay detection limit and, therefore, cannot be used for diagnosis of early-phase pathogenic infectious diseases. Also, being proteins, antigens are more vulnerable to environmental conditions, such as temperature and pH, and have a much shorter shelf-life than nucleic acids. Typically, antigen recognition requires a specific, monoclonal antibody, which is expensive and usually requires storage at -20 °C. Conversely, nucleic acids can serve as targets for early diagnosis due to their stability even in harsh conditions.

They are usually captured and/or detected with antisense nucleic acids, which are inexpensive to synthesize and very stable compared to antibody. Oligonucleotides with different modifications are commercially available, resulting in easy labeling or conjugation of oligonucleotide probes. Furthermore, nucleic acids are amenable to amplification using techniques such as polymerase chain reaction (PCR) [19], rolling circle amplification (RCA) [162], and loop-mediated isothermal amplification (LAMP) [78]. For these reasons, nucleic acids are suitable targets for point-of-care (POC) detection.

Common detection methods for viral nucleic acids include PCR [163-165], electrochemistry [166-168], surface plasmon resonance (SPR) [169], and piezoelectric biosensors (quartz crystal microbalance (QCM) [170], cantilever [171], etc.). These detection methods are very sensitive, but they all have some disadvantages which prevent them from meeting the requirements of POC detection. SPR and piezoelectric biosensors are restricted to laboratory use only due to the requirement of sensitive instrumentation and highly-skilled personnel. Electrochemistry reactions can be performed on portable devices, but these devices have limited sensitivity. PCR reactions can be performed with a portable thermocycler, and the result can be detected without instrumentation but with the possibility of false-positive results. For on-site nucleic acid detection, some reports have included LAMP and monitored the result by turbidity or intercalating dye [74, 79, 172].

As an alternative approach to on-site virus detection, we decided to perform nucleic acid detection on a paper-based setup because of several

advantages of this format. It is inexpensive, easily disposable (biodegradable and flammable), conducive to native biomolecule conformations, and a good sample and reagent carrier. These benefits make paper a suitable material for POC detection in remote environments or in underdeveloped countries. PCR for DNA detection from dried blood spots is a well-developed technique [173, 174]. However, practical paper-based devices did not become viable platforms until an easy fabrication method was published in 2007 [175]. The paper 96-well plate used in our study was termed a “paper microzone plate” by its designer, the Whitesides’ group at Harvard University [176].

In this study, we tested our detection platform by sensing Epstein-Barr virus (EBV), also named human herpesvirus-4 (HHV4). EBV is a double-stranded DNA virus which is transmissible via nasopharyngeal secretions. EBV typically targets B lymphocytes due to strong receptor homology for EBV surface antigens, but other immune cells as well as unrelated cell types can be infected due to the complex surface antigen complement on herpes viruses [177]. Given its tendency to go latent, more than 90% of the world’s population is an EBV carrier. Reported targets for EBV detection include antigen and RNA (Epstein Barr encoded RNAs (EBER)), but RNA presents a more lucrative target given that, on average, there are 10^7 copies of EBER (EBER-1 and EBER-2) present in one latently infected cell [178, 179]. These two RNAs are small, non-coding RNAs which are usually bound to nuclear proteins [180]. We optimized our detection platform with EBV primarily due to the significant expression of EBER RNAs. To date, there has been only one paper-based virus detection method

published. The authors performed reverse transcription (RT)-LAMP prior to target detection using an intercalating dye. In this case, paper was only employed as a carrier for double-stranded DNA, and the assay was incapable of differentiating multiple targets in one assay. Here, we developed a multiplex viral diagnostic assay using DNA hybridization on a paper surface.

As shown in Figure 3.1, a biotinylated-capture probe is immobilized on a paper surface that has been previously coated with physically absorbed NA. The single-stranded cDNA target generated from RT of extracted total RNA was captured on a paper microzone surface by DNA hybridization. The cDNA was detected with an Alexa Fluor 647-labeled reporter probe, and the fluorescent result was imaged with a LI-COR instrument and analyzed with ImageJ.

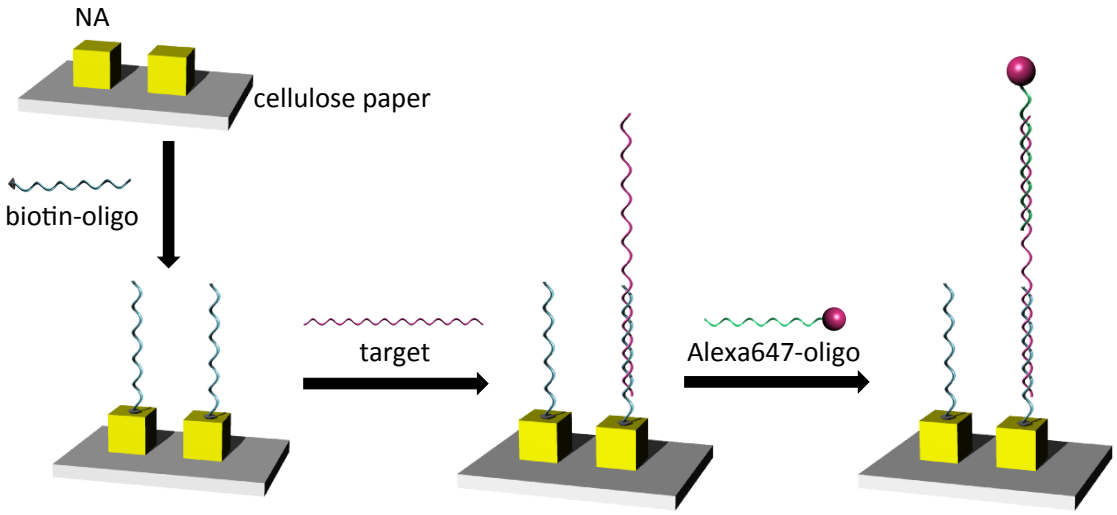

Figure 3.1 Scheme of paper-based virus detection system. NeutrAvidin® (NA) was physically absorbed onto the paper surface for immobilization of the biotinylated capture probe. After sample loading, target was selected by hybridization to the capture probe. Target was detected by its subsequent capture of an Alexa Fluor 647-labeled probe. Increasing concentrations/volumes of target were indicated as higher fluorescence intensity.

3.3 Material and Methods

3.3.1 Materials

The NeutrAvidin® (NA), dNTPs, Alexa Fluor 647-oligo, herring sperm, TRIzol reagent, and RNaseOUT were from Invitrogen (Grand Island, NY). The RPMI media, fetal bovine serum, biotinylated capture probe, and unmodified oligo were purchased from Sigma-Aldrich (St. Louis, MO). StartingBlock blocking buffer was from Pierce (RIckford, IL). The Raji B cell line was purchased from American Type Culture Collection (Manassas, VA). The RNeasy Mini Kit was from Qiagen (Valencia, CA). The M-MLV reverse transcriptase was from Epicentre (Madison, WI). Whatman #1 cellulose paper was purchased from Whatman (Piscataway, NJ).

3.3.2 Cell preparation and RNA extraction

Raji cells were cultured at 37 °C, 5% CO_2 in RPMI media with 10% fetal bovine serum. After centrifugation, total RNA was extracted using an RNeasy Mini Kit based on the Qiagen protocol. Briefly, approximately 1×10^7 cells were lysed in 0.5 mL Buffer RLT. Proteinase K (100 µg/ml) was added prior to a 10-min incubation at 60 °C to reduce RNase activity. Then, a 0.5 mL aliquot of 70% ethanol was added to the mixture. The solution was transferred to the filter column, and RNA was collected by centrifuging for 15 s. The filter was washed with 700 µL of Buffer RW1 and centrifuged for 15 s. Then, a 500 µL aliquot of Buffer RPE was added to the column, and the column was centrifuged for 2 min. The empty column was centrifuged for 1 min before adding 30 µL of 65 °C

RNase-free water. The filter was incubated for an additional 1 min before centrifuging for 1 min. All centrifuge steps were performed at 4 °C and 10,000 × *g*. The concentration of total RNA was checked with a GE NanoVue Plus spectrophotometer (Hollywood, FL).

3.3.3 Single strand cDNA synthesis

Reverse transcription was performed according to Epicentre M-MLV protocol. Briefly, extracted total RNA was mixed with 10 pmol RT primer and RNase-free water to a total volume of 10 µL. After denaturing at 65 °C for 2 min, the mixture was cooled on ice for 1 min. For a 20 µL reaction, 2 µL of 10X buffer, 200 nmol DTT, 10 nmol of each dNTP, 0.5 µL M-MLV reverse transcriptase, 0.5 µL RNAseOUT, and RNAse-free water to volume were added to the mixture. The solution was incubated at room temperature for 10 min, followed by 10 min at 37 °C. The reverse transcriptase was denatured by heating the reaction to 85 °C for 5 min. RNA was hydrolyzed at 70 °C for 10 min with 0.33 M NaOH. Following neutralization with HCl, the single stranded cDNA was ready for detection.

3.3.4 Design and use of paper microzones for synthesized oligo and cDNA detection

96-well paper microzones were fabricated according to previous literature protocols [176, 181]. Briefly, the 96-well pattern was designed with Adobe Illustrator and printed on the filter paper surface using a Xerox ColorQube 8570

solid ink printer (Xerox; Norwalk, CT). The wax was melted using an oven by incubating for 1 min at 110 °C. To assemble the paper capture construct, a 4 µL aliquot of 0.25 mg/mL NA was allowed to adsorb for 30 min in each fabricated reaction zone. After washing once with PBS buffer (10 mM sodium phosphate, 150 mM sodium chloride pH 7.2), a 4 µL aliquot of 4 µM biotinylated capture probe (b-Tar, Table 3.1) was incubated in the well for 15 min. Then, the wells were washed once with PBS and blocked with blocking buffer (StartingBlock blocking buffer with 10 µg/mL herring sperm) for 40 min, followed by drying for 20 min under ambient conditions.

For synthesized oligo detection, the blocked paper wells were washed once with PBS before incubating with target (Tar, 7 nM to 1 mM, Table 3.1) for 30 min. Then the wells were washed once with PBS, and 4 µL reporter probe (Alexa-Tar, Table 3.1) was added to a final concentration of 300 nM. After 30-min incubation, the wells were washed three times with PBST (PBS with 0.05% Tween-20 (v/v)). The procedure for cDNA detection was similar to the synthesized oligo detection, except for the sample capture step. Each tube of neutralized cDNA sample (about 26 µL) was loaded in one well and incubated for 1 h. The capture probe and reporter probe employed for cDNA detection are referred to as b-cDNA and Alexa-cDNA, respectively, as shown in Table 3.1.

The positive control consisted of a biotinylated oligo (b-pos) and Alexa Fluor 647-oligo (Alexa-pos) (100 nM) pair with complementary sequences, as shown in Table 3.1. Thus, positive control wells were left empty during the target incubation step. The fluorescence result was recorded with a LI-COR Odyssey

Fc imaging system from LI-COR Biosciences (Lincoln, Nebraska) using a 30 s exposure at 700 nm. The brightness was calculated with ImageJ software by normalizing the brightness of each well against the positive control well.

Name	**Sequence (5′→3′)**
b-pos	CTTAGCTTCCGAGATCAGACGAGA - biotin
Alexa-pos	Alexa Fluor 647-TCTCGTCTGATCTCGGAAGCTAAG
b-Tar	GCTACAGCCACACACGTCTCCTC - biotin
Tar	GACGTGTGTGGCTGTAGCCACCCGTCCCGGGTACAAGTCCCGGGTGGTGAG
Alexa-Tar	Alexa Fluor 647 - CTCACCACCCGGGACTTGTACCC
Ran-Tar	TTATACAGATGATATTAGATGATCTCAATAGGAGCATCATTACTATATTAA
b-cDNA	GGGTACAAGTCCCGGGTGGTGAG - biotin
Alexa-cDNA	Alexa Fluor 647 - GAGGAGACGTGTGTGGCTGTAGC

Table 3.1 Sequences of all probes and synthesized oligonucleotide targets. The first two oligos were used as the complementary positive control pair. The next three oligonucleotides comprised the set of probes for synthesized target detection. The single and double underlined regions in the Tar sequence are complementary to b-Tar and Alexa-Tar, respectively. The bottom two oligos were used as capture probe and reporter probe for cDNA detection.

3.3.5 Concentrate sample with paper microzone

All the steps were identical to the synthesized oligo sensing assay, except for target loading and incubation. Different volumes (4, 8, 16, 32, 64, 128 µL) of Tar or Ran-Tar (Table 3.1) were loaded and dried under ambient conditions. Then, a 4 µL aliquot of PBS was added to each well and incubated for 30 min, followed by a 30-min hybridization to the Alexa Fluor 647-oligo. The result was

imaged using a LI-COR Odyssey Fc imaging system, and target wells were normalized against the positive control well.

3.4 Results and Discussion

Viruses only replicate inside living cells. Except for the unusual case of prions, the starting material for viral replication is DNA or RNA [182]. Based on the Baltimore classification, viruses fall into seven catagories based upon the starting material: dsDNA, ssDNA, dsRNA, (+)ssRNA, (-)ssRNA, ssRNA-RT, and dsRNA-RT [183]. Because RNA is a common product of all viral replication strategies, we chose the small non-coding RNA EBER-1 as our target. However, a reverse transcription step was performed to generate complementary cDNA as the direct target for detection due to the instability of RNA. Typically, special buffer (DEPC-treated or RNase-free buffer) is employed and careful handling is required in RNA detection methods in order to prevent RNA degradation [184]. Therefore, RNA is not suitable as target for POC detection. Thus, the RT process for cDNA generation was included.

We detected the cDNA target on cellulose paper printed with a 96-well pattern. Compared to prevalent viral nucleic acid detection methods such as PCR, electrochemistry, and SPR, paper-based detection platforms can provide the basis for POC detection in resource-limited settings because paper is inexpensive, lightweight, disposable, and easy to functionalize and modify [185]. Also, filter paper is commonly used to store samples and reagents in a dry form for long periods without refrigeration [17, 18]. Paper-based sensing assays have

garnered much attention since an easy and reliable fabrication method was published in 2007 by the Whitesides' group [175]. Now, the two major paper fabrication methods are photolithography [175] and wax printing [181]. We decided to pursue the wax printing method due to the ease of fabrication with current instrumentation. First, the 96-well pattern was designed using Adobe Illustrator. The pattern was printed with a solid ink printer, which printed wax on the paper surface. Then, the printed paper was heated in order to allow the wax to fill the pores of the paper and form hydrophobic barriers. The resulting paper microzone can be stored in ambient conditions for a substantial period of time.

We targeted cDNA transcribed from EBER-1, which produced a 167 nucleotide product (Figure 3.2). Therefore, a 10-min RT reaction was performed to generate cDNA instead of the typical >1-hour PCR for double-stranded product. Then, the single-stranded cDNA was isolated after hydrolyzing the RNA template with NaOH for 10 min, which is a widely used technique in DNA microarray analysis. In order to detect the neutralized cDNA, two probes were utilized - a capture probe and a reporting probe, both of which contain sequence that was complementary to adjacent regions in the target strand. The cDNA target was initially captured by the biotinylated capture probe, which was tethered to the paper surface via non-covalent binding of its 3′ biotin to physically adsorbed NA. The captured target was detected by hybridization to a reporter probe labeled with Alexa Fluor 647. The fluorescence intensity was imaged using a LI-COR instrument and analyzed with ImageJ software.

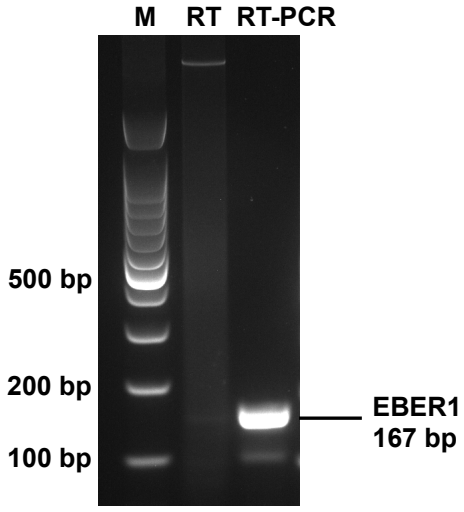

Figure 3.2 RT and RT-PCR product using total RNA extract from Raji B cells as template. As shown in lane 2, the variable length of RT products was the result of truncated product that was incompletely transcribed at the end of the 10 min cycle. In lane 3, the desired 167 bp PCR product is visible.

Before moving to real-sample detection, we characterized the paper-based detection system first by testing synthesized oligonucleotide target (Tar). A 4 μL aliquot of Tar with different concentrations (7 nM to 1 μM) was detected using this platform. As shown in Figure 3.3, a linear calibration curve was obtained in a range of 50 to 500 nM (0.2 to 2 pmol) from three independent assays. The detection limit of 66.4 nM (265 fmol) was calculated by the blank value + 3σ. For normalization, 100% signal was defined as the brightness of Alexa-pos captured by b-pos, while 0% was the background brightness of the negative control (no target addition). All data was analyzed using this same method.

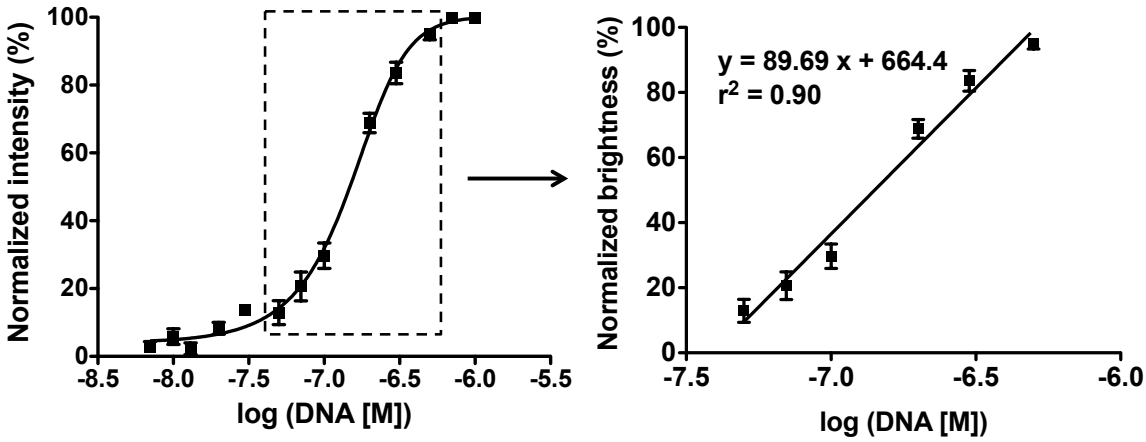

Figure 3.3 Detection of synthesized oligonucleotide target on the paper microzone. Oligonucleotide target was detected within a linear range from 50 to 500 nM. The detection limit was calculated to be 66.4 nM.

Then, we evaluated this method by detecting EBER-1 extracted from Raji B cells. Total RNA was extracted with an RNA isolation kit, the RNA concentration was measured, and three calculated RNA volumes corresponding to different cell counts (2×10^6 to 8×10^6) were added as template for RT. After cDNA synthesis and RNA hydrolysis, each neutralized mixture (about 26 μL) containing single-stranded cDNA was added to one well on the paper microzone and incubated for 1 h. As shown in Figure 3.4, there was a significant increase in fluorescence corresponding to the addition of more RNA template.

Because of the porous structure of the paper, it served as an effective carrier. Thus, we tested the ability of the paper to concentrate samples in order to improve the detection limit. In each well, we loaded different volumes (4, 8, 16, 32, 64, and 128 μL) of Tar and Ran-Tar. The paper microzone was dried

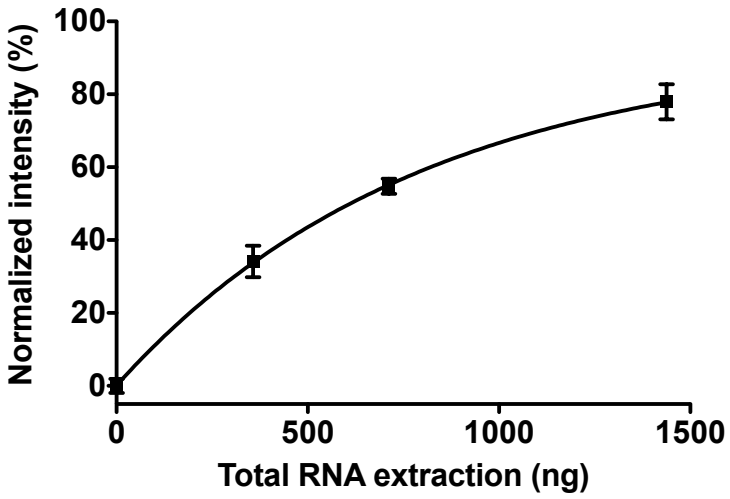

Figure 3.4 Detection of EBER-1 extracted from Raji B cells with different cell counts on the paper microzone. There was a significant increase in fluorescence intensity that corresponded to increasing cell count.

prior to the addition of 4 µL PBS and 30-min hybridization. The captured target was detected with the same method used for the synthesized oligo detection. As shown in Figure 3.5, Ran-Tar could be easily distinguished even in high concentrations. Meanwhile, the detection limit was also enhanced with the addition of the concentration step. Comparing Figure 3.5 to Figure 3.4, the signal generated from similar amounts of concentrated sample was close to or higher than the corresponding signals in the direct target detection. In Figure 3.4, the signals of 0.4 pmol and 2 pmol Tar (0.1 µM and 0.5 µM) were 29.6% and 95.0%, respectively, of the maximum signal, while the intensities of 0.16 pmol and 1.28 pmol Tar (16 µL and 128 µL) in Figure 3.5 were 27.7% and 91.8%, respectively. This indicated that there was almost no loss of DNA target in the concentration process. The higher signal at low DNA amounts may have been due to the

longer total hybridization time (time for sample drying process plus 30-min hybridization).

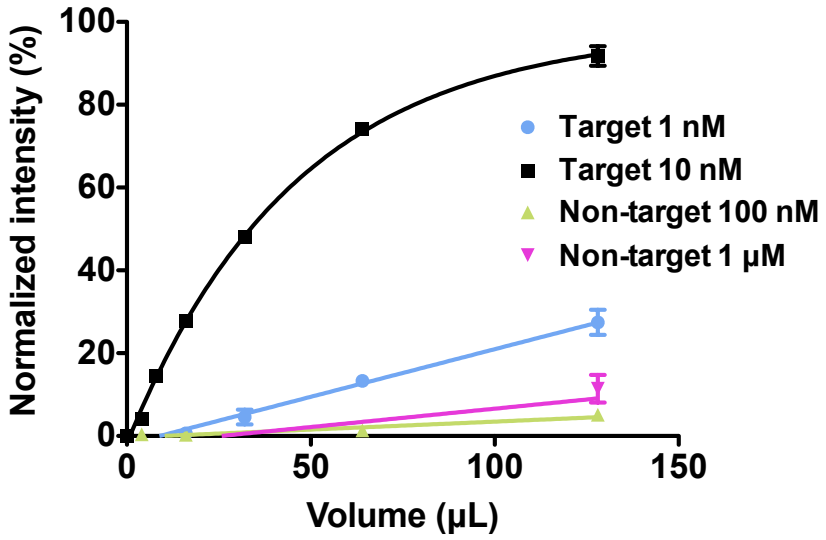

Figure 3.5 Detection of sample concentrated on the paper microzone. Different volumes of target (Tar, circle and square) and non-target (Ran-Tar, triangles) were concentrated on the paper microzone, and the dried sample was detected with Alexa-Tar. Target and non-target could be easily distinguished even with higher concentration and large loading volumes. The process of concentrating the sample also served to improve the detection limit.

We also tested the shelf life of the paper microzone subsequent to capture probe immobilization for periods of up to 3 months. There was no observed signal loss if the paper microzone was stored in dry conditions. Additionally, there was no decrease in the fluorescence intensity if the assay was completed and stored without imaging. Thus, the assay could be performed and then stored for a period of time prior to signal analysis, which would be a potential strategy for detection in resource-poor conditions. As this method was only a proof-of-

concept platform for paper-based virus detection, further changes can be made in order to better suit this method for POC detection. First, the RT process can be performed at room temperature. There were two steps for RT, annealing and elongation, which were performed at room temperature and 37 °C, respectively, as suggested by the protocol. For our demonstration, the elongation step was performed at 37 °C because this was the optimal temperature for M-MLV reverse transcriptase. Although M-MLV has less activity at room temperature, our target was short (167 nt) and would allow room temperature RT if the elongation time was extended. Second, a colorimetric reporter probe (such as gold nanoparticle-functionalized probe) can be employed to eliminate instrumentation completely. Besides virus detection, this method could be utilized as a general DNA or RNA diagnostic platform. It could also serve as an alternative to traditional Northern blot because of the reduction of experimental steps, smaller sample size, shorter incubation time, and inexpensive buffer.

3.5 Conclusion

We developed a paper-based virus detection method which is suitable for resource-poor settings. This method includes two steps, RT and paper-based detection. The isothermal RT process was performed to generate cDNA, which is much more stable than RNA, as the nucleic acid target. Paper-based detection was chosen as a way to increase portability, reduce platform expense, and provide an easy means of disposal. Also, the porous structure of paper increased the effective surface area, which provided a commensurately

decreased detection limit. The paper microzone required less reagent and sample size (4 μL for synthesized oligonucleotide detection), which reduced the cost of each test. Meanwhile, the paper substrate was shown to provide a means to concentrate the samples in order to further decrease the detection limit. This testing platform could be stored at room temperature for at least 3 months prior to use, and the result of a completed assay can be imaged after 3 months. We believe that this paper-based detection method is suitable for diagnostic use in resource-limited environments. In addition, it has the potential to be employed as a general assay for DNA or RNA detection.

CHAPTER 4: RAPID, INEXPENSIVE, MULTIPLEXED DNA DETECTION USING NOVEL ZINC FINGER PROTEIN TAGS AND A PAPER-BASED MICROFLUIDIC DEVICE

4.1 Overview of Study

Multiplexed, DNA-based diagnostics for resource-poor settings are urgently needed for accurate pathogen detection at the point-of-care (POC). Yet, current limitations of the available DNA detection methodologies significantly limit the development of economical diagnostic devices. Here, we describe a novel zinc finger protein (ZFP)-based method for direct multiplex detection of double-stranded DNA using a paper-based microfluidics device. We encoded unique ZFP DNA recognition sequences (termed “ztags”) in the DNA amplification primers themselves, thereby tagging each product DNA for recognition by a specific, pre-designed ZFP. Given the unlimited number of unique ZFP recognition sequences that can be placed as tags in different amplification primers, our design allows for detection of many DNA biomarkers by using multiple ztagged DNA products along with their respective capture ZFPs. We applied our methodology to detect two different tuberculosis (TB) biomarkers using immobilized ZFPs and showed specific and selective detection in uniplex and multiplex assays. We also developed a paper-based microfluidic device platform and applied our novel DNA detection methodology to it. Here, in a proof-of-concept experiment, we show that this paper-based microfluidic device can accurately detect two different TB genes and provides simple, visible readout of the assay. Our results suggest that primer-encoded ZFP tags, in combination

with the corresponding ZFPs, can be used to easily detect multiple DNA targets in a single assay and can be utilized with simple, paper-based microfluidic devices for accurate and rapid pathogen detection. This novel methodology has the potential to be developed into a simple method for DNA diagnostics at the POC in resource-poor settings.

4.2 Background

Early and accurate diagnosis of disease-causing agents in resource-poor settings is critical for effective treatment of patients and for disease containment. Yet, cost-effective methods and technologies for identifying infected patients are sorely lacking. For example, tuberculosis (TB) is a leading cause of death worldwide due to infections and is especially prevalent in the developing world [186, 187], but the pathway for accurate diagnosis requires an assessment of clinical symptoms, chest radiography, and microscopy of sputum specimens, followed by isolation and culture of *Mycobacterium tuberculosis* (*M. Tb*), the gold standard for positive identification of TB and its strain [188, 189]. However, culture of the pathogenic bacteria takes weeks due to the slow growth rate of TB in culture. While newer, faster molecular diagnostics based upon nucleic acid amplification are available in the western countries for the identification and typing of TB, diagnostic assays in resource-poor settings still rely on older methods due to the high costs of molecular diagnostic tests and their need for sophisticated equipment [190-193]. Thus, there is an urgent need for rapid and specific diagnostic assays for such pathogens [194]. Furthermore, having such

diagnostic tests available at point-of-care (POC) clinical settings is also critical for the effective treatment of patients, as many do not return for a follow-up visit. This necessitates a major re-think of the currently available nucleic acid amplification-based diagnostic assays that are commonly used in the more affluent countries. Some tests that are available for use and are potentially applicable in a low-resource setting rely on amplification and detection of a single target per test [78, 195, 196], thus requiring multiple assays for the detection of multiple nucleic acid biomarkers of infectious agents in each sample. In terms of technical challenges, while many methods have been developed to easily and cost-effectively amplify different DNA/RNA sequences in a single test tube [195], detection of amplified DNA products in a single assay at the POC in a resource-poor setting still remains a big challenge [197, 198], as most methods for detecting multiple amplified targets in a single assay require expensive or complex technological solutions that are beyond the on-site capabilities in resource-poor communities [199]. One key challenge with detection of multiple different amplified DNA sequences is the issue of DNA denaturation and subsequent hybridization to specific detection probes, which requires at least a few separate steps [63, 200]. A second challenge is the implementation of reliable multiplexed DNA detection assay onto a low-cost, instrument-free, POC device. While paper-based microfluidic devices [181, 201-203] are ideally suited for this, and paper-based devices have been reported as platforms for DNA amplification [204, 205], no such devices have yet been described in literature for multiplexed DNA diagnostics, perhaps owing to the difficulties associated with

implementing the commonly-used methods for DNA detection onto the paper-based microfluidics platform. One recent report describes utilization of a paper-based lateral-flow strip for detecting PCR products, which required a separation step after PCR for single DNA species generation [206].

Zinc finger proteins (ZFPs) are common DNA-binding proteins present in the human genome and form a large subset of all transcription factors encoded by the genome. We utilized two C2H2 ZFPs, which contain multiple Cys2-His2 class zinc finger domains that recognize a specific sequence of dsDNA [207-209]. Each zinc finger domain consists of a linear chain of approximately 30 amino acids that folds into a compact “finger-like” structure with two antiparallel β-sheets and one α-helix. The α-helix contains two key histidine residues that, together with two cysteine residues from the hairpin region of the antiparallel β-sheets, form a tetrahedral coordinate bond structure around a single zinc ion [210]. Specific residues in the α-helix of a typical zinc finger domain recognize a 3 DNA base pair (bp) sequence and do so in a highly selective manner. Using insights gained from structural studies and structure-function relationship studies, substitution of different residues in the α-helix has been used to engineer zinc finger domains that can target almost any three to four bp DNA sequence [211]. A typical ZFP contains a tandem array of three zinc finger domains, which facilitates recognition of an approximately nine bp linear DNA sequence. Thus, a variety of rational design methodologies with interchangeable zinc finger domains in a tandem array have been used to generate ZFPs against almost any DNA sequence of 9-18 bp in length [207, 212, 213], and computational algorithms for

designing ZFPs against almost any 9-12 bp DNA sequence are widely available. ZFPs containing three zinc finger domains have been the most commonly engineered proteins because, in general, they are easier to design and produce as compared to larger ZFPs and bind with high specificity to their target binding sites on DNA [213]. Recently-described transcription activator-like effector (TALE) proteins would also be useful for this purpose [214]. Engineered ZFPs have been developed and tested as synthetic transcription factors as well as novel enzymes such as targeted endonucleases and integrases [207, 211-213].

Given their ability to sequence-selectively bind dsDNA, ZFPs have been proposed for use in diagnostics ever since their discovery and structural elucidation in the 1990s. The ZFPs Sp1, Sp2 and Zif268 have been used to detect their respective endogenous recognition sequences that are naturally present in genomic DNA from different bacteria [68, 215-217]. Similarly, sequence-enabled reassembly (SEER) of two different ZFPs linked to split-proteins has been developed to detect long stretches of endogenous DNA sequences that correspond to the natural recognition sites for a pair of ZFPs [218, 219]. Furthermore, hydrogel immobilization of one of the two ZFPs from the SEER pair drove the dsDNA-dependent ZFP-based reassembly of β-lactamase in a recent study. This allowed for rapid, multiplexed detection of dsDNA on an array [70], proving that ZFPs can be used to create inexpensive diagnostic devices for use in the POC setting. However, a critical drawback of the current ZFP-based diagnostic assays is their reliance on the detection of pre-existing ZFP recognition sequences in their target DNA, which greatly limits the

dsDNA biomarkers that can be detected due to the challenge of designing multiple unique ZFPs against related sequences. Although engineered, novel ZFPs that can be directed against almost any target DNA sequence would provide an alternative method, it has been difficult to transition from theory to practice.

Here, we present a solution for the direct detection of multiple dsDNA sequences in a single assay that circumvents the need for denaturation and hybridization steps by using ZFPs as dsDNA detection agents in a novel fashion. In our assay, ZFP DNA recognition sequences are incorporated as tags in the primers used to amplify target biomarkers (Figure 4.1). Subsequently, we use the incorporated ZFP binding sequence (which we refer to as “ztag”) to detect the amplified target DNA using its corresponding ZFP as a detection agent. Because almost any ZFP recognition site can be incorporated in amplification primers, our design circumvents previous limitations of ZFPs and allows for multiplexed detection of DNA biomarkers by using multiple, independent amplification primer pairs for different DNA targets that are selectively assayed using their respective capture ZFPs. Additionally, we incorporated biotin tags in the amplified DNA for ease of detection with a variety of commonly available, avidin-based detection agents. As with the previous ZFP-based DNA detection methods, our approach does not require any denaturation or additional processing steps for the multiplexed detection of target dsDNA. We present results from the testing of our approach using TB genomic DNA as a model system. Additionally, we show implementation of our novel, multiplexed DNA detection assay on a paper-based

microfluidics device to overcome some of the existing difficulties in creating an appropriate device for use at the POC in a resource-poor setting. Our newly developed assay methodology and its incorporation into a paper-based microfluidics device provides a novel approach for designing economical devices for pathogen detection in a resource-poor setting.

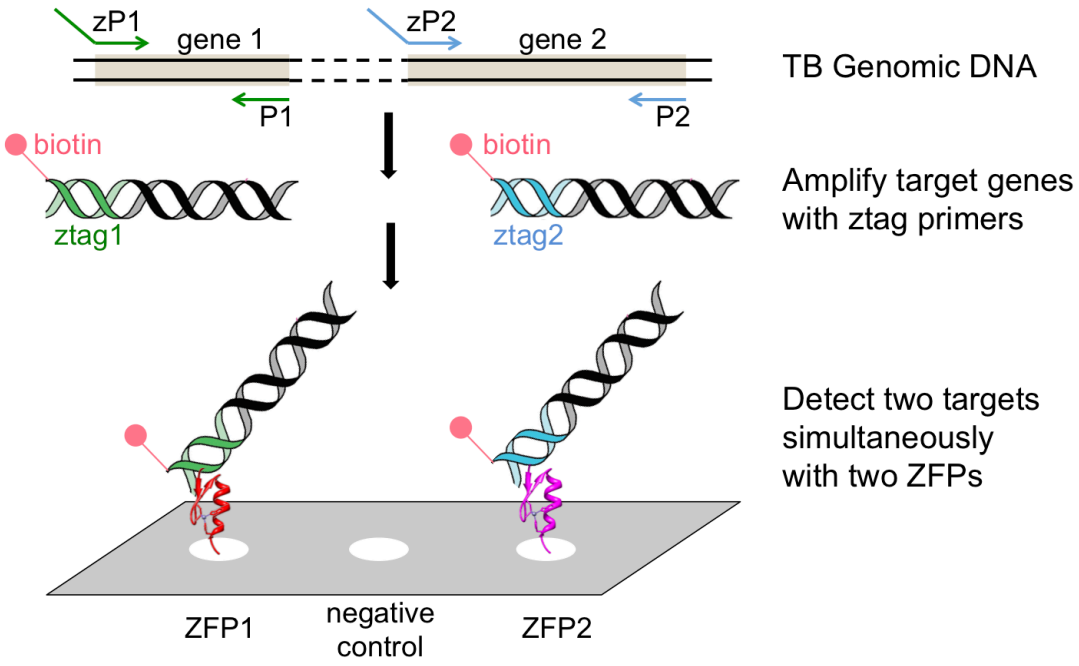

Figure 4.1 Schematic representation of the primer-encoded ZFP tag (ztag) methodology for the multiplex detection of DNA sequences using ZFPs. The ZFP recognition sequences are encoded in DNA amplification primers so that predesigned ZFP binding sites are added to each amplified DNA product. A biotin moiety is also incorporated into the DNA products during the amplification step for ease of detection. Multiple amplified DNA products are selectively captured on a detection device using site-selectively immobilized ZFPs that correspond to each of the encoded ztags and are detected via the biotin moiety. The ZFP structure was obtained from RCSB protein data bank (1A1L).

4.3 Materials and Methods

4.3.1 Materials

Primers for polymerase chain reaction (PCR), the 0.01% poly-L-lysine solution, nitrocellulose membranes, sodium periodate, chitosan (low molecular weight), and sodium cyanoborohydride were purchased from Sigma-Aldrich (St. Louis, MO). The Choice Taq DNA polymerase was purchased from Denville (Metuchen, NJ). The Ni^{2+}-NTA agarose beads and QIAprep Miniprep plasmid DNA purification kits were purchased from Qiagen (Valencia, CA). Amylose resin and anti-maltose binding protein (MBP) antibody were obtained from New England BioLabs (Ipswich, MA). The *M. Tb* genomic DNA (H37Ra, catalog # 25177) and human K562 erythroleukemic cell line were purchased from American Type Culture Collection (Manassas, VA). The 96-well microtiter plates were obtained from Corning (Corning, NY). The anti-His antibody, *E.coli* BL21 cells, herring sperm, and NeutrAvidin®-horseradish peroxidase conjugate (NA-HRP) were purchased from Invitrogen (Grand Island, NY). Glutaraldehyde solution (20%) was obtained from Electron Microscopy Science (Hatfield, PA), the streptavidin-horseradish peroxidase (SA-HRP) and SDS-PAGE were from Bio-Rad (Hercules, CA), the 3,3,5,5-tetramethylbenzidine (TMB) substrate was from Vector Laboratories (Burlingame, CA) and the SuperSignal West Pico Chemiluminescent Substrate was from Pierce (Rockford, IL). The Bio-Dot microfiltration apparatus and StartingBlock Blocking buffers were purchased from Thermo Fisher Scientific (Waltham, MA). Whatman #1 cellulose paper was from Whatman (Piscataway, NJ). Pooled human genomic DNA was purchased from

Promega (Madison, WI). The anti-MBP polyclonal antibody was from Rockland (Gilbertsville, PA).

4.3.2 Expression and purification of ZFPs

The construct (residues 331-430) of human EGR1, corresponding to three tandem copies of C_2H_2-type zinc fingers, was cloned into an Invitrogen TOPO® pET102 bacterial expression vector that included an N-terminal thioredoxin (Trx)-tag and a C-terminal polyhistidine-tag. Notably, Trx-tag was included to maximize protein expression in soluble fraction, while the His-tag was added to aid in protein purification through Ni^{2+}-NTA affinity chromatography. The bacterial expression plasmid pMAL-c2X containing the ZFP rrsA1175 has been previously described [70]. ZFPs were expressed by transforming *E. coli* BL21 cells with each of the plasmids according to manufacturer's protocol. BL21 cells were cultured in LB media containing ampicillin (100 μg/mL) at 37 °C until the cell density reached an OD_{600} of 0.6-0.8. Expression of EGR1 was induced in the cells by cooling the cells in culture to 15 °C, then adding isopropyl-1-thio-β-D-galactopyranoside (IPTG, 0.5 mM) and culturing the cell at 15 °C overnight. Expression of rrsA1175 was induced in the cells by cooling the cells in culture to 15 °C, then adding IPTG (0.3 mM) and culturing the cell at 15 °C overnight. Reduced expression temperatures were employed to reduce basal protein levels and retain solubility for the induced protein fraction. The cells were pelleted at 7000 × *g* for 20 min and resuspended in lysis buffer. The EGR1 lysis buffer consisted of 100 mM Tris base, 150 mM NaCl, 10 mM imidazole, 90 μM $ZnSO_4$,

0.05% (v/v) Tween-20, 2 mM β-mercaptoethanol pH 8.0, while the rrsA1175 lysis buffer included 50 mM Tris base, 200 mM NaCl, 90 μM $ZnSO_4$, 0.05% Tween-20 (v/v), and 10 mM β-mercaptoethanol pH 7.5. The cell lysate was sonicated, and the crude protein was isolated by centrifugation for 10 min at 18000 × *g*. EGR1 protein (His-tagged) was purified using a Ni^{2+}-NTA column according to manufacturer's directions. Briefly, Ni^{2+}-NTA agarose beads were loaded on a column and pre-equilibrated with EGR1 lysis buffer. The crude protein lysate from EGR1 culture was loaded onto the column, and the bound protein was washed using imidazole wash buffer (30 mM imidazole in 100 mM Tris base, 150 mM NaCl, 90 μM $ZnSO_4$, 0.05% Tween-20 (v/v), 2 mM β-mercaptoethanol pH 8.0). EGR1 was eluted using imidazole elution buffer (200 mM imidazole in 100 mM Tris base, 150 mM NaCl, 90 μM $ZnSO_4$, 0.05% Tween-20 (v/v), 2 mM β-mercaptoethanol pH 8.0) and pooled. Amylose was used to purify rrsA1175. The amylose column was pre-equilibrated with rrsA1175 lysis buffer, and the crude protein lysate was loaded onto the column. The resin-bound protein was washed using rrsA1175 lysis buffer, and was eluted from the column using the maltose elution buffer (10 mM maltose in 50 mM Tris base, 200 mM NaCl, 90 μM $ZnSO_4$, 0.05% Tween-20 (v/v), 10 mM β-mercaptoethanol pH 7.5). Purified protein was dialyzed in PBST/Zn^{2+} buffer (100 mM phosphate, 150 mM NaCl, 0.05% Tween-20 (v/v), 90 μM $ZnSO_4$ pH 7.4) and stored at 4 °C. Purity of the recombinant ZFP protein was confirmed using SDS-PAGE (Figure 4.2).

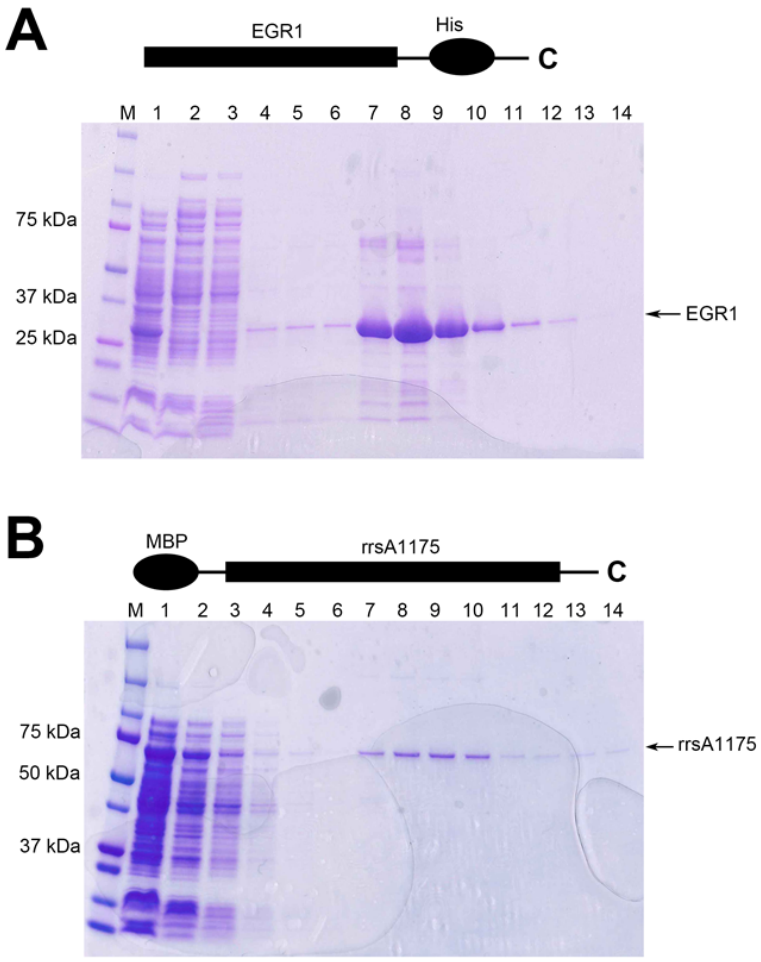

Figure 4.2 Cloning and expression of the recombinant ZFPs. **A)** Coomassie-stained SDS-PAGE (4%-12% gradient) gel showing purification of His-tagged EGR1 from bacterial lysates using Ni^{2+}-NTA column. A cartoon diagram depicting the construct used for the expression of the recombinant EGR1 in *E. coli* is shown above the gel. Lane M, molecular weight standards; lane 1, crude bacterial lysate; lane 2, flow-through fraction from a Ni^{2+}-NTA column after loading the EGR1-containing crude bacterial lysate on the column; lanes 3-6, wash fraction from the column, lanes 7-14, various elution fractions from the column upon treatment with imidazole-containing elution buffer. Arrow points to the correct size of the purified protein. **B)** Coomassie-stained SDS-PAGE (4%-12% gradient) gel showing purification of MBP-tagged rrsA1175 from bacterial lysates using amylose-resin column. A cartoon diagram depicting the construct used for the expression of the recombinant rrsA1175 in *E. coli* is shown above the gel. Lane M, molecular weight standards; lane 1, crude bacterial lysate; lane 2, flow-through fraction from the amylose resin column after loading the rrsA1175-containing crude bacterial lysate on the column; lanes 3-6, wash fraction from the column, lanes 7-14, various elution fractions from the column upon treatment with maltose-containing elution buffer. Arrow points to the correct size of the purified protein.

4.3.3 Tissue Culture

K562 cells were maintained at 37 °C and 5% CO_2 in Iscove's Modified Dulbecco's Medium (IMDM) supplemented with 10% FBS according to the provider's protocol (ATCC, Manassas, VA). Cells from confluent cultures were used for the isolation of human genomic DNA.

4.3.4 PCR amplification for the incorporation of ztags in the PCR products

The sequences of PCR primers used in this study are listed in Table 4.1. All PCR amplification reactions were performed using an Eppendorf Mastercycler gradient thermocycler (Hauppauge, NY) and the concentration of purified DNA products was determined using a GE Nanovue Plus spectrophotometer (Hollywood, FL). PCR amplifications were performed in a total volume of 50 µL containing 4 ng of *M. Tb* genomic DNA, 0.5 µM primers (each), 1.5 mM Mg^{2+}, 50 µM dNTPs (each), and 0.5 µL Choice Taq DNA polymerase. The reaction conditions for PCR with non-biotinylated primers were: initial denaturation at 95 °C for 2 min, followed by 30 reaction cycles (95 °C for 30 s, 56 °C for 30 s, and 72 °C for 1 min), followed by incubation at 72 °C for 10 minutes. The reaction conditions for PCR with biotinylated forward primers containing ztag sequences were: initial denaturation at 95 °C for 2 min, followed by 40 reaction cycles (95 °C for 5 min, 70 °C for 90 s, and 72 °C for 1 min), followed by incubation at 72 °C for 10 minutes. The same protocol was used in PCR reactions using human K562 cell genomic DNA as template. PCR products were analyzed using agarose gel electrophoresis (2%). The PCR products were purified and concentrated using a

standard QIAprep spin Miniprep plasmid DNA purification kit (Qiagen). DNA concentration of the PCR products was determined using a Nanovue Plus spectrophotometer by absorbance measurements at 260 nm and 280 nm. For using the amplified product in the paper-based microfluidic device, the PCR reactions were performed in a total volume of 50 µL containing 4 ng of pooled human genomic DNA and 400 pg of *M. Tb* genomic DNA, 0.4 µM primers (each) against human 18S rRNA gene, 0.8 µM primers (each) against each of the TB genes, 1.5 mM Mg^{2+}, 125 µM dNTPs (each), and 1 µL Choice Taq DNA

Name	**Description**	**Forward primer sequence (5'-3')**	**Reverse primer sequence (5'-3')**
inhA	Drug resistance region. Expected PCR product size = 203 bp.	TGC TGA GTC ACA CCG	CGT AAC CAG GAC TGA AC
katG	TB principal genotypic region. Expected PCR product size = 300 bp.	GTT GCG AGA TAC CTT	TGC GAA TGA CCT TG
EGR1-inhA	inhA primer encoded with EGR1 tag. Expected PCR product size = 211 bp.	TTT **GCG TGG GCG** TCT TGC TGA GTC ACA CCG	TCC GGT AAC CAG GAC TGA ACG GGA TAC GAA TGG G
EGR1-katG	inhA primer encoded with EGR1 tag. Expected PCR product size = 297 bp.	TTT **GCG TGG GCG** TCT AGG GTT GCG AGA TAC CTT	AGG GTG CGA ATG ACC TTG CGC AGA TCC C
rrsA1175-inhA	inhA primer encoded with EGR1 tag. Expected PCR product size = 218 bp.	TCT **GAG GAA GGT** TCT CGA AGT GTG CTG AGT CAC ACC GAC A	TCC GGT AAC CAG GAC TGA ACG GGA TAC GAA TGG G
rrsA1175-katG	inhA primer encoded with EGR1 tag. Expected PCR product size = 315 bp.	TCT **GAG GAA GGT** TCT TCC CGT TGC GAG ATA CCT TGG G	AGG GTG CGA ATG ACC TTG CGC AGA TCC C
H-RNA	Primers specific for human 18s rRNA. Expected PCR product size = 315 bp	GTA ACC CGT TGA ACC CCA TT	CCA TCC AAT CGG TAG TAG CG

Table 4.1 DNA sequences of the primers used in this study. Standard forward and reverse primers for the amplification of regions of TB genes inhA and katG were from literature [220]. The ztags for ZFPs EGR1 or rrsA1175 were included only in the forward primers, which were also biotinylated at the 5'-end. DNA sequences of primers containing the encoded ZFP tags are shown with the ztag sequence in bold and the sequence from the standard primer underlined.

polymerase. The reaction conditions for PCR were: initial denaturation at 95 °C for 2 min, followed by 40 reaction cycles (95 °C for 5 min, 70 °C for 90 s, and 72 °C for 1 min), followed by incubation at 72 °C for 10 minutes. Prior to their use in the paper-based microfluidic device, 0.1 μL Zn^{2+} solution (50 mM) and 2.5 μL of channel-blocking buffer (StartingBlock Blocking buffers containing 10 μg/mL herring sperm) were added to each 50 μL PCR product.

4.3.5 Detection of ZFP-tagged PCR products

First, DNA detection limits in the SA-HRP based colorimetric assay were tested in absence of ZFPs. A 50 μL aliquot of 0.01% poly-L-lysine was coated to each well of a 96-well microtiter plate at 4 °C overnight. After washing, various amounts of biotinylated DNA alone (0.01 pmol to 4 pmol) was added and reacted for 2 h. After incubating with glutaraldehyde (1.25%, 50 μL) for 1 h, the wells were blocked with plate-blocking buffer (0.125 M glycine, 1% milk (w/v) in PBST/Zn^{2+}) for 1 h. Then 50 μL of SA-HRP (1:5000) in PBST/Zn^{2+} was added and incubated for 2 h at room temperature. After washing the plate with PBST/Zn^{2+}, TMB substrate was added according to manufacturer's protocol. The reaction was stopped with addition of a 50 μL aliquot of 1 M H_2SO_4 following a 10-min incubation. To quantify the amount of bound DNA, absorbance of the TMB product was read at 450 nm using a Spectramax M5 spectrophotometer (Molecular Devices, Sunnyvale, CA). Each concentration point was performed in triplicate.

Detection for PCR products with a specific ztag was performed as follows. Wells of 96-well microtiter plates were coated with poly-L-lysine (0.01%, 50 µL) at 30 °C for 2 h. Coating solution was removed and the wells were washed 1X with PBS (100 mM phosphate, 150 mM NaCl pH 7.4). The wells were then coated with anti-His or anti-MBP antibodies (1 µg/mL) in PBS (50 µL) at 4°C overnight. The unbound antibody was washed 1X with PBST/Zn^{2+} buffer and the wells were blocked using plate-blocking buffer for 1 h at room temperature. The wells were then washed 1X with PBST/Zn^{2+} and subsequently used in DNA binding studies. For binding studies, the ztag-containing PCR product was mixed with the appropriate ZFP in PBSTM (0.1% milk (w/v) in PBST/Zn^{2+}, 50 µL), and this mixture was added to the antibody-coated wells and incubated for 2 h at room temperature. The unbound DNA-ZFP complex was washed with PBST/Zn^{2+} and the remaining DNA-ZFP complex was cross-linked to the bound antibody with glutaraldehyde (1.25% in PBS, 100 µL) for 30 min at room temperature, followed by blocking with plate-blocking buffer (150 µL) for 1 h at room temperature. To quantify the amount of bound biotinylated DNA, the wells were incubated with SA-HRP (1:5000, 80 µL) in PBSTM for 90 min at room temperature, followed by washing 3X with PBST/Zn^{2+} to remove the unbound SA-HRP. Colorimetric detection of bound DNA was performed using the TMB substrate kit according to manufacturer's protocol. The reaction was stopped with addition of a 50 µL aliquot of 1 M H_2SO_4 after 10-min incubation. Absorbance of the TMB product was read at 450 nm using a Spectramax M5 spectrophotometer (Molecular

Devices, Sunnyvale, CA). Each concentration point was performed in triplicate, and the data shown is from one of at least three independent experiments.

4.3.6 Multiple-target DNA detection on ZFP-coated nitrocellulose membrane

Nitrocellulose membranes were coated with varying amounts of each protein using a Bio-Dot microfiltration apparatus under vacuum following the manufacturer's instructions. The membrane was placed in the microfiltration apparatus chamber, and the protein dilution series with either EGR1 (150, 300, 500, 1000 pmol/well) or rrsA1175 (5, 10, 12.5, 15 pmol/well) was loaded into different wells of the chamber. Application of vacuum applied the protein onto a defined area on the membrane by moving the protein solution through the chamber. Subsequently, the membrane was removed and dried for 30 min at room temperature. Next, the protein-coated membranes were washed twice with PBST/Zn^{2+} buffer, followed by blocking with 5% milk in PBST/Zn^{2+} for 1 h at room temperature.

For the multiplex detection of two amplified *M. Tb* genes in a single assay, the amplified PCR products containing the ztags EGR1-inhA (300 pmol) and rrsA1175-inhA (80 pmol) were applied to the ZFP-coated membranes in PBSTM (5 mL) for 2 h at room temperature. The membranes were subsequently washed with PBST/Zn^{2+} and treated with SA-HRP (1:10000 dilution in PBSTM) for 1 h at room temperature for the detection of ztagged DNA product bound to the immobilized ZFPs. After washing 1X with PBST/Zn^{2+}, the DNA was detected with an X-ray film using SuperSignal West Pico chemiluminescent substrate after

a 30 sec exposure. The spot intensity was quantified using NIH ImageJ [221]. Data presented is representative of at least three independent experiments.

4.3.7 Design and use of paper-based microfluidic devices for multiplexed DNA detection

The devices were fabricated according to literature protocols [181, 222]. Briefly, Whatman #1 cellulose paper was used for creating the device. The pattern for the device was designed using Rhinoceros software (Robert McNeel & Associates, Seattle, WA). The channel design for each layer of the device was printed on the cellulose paper with solid wax using a Xerox ColorQube 8570 solid ink printer. To create a hydrophobic barrier for the channels, the wax printed on the cellulose paper surface was rapidly melted by baking the sheet of paper for 1 min in a 110 °C oven. Subsequently, the circular detection area on the detection layer of the cellulose paper was prepared by oxidizing the cellulose surface according to published protocol [223] and adsorbing the antibody and proteins to it. Briefly, an aliquot of 6.5 µL $NaIO_4$ (0.5 M in Milli-Q H_2O) was applied onto the circular wells. After 30-min incubation in the dark, the oxidant was washed off with 24 µL Milli-Q H_2O, and antibodies (20 µg/mL anti-His for the left well and 10 µg/mL polyclonal anti-MBP for the middle and right wells) were linked to the oxidized surface for 30 min. The Schiff base was reduced with 24 µL $NaCNBH_3$ (25.5 mM in Milli-Q H_2O, Sigma-Aldrich) for 30 min. The reaction was stopped with 24 µL Tris-HCl (1 M, pH 5.0) and blocked using channel-blocking buffer (StartingBlock blocking buffer containing 10 µg/mL herring sperm). Test

validation wells (ellipse wells) were coated with chitosan as follows. An aliquot of 40 µL chitosan (1 mg/mL) was applied to the ellipse wells for 1 hour. Unbound chitosan was removed and the wells were washed using 40 µL Milli-Q water. Subsequently, all the channels and wells were blocked with channel-blocking buffer. To load ZFPs in the circular detection zones, recombinant, purified ZFPs (EGR1 and rrsA1175, 300 pmol each) were applied in the appropriate paper layer and respective antibody-coated circular wells (EGR1 in the left well and rrsA1175 in the right well, Figure 4.10B). The paper layer was incubated at room temperature for 30 min, and any unbound ZFP was removed by washing with PBST/Zn^{2+} buffer.

For the multiplex detection of two amplified *M. Tb* genes in the presence of human DNA, the device containing the amplified PCR products incorporating the ztags EGR1-inhA and rrsA1175-inhA was assembled using paper clips according to Figure 4.7B. The device was pre-equilibrated with PBST/Zn^{2+} buffer by dipping the device into an Eppendorf tube containing the buffer. For the multiplex assay, a device with only the top two layers was dipped into an Eppendorf tube containing 100 µL of amplified DNA solution for approximately 1 h at room temperature. Next, the third paper layer was added onto the device, and the device was dipped into a new Eppendorf tube containing 80 µL of NA-HRP (1 µg/mL) for 20 min. Subsequently, the device was dipped into Eppendorf tubes containing the wash buffer (PBST/Zn^{2+}). The device was then treated with TMB solution to develop colored zones for detection. After approximately 5 min, the device was disassembled, and the layers were images using the camera of a

mobile phone. Data presented is representative of two to three independent experiments.

4.4 Results and discussion

4.4.1 Assay design using zinc finger protein binding sites as tags

ZFPs recognize double-stranded DNA (dsDNA) in a sequence-specific fashion and are easily designed against almost any 9-12 bp DNA sequence [207]. Here, we propose using ZFP-binding sequences as tags that are directly incorporated into a target dsDNA during amplification. In our design, a unique ZFP binding site (referred to as “ztag”) is incorporated close to the 5′-end of amplification primers for each target DNA sequence in order to introduce this sequence into the PCR product during amplification (Figure 4.1). The unique ztags introduced during amplification are then used to identify a target DNA sequence using a corresponding immobilized ZFP as a capture reagent. Our design overcomes a key limitation of the current ZFP-based methods that detect only pre-existing ZFP recognition sequences in the target genomes [68, 69, 215-217]. It also allows for using multiple, independent ZFP-primer pairs for sequence-specific DNA detection using multiple cognate ZFPs that selectively bind to each of their respective ztags. Additionally, our design uses biotin-tags that are incorporated via biotinylated nucleotides in the amplified DNA in order to easily detect the amplified product using a variety of commonly available, streptavidin-based detection agents.

To demonstrate feasibility of our approach, we chose the *M. Tb* genome as a model system. We targeted two known TB genes as biomarkers in our experiments – a genotype marker (inhA-15, referred to as "inhA" here) and a drug resistance marker (katG463, referred to as "katG" here) [220]. We employed standard PCR amplification to amplify these genes in our experiments, which are mainly designed to validate the concept of ztagged primers and ZFP-based capture agents as a potential diagnostic. However, the method is applicable to DNA amplified using any protocol, including isothermal amplification methods [78, 224, 225]. Sequences of these primers (both forward and reverse, modified from their original references) are shown in Table 4.1. These DNA segments were chosen based on prior literature reports that showed that these segments to be specific for the *M. Tb* genome [220]. We chose two different ZFPs as capture agents: EGR1 (also known as zif268 [226]) and rrsA1175 [70]. EGR1 is a natural three-finger ZFP that has been well characterized in the literature and recognizes a nine base pair sequence (5′-GCGTGGGCG-3′) in the target EGR binding element [218]. Conversely, rrsA1175 is a synthetic ZFP that has been recently described [70] and was designed to bind a predefined nine base pair dsDNA sequence (5′-GAGGAAGGT-3′). The binding sequences of each ZFP were incorporated into two different forward primers near their respective 5′-ends. Sequences of these primers are also shown in Table 4.1. We also verified that the target TB genes do not contain these sequences, indicating that the ZFPs will only detect ztagged amplification product. Furthermore, our design included a 5′-biotin tag in the primers and the use of biotinylated dUTP

during the DNA amplification steps so that the ZFP-bound DNA product could easily be detected with commonly used, streptavidin-based detection reagents.

4.4.2 Zinc finger-based detection of amplified TB genes

First, to test the efficiency of the ztag-modified primers, we amplified diagnostic segments of the two target TB genes, katG and inhA, from TB genomic DNA using standard amplification primers and with primers containing the encoded ztags for EGR1 or rrsA1175. Analysis of the amplified DNA products using gel electrophoresis showed amplified products of the expected length from each primer pair and visible increases in product length for the DNA products amplified using the two types of ztagged primers (Figure 4.3, lanes 2, 5, 8, and 11). This suggests that the addition of ztags in the primers did not affect primer specificity and that the ztags were successfully incorporated into the products. Additionally, since TB genomic DNA material can often contain contaminating human genomic DNA material, we also performed the amplification reactions on human genomic DNA template using the newly designed primers. Analysis of the amplified DNA products using gel electrophoresis showed no DNA amplification product band on the gel, confirming the selectivity of the designed primers for the TB genomic DNA (Figure 4.3, lanes 3, 6, 9, and 12).

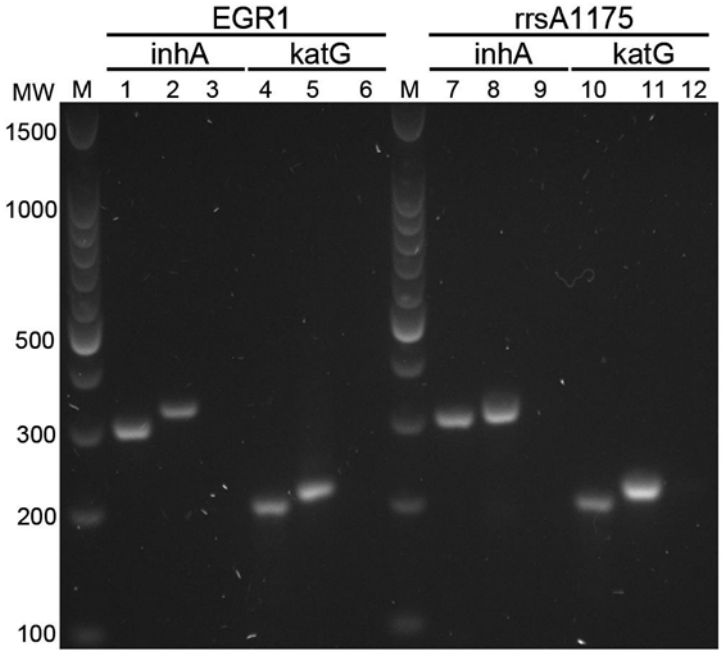

Figure 4.3 Gel electrophoresis of DNA products amplified from genomic DNA. The image shows TB biomarkers amplified using standard primers for inhA (lanes 1 and 7) and katG (lanes 4 and 10), primers containing the encoded EGR1 ztag (lanes 2 and 5), or the primers containing rrsA1175 ztag (lanes 8 and 11). TB genomic DNA was used as the template for all amplifications except for product in lanes 3, 6, 9, and 12, where human genomic DNA isolated from K562 cells was used. A 100 bp DNA ladder is shown in lane M.

Next, we tested the ability of the two ZFPs (EGR1 and rrsA1175) to capture and detect ztag-containing, amplified DNA products using an enzyme-linked immunosorbent assay (ELISA) [227]. Our assay scheme is shown in Figure 4.5A. The two ZFPs were expressed in bacteria and were affinity purified prior to use in the assay (Figure 4.2). In order to preserve the DNA binding region of ZFPs and provide appropriate orientation for efficient binding of target DNA, we decided to capture the ZFPs on the interior surface of microtiter plate wells via capture antibodies specific to the tags available in the two recombinant proteins. EGR1 contained a histidine tag (His-tag) and rrsA1175 contained a

MBP tag. We immobilized the two different antibodies (anti-His and anti-MBP) in individual wells of a 96-well plate. The ZFPs EGR1 (150 µg/mL, 250 pmol) and rrsA1175 (150 µg/mL, 100 pmol) were mixed with their respective ztagged DNA products (varying amounts ranging from 0.01 pmol to 3 pmol), and the complexes were added to the antibody-coated wells. Since the amplified DNA was biotin-tagged during the amplification reaction, the amount of bound ZFP/DNA complex was detected using a streptavidin-horse radish peroxidase (SA-HRP) conjugate by measuring the absorbance of its substrate (TMB) in each well (Figure 4.5B-J). First, in order to quantify the amount of bound, ztagged DNA, we generated a calibration curve by immobilizing various amounts of biotinylated DNA alone (0.01 pmol to 4 pmol, linear range of 0.08 pmol to 2 pmol) on poly-L-lysine coated wells and detecting the immobilized DNA using SA-HRP and TMB substrate (Figure 4.4). Control wells contained no input DNA. The resulting dose-response curve shows that the calculated detection limit (background absorption + 3σ) of this absorbance-based system is 0.066 pmol of input DNA. Next, we detected the amount of DNA containing specific ztags using ZFPs. The results show that our ZFP-based detection system generated a DNA dose-dependent response that was linear and quantitative in the range of 1 nM to 16 nM for the EGR1-tagged DNA (R^2 correlation coefficients of 0.93 and 0.87 for the two EGR1-tagged DNA) and 20 nM to 100 nM for the rrsA1175-tagged DNA (R^2 correlation coefficient of 0.94 for the two rrsA1175-tagged DNA). Our calculations show that the ZFPs have low nanomolar sensitivity for the detection of ztagged DNA (approximately 1.0 nM to 6.2 nM for EGR1-tagged DNA and

18.8 nM to 20.0 nM of the rrsA1175-tagged DNA). These data show that our novel ZFP-based assay system can sensitively and efficiently detect amplified TB biomarkers via the primer-encoded ztags.

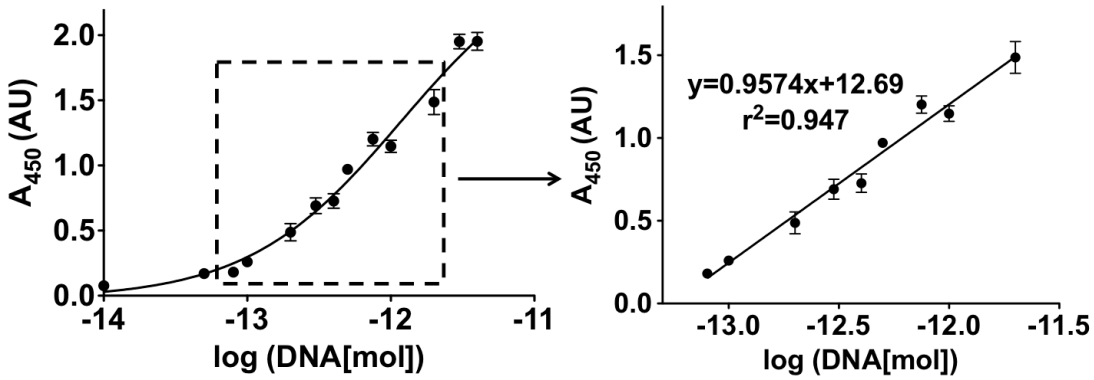

Figure 4.4 Determination of DNA detection limits in the SA-HRP-based colorimetric assay. A dose-response curve showing detection of biotinylated DNA immobilized on poly-L-lysine coated wells. An increasing amount of DNA was added to each well and the amount of immobilized DNA was measured using SA-HRP-based colorimetric assay. The linear correlation coefficient is also shown. Data shown is the mean ± SEM from three independent wells and is representative of at least three independent experiments.

4.4.3 Multiplex detection of TB genes using ZFPs

Next, we designed an assay to detect multiple, ztagged DNA targets using the two different ZFPs in a single assay. As shown schematically in Figure 4.6A-B, we immobilized varying amounts of the recombinant EGR1 (150-1000 pmol) and rrsA1175 (5-15 pmol) ZFPs on a nitrocellulose membrane to capture and detect the corresponding ztagged DNA. We found that membrane loading required more EGR1 than rrsA1175 due to a large fraction of EGR1 that passed

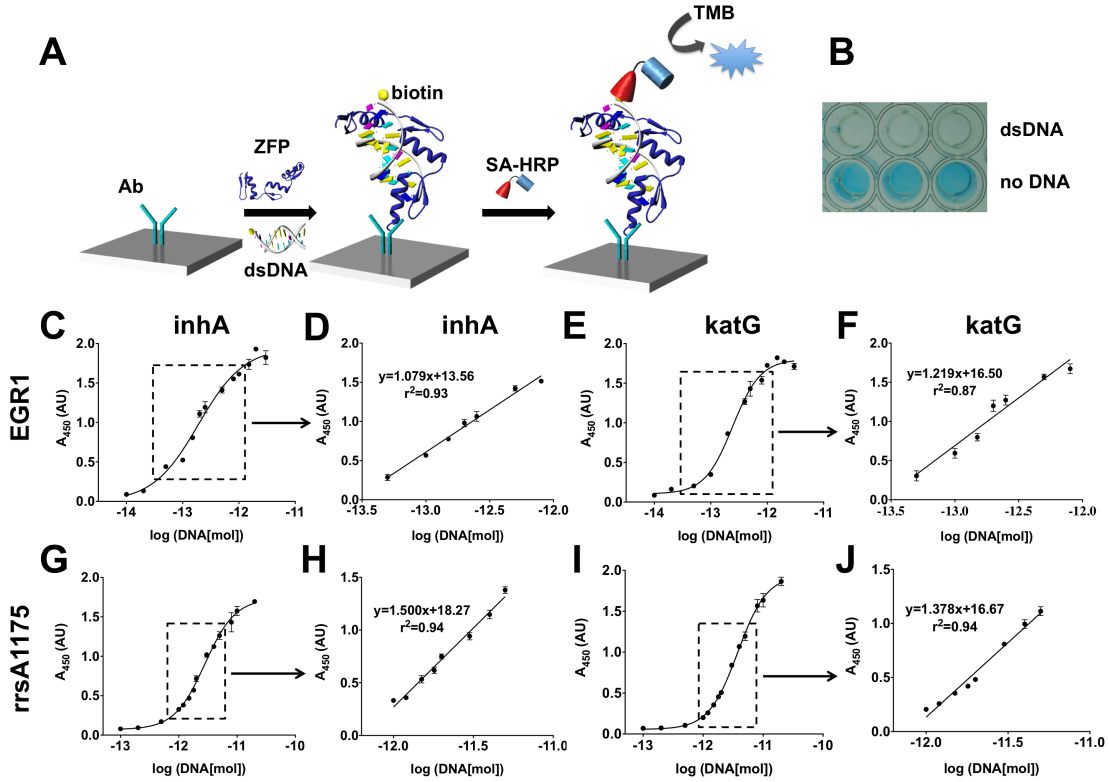

Figure 4.5 Colorimetric detection of ztagged, amplified DNA products using ZFPs. **A-B)** Schematic representation of our assay design for the colorimetric assay. The ztagged DNA (biotinylated) was detected with the SA-HRP system and was quantified by measuring the intensity of blue color generated by HRP-dependent, TMB substrate oxidation. An example image of the assay plate is shown in **B**. **C-J)** Dose-response curves showing detection of ztagged DNA by its corresponding ZFP. **C-F)** Primers containing EGR1 ztag were used to amplify TB biomarker inhA (**C-D**) or katG (**E-F**). An increasing amount of the amplified DNA product was mixed with recombinant EGR1 (250 pmol) containing a His-tag and added to wells coated with anti-His antibody, and the amount of ZFP-bound DNA was measured using the colorimetric assay described above. Data from the full range of input DNA amounts used in the assay are shown in the dose-response curves in **C** and **E**, where the absorbance signal saturates at higher amounts of input DNA:ZFP mixture. The linear portion of the data curves (**D** and **F**) was extracted from the two data sets to determine the linear correlation coefficients. Data shown represent the mean ± SEM from three independent wells and are representative of at least three independent experiments. **G-J)** Primers containing rrsA1175 ztag were used to amplify TB biomarker inhA (**C-D**) or katG (**E-F**). An increasing amount of the amplified DNA product was mixed with recombinant rrsA1175 (100 pmol) containing a MBP-tag and added to wells coated with anti-MBP antibody, and the amount of ZFP-bound DNA was measured using the colorimetric assay described above. Data from the full range of input DNA amounts used in the assay are shown in the dose-response curves

in **G** and **I**, where the absorbance signal saturates at higher amounts of input DNA:ZFP mixture. The linear portion of the data curves (**H** and **J**) was extracted from the two data sets to determine the linear correlation coefficients. Data shown represent the mean ± SEM from three independent wells and are representative of at least three independent experiments. The ZFP and ZFP-DNA binding structure were obtained from RCSB protein data bank (1A1L).

through the membrane without interaction, perhaps a consequence of its smaller size (30 kDa) as compared to rrsA1175 (67 kDa). First, the amplified, ztagged DNA product containing either the EGR1 (60 nM) or the rrsA1175 (16 nM) tag was applied to the nitrocellulose membrane. The captured DNA was detected using SA-HRP by measuring the chemiluminescence intensity generated from luminol oxidation, which has higher sensitivity as compared to the absorbance-based system using TMB. The results show that dsDNA products were selectively captured by each of the two immobilized ZFPs, with increasing concentrations of ZFP capturing the DNA product in a dose-dependent fashion (Figure 4.6C-D). We demonstrated that the ZFPs were highly selectivity and would only bind dsDNA if the appropriate ztag was present in the amplified product. It has been shown that rrsA1175 has a higher binding affinity for its target sequence (determined K_d < 0.06 nM [70]) as compared to EGR1 (determined K_d = approximately 0.34-6 nM [210]), perhaps explaining the lower LOD for rrsA1175. Assay conditions and the G-C content of the recognition sequence in the target DNA would also influence this parameter. Finally, incubation of amplified DNA product tagged with either EGR1 or rrsA1175 on the nitrocellulose membrane showed high signal intensity at spots where either of the two ZFPs were immobilized and a linear increase in spot intensity with increasing

concentrations of immobilized ZFPs (Figure 4.6E). These results suggest that the ZFP/ztag pairs can be used for multiplex detection of TB biomarkers in diagnostic assays.

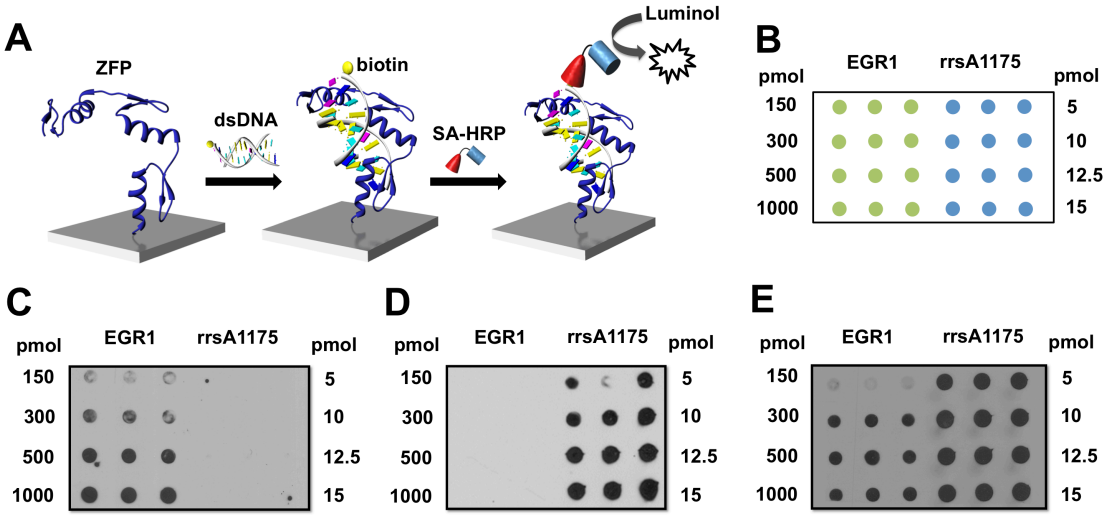

Figure 4.6 Multiplex detection of ztagged DNA using immobilized ZFPs and luminescence. **A)** Schematic representation of our assay design for the luminescence-based multiplex assay. **B)** Varying amounts of EGR1 (150-1000 pmol) and rrsA1175 (5-15 pmol) were immobilized as an array on a single nitrocellulose membrane in a spatially separated manner. **C-E:** The ztagged DNA (biotinylated) was detected on X-ray films with the SA-HRP-based luminescence system and was quantified by measuring spot density on the digitized films. **C)** Image showing chemiluminescent detection of EGR1-ztagged DNA product (inhA, 60 nM) on a nitrocellulose membrane containing immobilized EGR1 and rrsA1175 proteins. **D)** Image showing chemiluminescent detection of rrsA1175 ztagged DNA product (inhA, 16 nM) on a nitrocellulose membrane containing immobilized EGR1 and rrsA1175 proteins. **E)** Image showing chemiluminescent detection of a mixture containing DNA product encoded with ztags for EGR1 or rrsA1175 and incubated on a nitrocellulose membrane containing immobilized EGR1 and rrsA1175 proteins. Data presented in this figure are representative of at least three independent experiments. The ZFP and ZFP-DNA binding structures were obtained from the RCSB protein data bank (1A1L).

4.4.4 Paper-based microfluidic device for multiplexed detection of amplified TB genes

Paper-based diagnostics has recently emerged as the method of choice for multiplex detection of various markers in resource-poor settings [228-231]. Such devices are inexpensive to manufacture and easy to use in almost any condition. However, paper-based devices have not been developed for multiplexed, DNA-based tests, primarily due to the limitations inherent in transitioning current methods onto paper-based platforms. Here, we developed a novel, simple, paper-based microfluidic device around our ZFP-based detection platform to test its applicability for multiplexed DNA detection.

As shown in Figure 4.10A, our paper-based microfluidic device is based on three differentially-patterned paper layers assembled in a 3-D composite structure. A fully assembled device can be seen in Figure 4.7B. The device design (Figure 4.10B) consists of two circular regions for the detection of unique dsDNA products via the immobilized ZFPs EGR1 and rrsA1175, a circular control region (marked “C”) without ZFP as a background signal control, and elliptical regions to capture flow-through dsDNA via immobilized chitosan (a positively-charged polymer to bind any DNA and provide test confirmation). The assay detection chemistry utilized the NeutrAvidin®-HRP (NA-HRP) system, similar as SA-HRP, which was used in the ELISA assays described in Figure 4.5A, resulting in a blue/brown color that could be visually identified. Thus, the device contained several highly informative design features that convey test result information as a visual readout. A positive result would be indicated by colored

outputs in the ZFP-containing circular regions and the chitosan-containing elliptical regions with no/little background color in the non-ZFP control region. In case none of the ZFP-containing regions was positive but the elliptical DNA-binding control region showed a positive result, the assay would be valid and would lead to a conclusion that the tested TB genes were absent in the sample. On the other hand, if the elliptical control region showed no color, the test would be considered invalid and would need to be re-run.

To develop the device, we fabricated the sensor on cellulose paper (Whatman #1) using published methods [181, 222]. Microfluidic path patterns for the three layers (Figure 4.10A) were printed onto the cellulose paper using a solid wax ink printer, and each of the three layers was obtained by manually cutting it from a single sheet of paper (Figure 4.8). On the middle paper layer, recombinant ZFPs, EGR1 and rrsA1175 were immobilized onto individual detection wells (EGR1 on left, rrsA1175 on right, Figure 4.10B) using capture antibodies (anti-His and anti-MBP, respectively), as illustrated in Figures 4.5A. No ZFP was added to the central circular region, which acts as a negative control (region “C”, Figure 4.10B). Chitosan was immobilized in the elliptical regions to capture all DNA (and, thus, define positive control regions) because of two considerations; a) previous reports mentioned that chitosan can be immobilized onto a cellulose membrane surface by physical adsorption [232], and b) the positively-charged chitosan is ideal for non-selectively capturing negatively-charged DNA molecules.

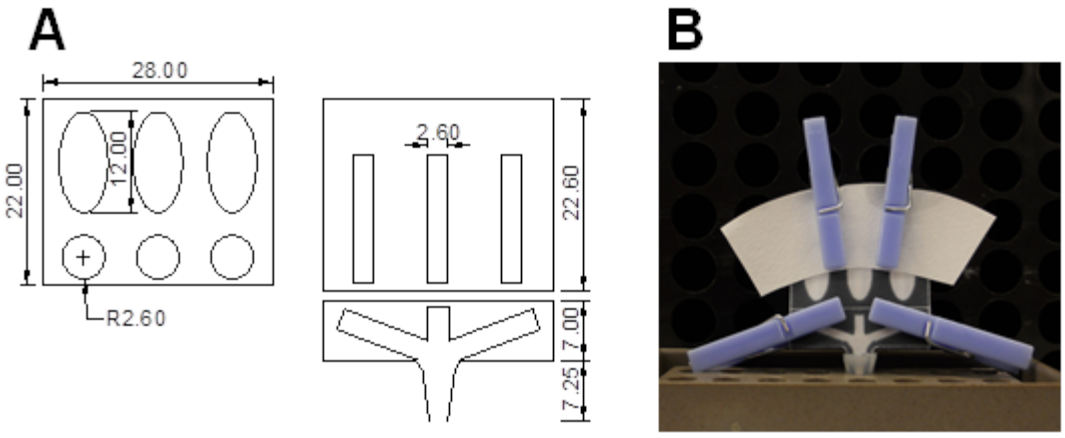

Figure 4.7 Design of paper-based channel. **A)** A schematic showing the design of each of the three layers of the paper-based microfluidic device and the dimensions (measurements are in mm) of the printed features. **B**) A photographic image of a fully assembled device (using paper-clips) and immersed in an cut Eppendorf tube.

First, the top two layers were assembled using a clip and were dipped into a solution containing target dsDNA in order to bind the target with the immobilized ZFPs. Subsequently, the third layer was added to the assembled device, and the unbound DNA was further washed to the chitosan-containing elliptical regions for confirmation that the platform is operational. Bound DNA was detected by sequentially loading solutions containing NA-HRP, wash buffer, and TMB substrate through the assembled device. Development of blue/brown color in the different regions of the device signified a “positive” for that region.

To evaluate its performance, we applied a variety of amplified dsDNA products to the device. We amplified TB genomic DNA using two different ztags, EGR1-katG and rrsA1175-inhA, as described above. As an additional specificity control, we

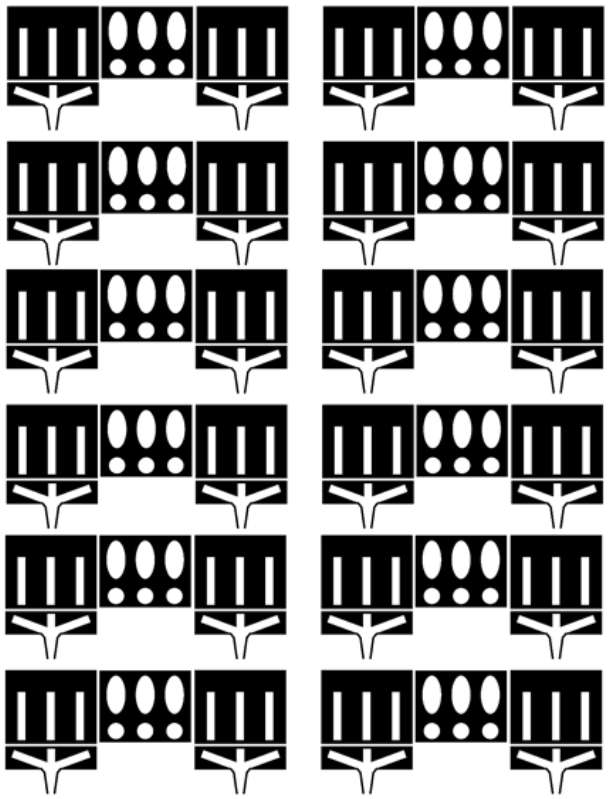

Figure 4.8 A schematic showing the final print layout of the paper-based microfluidic device. This shows how multiple devices could be printed on a single sheet of A4 paper.

also used human genomic DNA to amplify a human gene (18s rRNA gene product) without a ztag for use on the device. As shown in Figure 4.9, the gene-specific primers successfully amplified individual genes in the PCR reactions. Furthermore, in order to better mimic natural conditions, DNA amplification reactions were performed using human (4 ng) and TB genomic DNA (0.4 ng) mixture as the template. Figure 4.9 also shows that a mixture of all three sets of primers (TB EGR1-katG, TB rrsA1175-inhA and human 18S rRNA) successfully amplified the two specific TB genes and the human gene in a single amplification reaction containing both human and TB genomic DNA as template. Therefore,

DNA from combined amplification reactions was used on the paper-based microfluidic device for detection. In Figure 4.10C, a photograph of the device #1 clearly showed brown color in the elliptical regions, suggesting a “valid” assay. Additionally, no colored product could be seen in any of the ZFP-containing circular regions or the negative control region, validating the specificity of the ZFPs for actual target. Next, we determined the efficiency and selectivity of this device for measuring one of the two TB genes by applying dsDNA product mixture from an amplification reaction with either the human and the rrsA1175-inhA primer mixtures (Device #2, Figure 4.10C) or the human and the EGR1-katG primer mixtures (Device #3, Figure 4.10C). The blue color showed in corresponding ZFP immobilized region clearly demonstrated that the device could accurately detect the appropriate gene. Finally, analysis of dsDNA amplified using all three sets of primers (human 18S rRNA, EGR1-katG, and rrsA1175-inhA) showed visually-identifiable detection of both TB genes by a single device (Device #4, Figure 4.10C). Although the intensity of the product spots in the detection regions was slightly variable in different assays and devices (due to its dependence on the flow rate, concentration of the amplified dsDNA products, and the time of HRP-based color development), these results clearly show that this detection method is highly reproducible and is able to accurately perform multiplexed DNA detection in a simple and easy-to-read fashion.

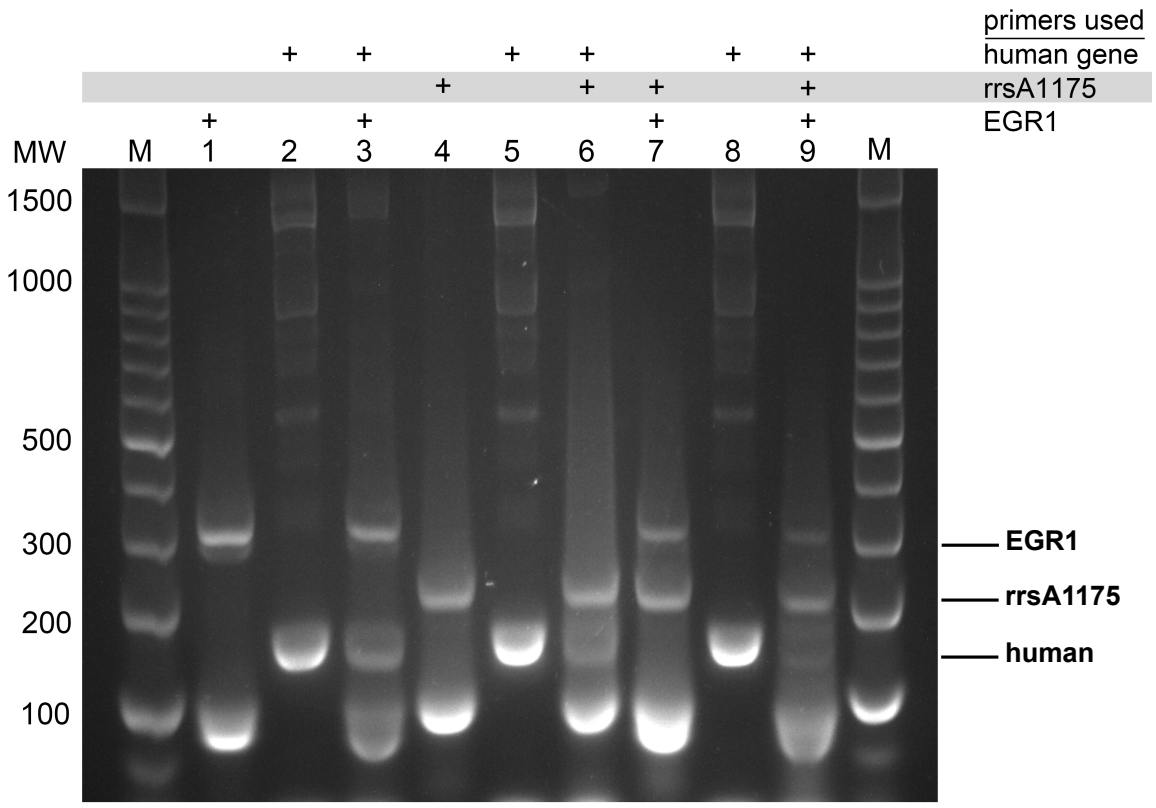

Figure 4.9 Gel electrophoresis of amplified DNA products detected on the paper-based microfluidic device. All PCR products shown were amplified with a mixed template containing 400 pg TB genomic DNA and 4 ng human pooled genomic DNA. Different lanes represented dsDNA product amplified with different primer sets. Lane M: 100 bp DNA ladder; Lane 1: dsDNA product amplified with only the EGR1-katG primers; lane 2: dsDNA product amplified with H-RNA specific for human 18s rRNA; lane 3: dsDNA product amplified with two sets of primers, the TB EGR1-katG primers and H-RNA; lane 4: dsDNA product amplified with only the rrsA1175-inhA primers; lane 5: dsDNA product amplified with H-RNA; lane 6: dsDNA product amplified with two sets of primers, the TB rrsA1175-inhA primers and H-RNA; lane 7: dsDNA product amplified with a mixture of TB primer sets, the EGR1-katG and the rrsA1175-inhA primers; lane 8: dsDNA product amplified with H-RNA; lane 9: dsDNA products from an amplification reaction with a mixture of all three primer sets, the TB EGR1-katG primers, the TB rrsA1175-inhA primers, and the H-RNA primers. Expected products for each of the specific sets of primers are also labeled.

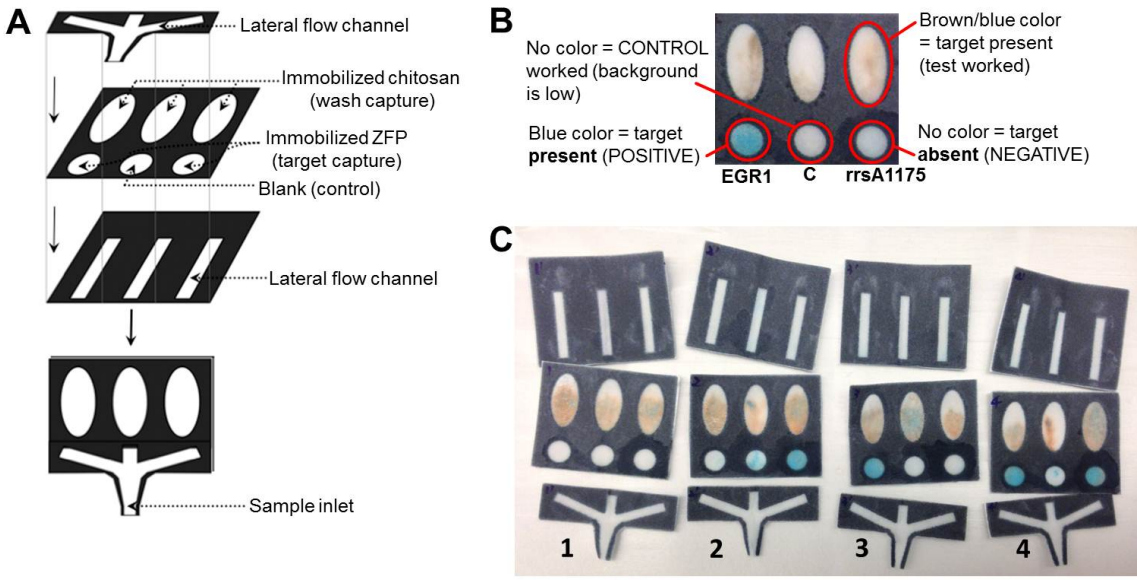

Figure 4.10 Multiplexed DNA detection using a paper-based microfluidic device. **A)** Schematic representation of the device. It consisted of three layers of patterned cellulose paper. The top-most layer carried the DNA mixture into the different detection zones on the next layer. The detection zones contained immobilized ZFPs and a separate zone for capturing flow-through dsDNA product via immobilized chitosan. The third layer contained channels to help transport liquids from detection zones to the control zones. **B)** Schematic of the detection zones on the detection layer of the device, the possible colorimetric readout, and its interpretation. **C)** Image of each of the three paper layers of the device after a test run with various samples. The test device "1" shows the results from a control experiment, where the device was incubated with a sample containing only the amplified human 18S rRNA gene product. The three circular detection zones show no increase in blue/brown color, suggesting a negative result. The elliptical zones show positive brown staining, suggesting that the test was valid. Similarly, the test device "2" shows results from a device incubated with a mixture of amplified human and rrsA1175-tagged TB product; the device "3" shows results from a device incubated with a mixture of amplified human and EGR1-tagged TB product and the test device "4" shows results from a device incubated with a mixture of amplified human gene, the rrsA1175-tagged TB product, and the EGR1-tagged TB gene product. The devices shown are representative of two to three independent tests.

4.5 Conclusion

A majority of the nucleic acid-based diagnostic assays that are currently available for pathogen detection in a low-resource setting rely upon amplification and detection of a single target per test [225, 233]. This necessitates multiple assays for the detection of multiple nucleic acid biomarkers in each sample. Alternative methods for detecting multiple targets in a single assay require expensive or complex technological solutions that are beyond the capabilities available in resource-poor settings. Here, we describe the development of a novel assay for the detection of multiple DNA sequences in a single assay by using ZFP binding sequences as tags that are directly incorporated into the amplification primers (Figure 4.1) and used in combination with immobilized ZFPs specific to the amplified binding sequences. Using TB as a model system, we show that our design can detect multiple TB genes in a single test and can do so on a number of different detection platforms, including a paper-based microfluidics device for use at the POC in a resource-poor setting. The data presented in this proof-of-concept study establishes that both the assay and the device are easy to design, use simple reagents, and provide visual readouts. This suggests that this novel assay/device has the potential to be implemented in underserved areas for rapid disease diagnostics and effective management strategies.

ZFPs have previously been used as a way to detect double-stranded DNA [68-70, 211, 215-219, 234]. By incorporating almost any desired ZFP recognition sequence in the amplification primers, our ZFP-based method offers significant

advantages in that it circumvents many limitations of previous ZFP-based detection methods that require their recognition sequences be endogenously present in the target sequence. Additionally, multiple, independent primers can be pre-encoded with unique ztags for amplification of different DNA targets, allowing for multiplex detection in a single assay. Using TB genomic DNA in our proof-of-concept assays, we showed that our novel design is simple and practical, enabling sensitive detection of two different TB biomarkers in a single assay. Thus, the results presented here provide a construct for the future addition of other ztag:ZFP combinations that would increase the multiplex capabilities of the system. A potential concern with our assay design could be that amplified DNA products may also contain endogenous ZFP recognition sites, which would make detection (and differential detection) problematic. However, the variety of endogenous and synthetic ZFPs enables a choice of ztags that are not represented in the amplified DNA targets. Additionally, in this report, we tested only two different ZFPs with very different binding affinities. Whether ZFPs with similar binding affinities would make better detection agents in this setting is not known and would be evaluated in the future. Similarly, we found that the immobilization efficiency of ZFPs played a role in the target detection limits, as the smaller EGR1 was not efficiently retained during immobilization on the nitrocellulose membranes. Future studies will also need to determine the effects of overall size and the various tags on the recombinant ZFPs. Furthermore, additional improvements such as incorporation of isothermal DNA amplification methods and increasing the overall dynamic range for the assay by

changing the concentration of capture ZFPs may further improve the performance of this assay. Moreover, there are a number of other approaches that are available in the literature for direct recognition and detection of dsDNA [234]. These include the triplex-forming oligos (TFOs, both linear and circular), a variety of natural and synthetic major groove binders and other transcription factors [234]. Currently, ZFPs are the most versatile and have higher applicability in diagnostics due to high affinities for their target DNA. However, all of the previously described assays have a key limitation in that they were designed to detect DNA sequences that are endogenously present or pre-exist in their target biomarkers, thus limiting their potential for use in a multiplex assay. While engineering novel transcription factors against almost any target DNA sequence has previously been proposed, this has been difficult to achieve experimentally. Our novel assay design avoids this critical limitation by directly encoding the detection sequences in the amplification primers, thus providing a greater degree of freedom in the choice of multiplex detection agents. Additionally, our design methodology can easily be extended to include TFOs, minor groove binders, and other DNA binding agents given that the DNA recognition sequence for almost any DNA binding agent can be encoded in the amplification primers.

Our paper-based microfluidics platform for multiplexed DNA detection also offers several technical advantages, including many that have already been reported to be associated with such paper-based devices [181, 185, 235]. The incorporation of multiple layers in the design allows multiplexed detection by

splitting the input channel into multiple channels. Although we show the device with three split channels to detect two unique DNA markers, the device design allows for easy incorporation of additional channels and detection zones for more ZFP:ztag combinations. Similarly, the device provides a visual, color-based test result that can either be read manually or with the help of any portable camera, such as those that are built into a majority of cell phones. The device platform is also versatile and is open to application of a variety of other detection strategies such as gold nanoparticles [236, 237], electrochemical detection [222, 238-240], electrical impedance-based detection [241], etc. A future goal is to demonstrate this newly developed methodology on patient samples in order to fully validate device performance. Similarly, future studies will also evaluate the long-term device stability, especially under conditions typically associated with a resource-poor POC setting.

In summary, we describe a successful proof-of-concept implementation of a multiplexed DNA detection platform using a simple, economical, paper-based microfluidic device. This research provides a framework for the implementation of simple, accurate, and reliable POC devices to help improve the quality of life for patients in resource-poor settings.

REFERENCES

1. Sanvicens, N., Pastells, C., Pascual, N., and Marco, M.P., Nanoparticle-based biosensors for detection of pathogenic bacteria*. Trac-Trends Anal Chem,* **2009**, 28(11): 1243-1252.

2. Banerjee, P. and Bhunia, A.K., Mammalian cell-based biosensors for pathogens and toxins*. Trends Biotechnol,* **2009**, 27(3): 179-188.

3. Vikesland, P.J. and Wigginton, K.R., Nanomaterial enabled biosensors for pathogen monitoring - a review*. Environ Sci Technol,* **2010**, 44(10): 3656-3669.

4. Ivnitski, D., Abdel-Hamid, I., Atanasov, P., Wilkins, E., and Stricker, S., Application of electrochemical biosensors for detection of food pathogenic bacteria*. Electroanalysis,* **2000**, 12(5): 317-325.

5. Velusamy, V., Arshak, K., Korostynska, O., Oliwa, K., and Adley, C., An overview of foodborne pathogen detection: in the perspective of biosensors*. Biotechnol Adv,* **2010**, 28(2): 232-254.

6. The top 10 causes of death. Fact Sheets 2013; World Health Organization, Available from: http://who.int/mediacentre/factsheets/fs310/en/index.html.

7. Black, R.E., Cousens, S., Johnson, H.L., Lawn, J.E., Rudan, I., Bassani, D.G., Jha, P., Campbell, H., Walker, C.F., Cibulskis, R., Eisele, T., Liu, L., Mathers, C., Child Health Epidemiology Reference Group of, W.H.O., and Unicef, Global, regional, and national causes of child mortality in 2008: a systematic analysis*. Lancet,* **2010**, 375(9730): 1969-1987.

8. TDR Accessible quality-assured diagnostics - 2009 annual report; TDR/BL7.10; World Health Organization: 2010; p 36.

9. Wu, G. and Zaman, M.H., Low-cost tools for diagnosing and monitoring HIV infection in low-resource settings*. Bull World Health Organ,* **2012**, 90(12): 914-920.

10. Lazcka, O., Del Campo, F.J., and Munoz, F.X., Pathogen detection: a perspective of traditional methods and biosensors*. Biosens Bioelectron,* **2007**, 22(7): 1205-1217.

11. Wang, Y., Ye, Z., and Ying, Y., New trends in impedimetric biosensors for the detection of foodborne pathogenic bacteria. *Sensors (Basel),* **2012**, 12(3): 3449-3471.

12. Wisdom, G.B., Enzyme-immunoassay. *Clin Chem,* **1976**, 22(8): 1243-1255.

13. Scharpe, S.L., Cooreman, W.M., Blomme, W.J., and Laekeman, G.M., Quantitative enzyme immunoassay: current status. *Clin Chem,* **1976**, 22(6): 733-738.

14. Voller, A., Bartlett, A., and Bidwell, D.E., Enzyme immunoassays with special reference to ELISA techniques. *J Clin Pathol,* **1978**, 31(6): 507-520.

15. Bostrom, J., Lee, C.V., Haber, L., and Fuh, G., Improving antibody binding affinity and specificity for therapeutic development. *Methods Mol Biol,* **2009**, 525: 353-376, xiii.

16. DNA Oligonucleotide Resuspension and Storage. 2013; Integrated DNA Technologies, Available from: http://www.idtdna.com/pages/decoded/decoded-articles/core-concepts/decoded/2011/03/16/dna-oligonucleotide-resuspension-and-storage.

17. Hsiang, M.S., Lin, M., Dokomajilar, C., Kemere, J., Pilcher, C.D., Dorsey, G., and Greenhouse, B., PCR-based pooling of dried blood spots for detection of malaria parasites: optimization and application to a cohort of Ugandan children. *J Clin Microbiol,* **2010**, 48(10): 3539-3543.

18. Boppana, S.B., Ross, S.A., Novak, Z., Shimamura, M., Tolan, R.W., Jr., Palmer, A.L., Ahmed, A., Michaels, M.G., Sanchez, P.J., Bernstein, D.I., Britt, W.J., Fowler, K.B., National Institute on, D., Other Communication Disorders, C.M.V., and Hearing Multicenter Screening, S., Dried blood spot real-time polymerase chain reaction assays to screen newborns for congenital cytomegalovirus infection. *JAMA,* **2010**, 303(14): 1375-1382.

19. Mullis, K.B. and Faloona, F.A., Specific synthesis of DNA in vitro via a polymerase-catalyzed chain reaction. *Methods Enzymol,* **1987**, 155: 335-350.

20. Saiki, R.K., Gelfand, D.H., Stoffel, S., Scharf, S.J., Higuchi, R., Horn, G.T., Mullis, K.B., and Erlich, H.A., Primer-directed enzymatic amplification of DNA with a thermostable DNA polymerase. *Science,* **1988**, 239(4839): 487-491.

21. Schochetman, G., Ou, C.Y., and Jones, W.K., Polymerase chain reaction. *J Infect Dis,* **1988**, 158(6): 1154-1157.

22. Eckert, K.A. and Kunkel, T.A., High fidelity DNA synthesis by the Thermus aquaticus DNA polymerase. *Nucleic Acids Res,* **1990**, 18(13): 3739-3744.

23. Porter-Jordan, K., Rosenberg, E.I., Keiser, J.F., Gross, J.D., Ross, A.M., Nasim, S., and Garrett, C.T., Nested polymerase chain reaction assay for the detection of cytomegalovirus overcomes false positives caused by contamination with fragmented DNA. *J Med Virol,* **1990**, 30(2): 85-91.

24. Berkhout, R.J., Tieben, L.M., Smits, H.L., Bavinck, J.N., Vermeer, B.J., and ter Schegget, J., Nested PCR approach for detection and typing of epidermodysplasia verruciformis-associated human papillomavirus types in cutaneous cancers from renal transplant recipients. *J Clin Microbiol,* **1995**, 33(3): 690-695.

25. Van Tuinen, D., Jacquot, E., Zhao, B., Gollotte, A., and Gianinazzi-Pearson, V., Characterization of root colonization profiles by a microcosm community of arbuscular mycorrhizal fungi using 25S rDNA-targeted nested PCR. *Mol Ecol,* **1998**, 7(7): 879-887.

26. Nuovo, G.J., Gallery, F., MacConnell, P., Becker, J., and Bloch, W., An improved technique for the in situ detection of DNA after polymerase chain reaction amplification. *Am J Pathol,* **1991**, 139(6): 1239-1244.

27. Birch, D.E., Simplified hot start PCR. *Nature,* **1996**, 381(6581): 445-446.

28. Don, R.H., Cox, P.T., Wainwright, B.J., Baker, K., and Mattick, J.S., Touchdown PCR to circumvent spurious priming during gene amplification. *Nucleic Acids Res,* **1991**, 19(14): 4008-4008.

29. Lundberg, K.S., Shoemaker, D.D., Adams, M.W.W., Short, J.M., Sorge, J.A., and Mathur, E.J., High-fidelity amplification using a thermostable DNA-polymerase isolated from Pyrococcus-furiosus. *Gene,* **1991**, 108(1): 1-6.

30. Burg, J.L., Grover, C.M., Pouletty, P., and Boothroyd, J.C., Direct and sensitive detection of a pathogenic protozoan, Toxoplasma gondii, by polymerase chain reaction. *J Clin Microbiol,* **1989**, 27(8): 1787-1792.

31. Josephson, K.L., Gerba, C.P., and Pepper, I.L., Polymerase chain reaction detection of nonviable bacterial pathogens. *Appl Environ Microbiol,* **1993**, 59(10): 3513-3515.

32. Wang, R.F., Cao, W.W., and Cerniglia, C.E., A universal protocol for PCR detection of 13 species of foodborne pathogens in foods. *J Appl Microbiol,* **1997**, 83(6): 727-736.

33. Pfaffl, M.W., A new mathematical model for relative quantification in real-time RT-PCR. *Nucleic Acids Res,* **2001**, 29(9): e45.

34. Higuchi, R., Fockler, C., Dollinger, G., and Watson, R., Kinetic PCR analysis - real-time monitoring of DNA amplification reactions. *Bio-Technology,* **1993**, 11(9): 1026-1030.

35. Heid, C.A., Stevens, J., Livak, K.J., and Williams, P.M., Real time quantitative PCR. *Genome Res,* **1996**, 6(10): 986-994.

36. Gibson, U.E., Heid, C.A., and Williams, P.M., A novel method for real time quantitative RT-PCR. *Genome Res,* **1996**, 6(10): 995-1001.

37. Belgrader, P., Benett, W., Hadley, D., Richards, J., Stratton, P., Mariella, R., and Milanovich, F., Infectious disease - PCR detection of bacteria in seven minutes. *Science,* **1999**, 284(5413): 449-450.

38. Heller, M.J., DNA microarray technology: devices, systems, and applications. *Annu Rev Biomed Eng,* **2002**, 4: 129-153.

39. Epstein, J.R., Biran, I., and Walt, D.R., Fluorescence-based nucleic acid detection and microarrays. *Anal Chim Acta,* **2002**, 469(1): 3-36.

40. Gresham, D., Ruderfer, D.M., Pratt, S.C., Schacherer, J., Dunham, M.J., Botstein, D., and Kruglyak, L., Genome-wide detection of polymorphisms at nucleotide resolution with a single DNA microarray. *Science,* **2006**, 311(5769): 1932-1936.

41. Kraynov, V.S., Chamberlain, C., Bokoch, G.M., Schwartz, M.A., Slabaugh, S., and Hahn, K.M., Localized Rac activation dynamics visualized in living cells. *Science,* **2000**, 290(5490): 333-337.

42. Lakowicz, J.R., Principles of fluorescence spectroscopy. 3rd ed. 2006: *Springer*. 954.

43. Tyagi, S. and Kramer, F.R., Molecular beacons: probes that fluoresce upon hybridization. *Nat Biotechnol,* **1996**, 14(3): 303-308.

44. Liang, R.Q., Li, W., Li, Y., Tan, C.Y., Li, J.X., Jin, Y.X., and Ruan, K.C., An oligonucleotide microarray for microRNA expression analysis based on labeling RNA with quantum dot and nanogold probe. *Nucleic Acids Res,* **2005**, 33(2): e17.

45. Bawendi, M.G., Wilson, W.L., Rothberg, L., Carroll, P.J., Jedju, T.M., Steigerwald, M.L., and Brus, L.E., Electronic structure and photoexcited-carrier dynamics in nanometer-size CdSe clusters. *Phys Rev Lett,* **1990**, 65(13): 1623-1626.

46. Alivisatos, A.P., Semiconductor clusters, nanocrystals, and quantum dots. *Science,* **1996**, 271(5251): 933-937.

47. Ho, Y.P., Kung, M.C., Yang, S., and Wang, T.H., Multiplexed hybridization detection with multicolor colocalization of quantum dot nanoprobes. *Nano Lett,* **2005**, 5(9): 1693-1697.

48. Doleman, L., Davies, L., Rowe, L., Moschou, E.A., Deo, S., and Daunert, S., Bioluminescence DNA hybridization assay for Plasmodium falciparum based on the photoprotein aequorin. *Anal Chem,* **2007**, 79(11): 4149-4153.

49. Galvan, B. and Christopoulos, T.K., Bioluminescence hybridization assays using recombinant aequorin. Application to the detection of prostate-specific antigen mRNA. *Anal Chem,* **1996**, 68(20): 3545-3550.

50. Siddiqi, A.M., Jennings, V.M., Kidd, M.R., Actor, J.K., and Hunter, R.L., Evaluation of electrochemiluminescence- and bioluminescence-based assays for quantitating specific DNA. *J Clin Lab Anal,* **1996**, 10(6): 423-431.

51. Cissell, K.A., Campbell, S., and Deo, S.K., Rapid, single-step nucleic acid detection. *Anal Bioanal Chem,* **2008**, 391(7): 2577-2581.

52. Broyles, D., Cissell, K., Kumar, M., and Deo, S., Solution-phase detection of dual microRNA biomarkers in serum. *Anal Bioanal Chem,* **2012**, 402(1): 543-550.

53. Cissell, K.A., Rahimi, Y., Shrestha, S., Hunt, E.A., and Deo, S.K., Bioluminescence-based detection of microRNA, miR21 in breast cancer cells. *Anal Chem,* **2008**, 80(7): 2319-2325.

54. Hunt, E.A. and Deo, S.K., Bioluminescent stem-loop probes for highly sensitive nucleic acid detection. *Chem Commun (Camb),* **2011**, 47(33): 9393-9395.

55. Cissell, K.A., Rahimi, Y., Shrestha, S., and Deo, S.K., Reassembly of a bioluminescent protein Renilla luciferase directed through DNA hybridization. *Bioconjugate Chem,* **2009**, 20(1): 15-19.

56. Conyers, R.A., Birkett, D.J., Neale, F.C., Posen, S., and Brudenell-Woods, J., The action of EDTA on human alkaline phosphatases. *Biochim Biophys Acta,* **1967**, 139(2): 363-371.

57. Girotti, S., Ferri, E., Ghini, S., Musiani, M., Zerbini, M.L., Gibellini, D., and Gentilomi, G., Direct quantitative chemiluminescent assays for the eetection of viral-DNA. *Anal Chim Acta,* **1991**, 255(2): 387-394.

58. Zhang, N. and Appella, D.H., Colorimetric detection of anthrax DNA with a peptide nucleic acid sandwich-hybridization assay. *J Am Chem Soc,* **2007**, 129(27): 8424-8425.

59. Ke, R., Zorzet, A., Goransson, J., Lindegren, G., Sharifi-Mood, B., Chinikar, S., Mardani, M., Mirazimi, A., and Nilsson, M., Colorimetric nucleic acid testing assay for RNA virus detection based on circle-to-circle amplification of padlock probes. *J Clin Microbiol,* **2011**, 49(12): 4279-4285.

60. Matthews, J.A., Batki, A., Hynds, C., and Kricka, L.J., Enhanced chemiluminescent method for the detection of DNA dot-hybridization assays. *Anal Biochem,* **1985**, 151(1): 205-209.

61. Forster, A.C., McInnes, J.L., Skingle, D.C., and Symons, R.H., Non-radioactive hybridization probes prepared by the chemical labelling of DNA and RNA with a novel reagent, photobiotin. *Nucleic Acids Res,* **1985**, 13(3): 745-761.

62. Wilson, R., Preparation of single-stranded DNA from PCR products with streptavidin magnetic beads. *Nucleic Acid Ther,* **2011**, 21(6): 437-440.

63. Hill, H.D., Vega, R.A., and Mirkin, C.A., Nonenzymatic detection of bacterial genomic DNA using the bio bar code assay. *Anal Chem,* **2007**, 79(23): 9218-9223.

64. Harcourt, E.M. and Kool, E.T., Amplified microRNA detection by templated chemistry. *Nucleic Acids Res,* **2012**, 40(9): e65.

65. Sato, K., Ishii, R., Sasaki, N., Sato, K., and Nilsson, M., Bead-based padlock rolling circle amplification for single DNA molecule counting. *Anal Biochem,* **2013**, 437(1): 43-45.

66. Sato, K., Tachihara, A., Renberg, B., Mawatari, K., Sato, K., Tanaka, Y., Jarvius, J., Nilsson, M., and Kitamori, T., Microbead-based rolling circle amplification in a microchip for sensitive DNA detection. *Lab Chip,* **2010**, 10(10): 1262-1266.

67. Hu, J. and Zhang, C.Y., Sensitive detection of nucleic acids with rolling circle amplification and surface-enhanced Raman scattering spectroscopy. *Anal Chem,* **2010**, 82(21): 8991-8997.

68. Abe, K., Kumagai, T., Takahashi, C., Kezuka, A., Murakami, Y., Osawa, Y., Motoki, H., Matsuo, T., Horiuchi, M., Sode, K., Igimi, S., and Ikebukuro, K., Detection of pathogenic bacteria by using zinc finger protein fused with firefly luciferase. *Anal Chem,* **2012**, 84(18): 8028-8032.

69. Osawa, Y., Ikebukuro, K., Motoki, H., Matsuo, T., Horiuchi, M., and Sode, K., The simple and rapid detection of specific PCR products from bacterial genomes using Zn finger proteins. *Nucleic Acids Res,* **2008**, 36(11).

70. Kim, M.S., Stybayeva, G., Lee, J.Y., Revzin, A., and Segal, D.J., A zinc finger protein array for the visual detection of specific DNA sequences for diagnostic applications. *Nucleic Acids Res,* **2011**, 39(5): e29.

71. Yin, B.C., Liu, Y.Q., and Ye, B.C., One-step, multiplexed fluorescence detection of microRNAs based on duplex-specific nuclease signal amplification. *J Am Chem Soc,* **2012**, 134(11): 5064-5067.

72. Huang, J.H., Su, X.F., and Li, Z.G., Enzyme-Free and Amplified Fluorescence DNA Detection Using Bimolecular Beacons. *Anal Chem,* **2012**, 84(14): 5939-5943.

73. Zhang, Y. and Zhang, C.Y., Sensitive detection of microRNA with isothermal amplification and a single-quantum-dot-based nanosensor. *Anal Chem,* **2012**, 84(1): 224-231.

74. En, F.X., Wei, X., Jian, L., and Qin, C., Loop-mediated isothermal amplification establishment for detection of pseudorabies virus. *J Virol Methods* **2008**, 151(1): 35-39.

75. Fang, X., Liu, Y., Kong, J., and Jiang, X., Loop-mediated isothermal amplification integrated on microfluidic chips for point-of-care quantitative detection of pathogens. *Anal Chem,* **2010**, 82(7): 3002-3006.

76. Mori, Y., Kitao, M., Tomita, N., and Notomi, T., Real-time turbidimetry of LAMP reaction for quantifying template DNA. *J Biochem Biophys Methods,* **2004**, 59(2): 145-157.

77. Mori, Y., Nagamine, K., Tomita, N., and Notomi, T., Detection of loop-mediated isothermal amplification reaction by turbidity derived from magnesium pyrophosphate formation. *Biochem Biophys Res Commun,* **2001**, 289(1): 150-154.

78. Notomi, T., Okayama, H., Masubuchi, H., Yonekawa, T., Watanabe, K., Amino, N., and Hase, T., Loop-mediated isothermal amplification of DNA. *Nucleic Acids Res,* **2000**, 28(12): E63.

79. Tourlousse, D.M., Ahmad, F., Stedtfeld, R.D., Seyrig, G., Tiedje, J.M., and Hashsham, S.A., A polymer microfluidic chip for quantitative detection of multiple water- and foodborne pathogens using real-time fluorogenic loop-mediated isothermal amplification. *Biomed Microdevices,* **2012**, 14(4): 769-778.

80. Vet, J.A.M., Majithia, A.R., Marras, S.A.E., Tyagi, S., Dube, S., Poiesz, B.J., and Kramer, F.R., Multiplex detection of four pathogenic retroviruses using molecular beacons. *Proc Nat Acad Sci U S A,* **1999**, 96(11): 6394-6399.

81. Liao, W.C. and Ho, J.A., Attomole DNA electrochemical sensor for the detection of Escherichia coli O157. *Anal Chem,* **2009**, 81(7): 2470-2476.

82. Cai, J., Yao, C.Y., Xia, J., Wang, J., Chen, M., Huang, J.F., Chang, K., Liu, C.J., Pan, H., and Fu, W.L., Rapid parallelized and quantitative analysis of five pathogenic bacteria by ITS hybridization using QCM biosensor. *Sensor Actuat B-Chem,* **2011**, 155(2): 500-504.

83. Kim, D.K., Yoo, S.M., Park, T.J., Yoshikawa, H., Tamiya, E., Park, J.Y., and Lee, S.Y., Plasmonic properties of the multispot copper-capped nanoparticle array chip and its application to optical biosensors for pathogen detection of multiplex DNAs. *Anal Chem,* **2011**, 83(16): 6215-6222.

84. Kang, T., Yoo, S.M., Yoon, I., Lee, S.Y., and Kim, B., Patterned multiplex pathogen DNA detection by Au particle-on-wire SERS sensor. *Nano Lett,* **2010**, 10(4): 1189-1193.

85. Cha, B.H., Lee, S.M., Park, J.C., Hwang, K.S., Kim, S.K., Lee, Y.S., Ju, B.K., and Kim, T.S., Detection of hepatitis B virus (HBV) DNA at femtomolar concentrations using a silica nanoparticle-enhanced microcantilever sensor. *Biosens Bioelectron,* **2009**, 25(1): 130-135.

86. Rojanathanes, R., Sereemaspun, A., Pimpha, N., Buasorn, V., Ekawong, P., and Wiwanitkit, V., Gold nanoparticle as an alternative tool for a urine pregnancy test. *Taiwan J Obstet Gynecol,* **2008**, 47(3): 296-299.

87. Elghanian, R., Storhoff, J.J., Mucic, R.C., Letsinger, R.L., and Mirkin, C.A., Selective colorimetric detection of polynucleotides based on the distance-dependent optical properties of gold nanoparticles. *Science,* **1997**, 277(5329): 1078-1081.

88. Storhoff, J.J., Marla, S.S., Bao, P., Hagenow, S., Mehta, H., Lucas, A., Garimella, V., Patno, T., Buckingham, W., Cork, W., and Muller, U.R., Gold nanoparticle-based detection of genomic DNA targets on microarrays using a novel optical detection system. *Biosens Bioelectron,* **2004**, 19(8): 875-883.

89. Nie, L., Tang, J., Guo, H., Chen, H., Xiao, P., and He, N., Colorimetric detection of polynucleotides on polypropylene slices. *Anal Sci,* **2004**, 20(3): 461-463.

90. Jelen, F., Yosypchuk, B., Kourilova, A., Novotny, L., and Palecek, E., Label-free determination of picogram quantities of DNA by stripping voltammetry with solid copper amalgam or mercury electrodes in the presence of copper. *Anal Chem,* **2002**, 74(18): 4788-4793.

91. Wang, J. and Kawde, A.N., Amplified label-free electrical detection of DNA hybridization. *Analyst,* **2002**, 127(3): 383-386.

92. Tosar, J.P., Branas, G., and Laiz, J., Electrochemical DNA hybridization sensors applied to real and complex biological samples. *Biosens Bioelectron,* **2010**, 26(4): 1205-1217.

93. de la Escosura-Muniz, A. and Merkoci, A., Nanoparticle based enhancement of electrochemical DNA hybridization signal using nanoporous electrodes. *Chem Commun (Camb),* **2010**, 46(47): 9007-9009.

94. Boon, E.M., Ceres, D.M., Drummond, T.G., Hill, M.G., and Barton, J.K., Mutation detection by electrocatalysis at DNA-modified electrodes. *Nat Biotechnol,* **2000**, 18(10): 1096-1100.

95. Yang, W.R., Ozsoz, M., Hibbert, D.B., and Gooding, J.J., Evidence for the direct interaction between methylene blue and guanine bases using DNA-Modified carbon paste electrodes. *Electroanalysis,* **2002**, 14(18): 1299-1302.

96. Zhu, L., Zhao, R.J., Wang, K.G., Xiang, H.B., Shang, Z.M., and Sun, W., Electrochemical behaviors of methylene blue on DNA modified electrode and its application to the detection of PCR product from NOS sequence. *Sensors,* **2008**, 8(9): 5649-5660.

97. Kelley, S.O., Jackson, N.M., Hill, M.G., and Barton, J.K., Long-range electron transfer through DNA films. *Angew Chem Int Ed,* **1999**, 38(7): 941-945.

98. Xiao, Y., Lubin, A.A., Baker, B.R., Plaxco, K.W., and Heeger, A.J., Single-step electronic detection of femtomolar DNA by target-induced strand displacement in an electrode-bound duplex. *Proc Natl Acad Sci U S A,* **2006**, 103(45): 16677-16680.

99. Tichoniuk, M., Gwiazdowska, D., Ligaj, M., and Filipiak, M., Electrochemical detection of foodborne pathogen Aeromonas hydrophila by DNA hybridization biosensor. *Biosens Bioelectron,* **2010**, 26(4): 1618-1623.

100. Soleymani, L., Fang, Z., Sun, X., Yang, H., Taft, B.J., Sargent, E.H., and Kelley, S.O., Nanostructuring of patterned microelectrodes to enhance the sensitivity of electrochemical nucleic acids detection. *Angew Chem Int Ed,* **2009**, 48(45): 8457-8460.

101. Das, J. and Kelley, S.O., Tuning the bacterial detection sensitivity of nanostructured microelectrodes. *Anal Chem,* **2013**, 85(15): 7333-7338.

102. Pinijsuwan, S., Rijiravanich, P., Somasundrum, M., and Surareungchai, W., Attomolar electrochemical detection of DNA hybridization based on enhanced latex/gold nanoparticles. *Adv Eng Mater,* **2010**, 12(11): B649-B653.

103. Subramanian, S., Aschenbach, K.H., Evangelista, J.P., Najjar, M.B., Song, W.X., and Gomez, R.D., Rapid, sensitive and label-free detection of Shiga-toxin producing Escherichia coli O157 using carbon nanotube biosensors. *Biosens Bioelectron,* **2012**, 32(1): 69-75.

104. Thuy, N.T., Tam, P.D., Tuan, M.A., Le, A.T., Tam, L.T., Thu, V.V., Hieu, N.V., and Chien, N.D., Detection of pathogenic microorganisms using biosensor based on multi-walled carbon nanotubes dispersed in DNA solution. *Curr Appl Phys,* **2012**, 12(6): 1553-1560.

105. Liu, F., Choi, K.S., Park, T.J., Lee, S.Y., and Seo, T.S., Graphene-based electrochemical biosensor for pathogenic virus detection. *Biochip J,* **2011**, 5(2): 123-128.

106. Su, X., Teh, H.F., Aung, K.M., Zong, Y., and Gao, Z., Femtomol SPR detection of DNA-PNA hybridization with the assistance of DNA-guided polyaniline deposition. *Biosens Bioelectron,* **2008**, 23(11): 1715-1720.

107. Huang, C.J., Dostalek, J., Sessitsch, A., and Knoll, W., Long-range surface plasmon-enhanced fluorescence spectroscopy biosensor for ultrasensitive detection of E. coli O157:H7. *Anal Chem,* **2011**, 83(3): 674-677.

108. Wang, Y., Knoll, W., and Dostalek, J., Bacterial pathogen surface plasmon resonance biosensor advanced by long range surface plasmons and magnetic nanoparticle assays. *Anal Chem,* **2012**, 84(19): 8345-8350.

109. Xia, H., Wang, F., Huang, Q., Huang, J.F., Chen, M., Wang, J., Yao, C.Y., Chen, Q.H., Cai, G.R., and Fu, W.L., Detection of Staphylococcus epidermidis by a quartz crystal microbalance nucleic acid biosensor array using Au nanoparticle signal amplification. *Sensors,* **2008**, 8(10): 6453-6470.

110. Zhou, H.Y., Gao, Z.X., Luo, G.H., Han, L., Sun, S.M., and Wang, H.Y., Determination of Listeria monocytogenes in milk samples by signal amplification quartz crystal microbalance sensor. *Analyt Lett,* **2010**, 43(2): 312-322.

111. Hao, R.Z., Song, H.B., Zuo, G.M., Yang, R.F., Wei, H.P., Wang, D.B., Cui, Z.Q., Zhang, Z.P., Cheng, Z.X., and Zhang, X.E., DNA probe functionalized QCM biosensor based on gold nanoparticle amplification for Bacillus anthracis detection. *Biosens Bioelectron,* **2011**, 26(8): 3398-3404.

112. Kleo, K., Kapp, A., Ascher, L., and Lisdat, F., Detection of vaccinia virus DNA by quartz crystal microbalance. *Anal Biochem,* **2011**, 418(2): 260-266.

113. Hur, Y., Han, J., Seon, J., Pak, Y.E., and Roh, Y., Development of an SH-SAW sensor for the detection of DNA hybridization. *Sensor Actuat A-Phys,* **2005**, 120(2): 462-467.

114. Xu, Q.H., Chang, K., Lu, W.P., Chen, W., Ding, Y., Jia, S.R., Zhang, K.J., Li, F.K., Shi, J.F., Cao, L., Deng, S.L., and Chen, M., Detection of single-nucleotide polymorphisms with novel leaky surface acoustic wave biosensors, DNA ligation and enzymatic signal amplification. *Biosens Bioelectron,* **2012**, 33(1): 274-278.

115. Mirasoli, M., Bonvicini, F., Dolci, L.S., Zangheri, M., Gallinella, G., and Roda, A., Portable chemiluminescence multiplex biosensor for quantitative detection of three B19 DNA genotypes. *Anal Bioanal Chem,* **2013**, 405(2-3): 1139-1143.

116. Liu, X., Farmerie, W., Schuster, S., and Tan, W., Molecular beacons for DNA biosensors with micrometer to submicrometer dimensions. *Anal Biochem,* **2000**, 283(1): 56-63.

117. Wang, H., Li, J., Liu, H., Liu, Q., Mei, Q., Wang, Y., Zhu, J., He, N., and Lu, Z., Label-free hybridization detection of a single nucleotide mismatch by immobilization of molecular beacons on an agarose film. *Nucleic Acids Res,* **2002**, 30(12): e61.

118. Yoshida, A., Nagashima, S., Ansai, T., Tachibana, M., Kato, H., Watari, H., Notomi, T., and Takehara, T., Loop-mediated isothermal amplification method for rapid detection of the periodontopathic bacteria Porphyromonas gingivalis, Tannerella forsythia, and Treponema denticola. *J Clin Microbiol,* **2005**, 43(5): 2418-2424.

119. Parida, M., Horioke, K., Ishida, H., Dash, P.K., Saxena, P., Jana, A.M., Islam, M.A., Inoue, S., Hosaka, N., and Morita, K., Rapid detection and differentiation of dengue virus serotypes by a real-time reverse transcription-loop-mediated isothermal amplification assay. *J Clin Microbiol,* **2005**, 43(6): 2895-2903.

120. Xiang, D.S., Zhai, K., and Wang, L.Z., Multiplexed DNA detection with a composite molecular beacon based on guanine-quenching. *Analyst,* **2013**, 138(18): 5318-5324.

121. Lam, B., Das, J., Holmes, R.D., Live, L., Sage, A., Sargent, E.H., and Kelley, S.O., Solution-based circuits enable rapid and multiplexed pathogen detection. *Nat Commun,* **2013**, 4: 2001.

122. Ravindranath, S.P., Wang, Y.L., and Irudayaraj, J., SERS driven cross-platform based multiplex pathogen detection. *Sensor Actuat B-Chem,* **2011**, 152(2): 183-190.

123. Varma-Basil, M., El-Hajj, H., Marras, S.A., Hazbon, M.H., Mann, J.M., Connell, N.D., Kramer, F.R., and Alland, D., Molecular beacons for multiplex detection of four bacterial bioterrorism agents. *Clin Chem,* **2004**, 50(6): 1060-1062.

124. Gubala, A.J. and Proll, D.F., Molecular-beacon multiplex real-time PCR assay for detection of Vibrio cholerae. *Appl Environ Microbiol,* **2006**, 72(9): 6424-6428.

125. Luo, X. and Hsing, I.M., Immobilization-free multiplex electrochemical DNA and SNP detection. *Biosens Bioelectron,* **2009**, 25(4): 803-808.

126. Li, X.M., Fu, P.Y., Liu, J.M., and Zhang, S.S., Biosensor for multiplex detection of two DNA target sequences using enzyme-functionalized Au nanoparticles as signal amplification. *Anal Chim Acta,* **2010**, 673(2): 133-138.

127. Zhao, Y.J., Zhao, X.W., Tang, B.C., Xu, W.Y., Li, J., Hu, L., and Gu, Z.Z., Quantum-dot-tagged bioresponsive hydrogel suspension array for multiplex aabel-free DNA detection. *Adv Funct Mater,* **2010**, 20(6): 976-982.

128. Algar, W.R. and Krull, U.J., Toward a multiplexed solid-phase nucleic acid hybridization assay using quantum dots as donors in fluorescence resonance energy transfer. *Anal Chem,* **2009**, 81(10): 4113-4120.

129. Freeman, R., Liu, X., and Willner, I., Amplified multiplexed analysis of DNA by the exonuclease III-catalyzed regeneration of the target DNA in the presence of functionalized semiconductor quantum dots. *Nano Lett,* **2011**, 11(10): 4456-4461.

130. Biju, V., Anas, A., Akita, H., Shibu, E.S., Itoh, T., Harashima, H., and Ishikawa, M., FRET from quantum dots to photodecompose undesired acceptors and report the condensation and decondensation of plasmid DNA. *ACS Nano,* **2012**, 6(5): 3776-3788.

131. Geissler, D., Charbonniere, L.J., Ziessel, R.F., Butlin, N.G., Lohmannsroben, H.G., and Hildebrandt, N., Quantum dot biosensors for ultrasensitive multiplexed diagnostics. *Angew Chem Int Ed,* **2010**, 49(8): 1396-1401.

132. Zhang, C.Y. and Hu, J., Single quantum dot-based nanosensor for multiple DNA detection. *Anal Chem,* **2010**, 82(5): 1921-1927.

133. Sandhu, A., Biosensing: new probes offer much faster results. *Nat Nanotechnol,* **2007**, 2(12): 746-748.

134. Drummond, T.G., Hill, M.G., and Barton, J.K., Electrochemical DNA sensors. *Nat Biotechnol,* **2003**, 21(10): 1192-1199.

135. Liu, J., Cao, Z., and Lu, Y., Functional nucleic acid sensors. *Chem Rev,* **2009**, 109(5): 1948-1998.

136. Sassolas, A., Leca-Bouvier, B.D., and Blum, L.J., DNA biosensors and microarrays. *Chem Rev,* **2008**, 108(1): 109-139.

137. Browne, K.A., Sequence-specific, self-reporting hairpin inversion probes. *J Am Chem Soc,* **2005**, 127(6): 1989-1994.

138. Bustin, S.A., Absolute quantification of mRNA using real-time reverse transcription polymerase chain reaction assays. *J Mol Endocrinol,* **2000**, 25(2): 169-193.

139. Raymond, C.K., Roberts, B.S., Garrett-Engele, P., Lim, L.P., and Johnson, J.M., Simple, quantitative primer-extension PCR assay for direct monitoring of microRNAs and short-interfering RNAs. *RNA,* **2005**, 11(11): 1737-1744.

140. Zhang, P., Beck, T., and Tan, W.H., Design of a molecular beacon DNA probe with two fluorophores. *Angew Chem Int Ed,* **2001**, 40(2): 402-405.

141. Zhang, C.Y., Yeh, H.C., Kuroki, M.T., and Wang, T.H., Single-quantum-dot-based DNA nanosensor. *Nat Mater,* **2005**, 4(11): 826-831.

142. Yao, G. and Tan, W., Molecular-beacon-based array for sensitive DNA analysis. *Anal Biochem,* **2004**, 331(2): 216-223.

143. Nallur, G., Luo, C., Fang, L., Cooley, S., Dave, V., Lambert, J., Kukanskis, K., Kingsmore, S., Lasken, R., and Schweitzer, B., Signal amplification by rolling circle amplification on DNA microarrays. *Nucleic Acids Res,* **2001**, 29(23): E118.

144. Wallner, G., Amann, R., and Beisker, W., Optimizing fluorescent in situ hybridization with rRNA-targeted oligonucleotide probes for flow cytometric identification of microorganisms. *Cytometry,* **1993**, 14(2): 136-143.

145. Medintz, I.L., Konnert, J.H., Clapp, A.R., Stanish, I., Twigg, M.E., Mattoussi, H., Mauro, J.M., and Deschamps, J.R., A fluorescence resonance energy transfer-derived structure of a quantum dot-protein bioconjugate nanoassembly. *Proc Natl Acad Sci U S A,* **2004**, 101(26): 9612-9617.

146. Sando, S. and Kool, E.T., Imaging of RNA in bacteria with self-ligating quenched probes. *J Am Chem Soc,* **2002**, 124(33): 9686-9687.

147. Paras, P.N., Introduction to Biophotonics. 2003, Hoboken, NJ: *John Wiley & Sons, Inc*. 624.

148. Fujii, R., Kitaoka, M., and Hayashi, K., Error-prone rolling circle amplification: the simplest random mutagenesis protocol. *Nat Protoc,* **2006**, 1(5): 2493-2497.

149. Zhao, X.J., Tapec-Dytioco, R., and Tan, W.H., Ultrasensitive DNA detection using highly fluorescent bioconjugated nanoparticles. *J Am Chem Soc,* **2003**, 125(38): 11474-11475.

150. Subramanian, C., Xu, Y., Johnson, C.H., and von Arnim, A.G., In vivo detection of protein-protein interaction in plant cells using BRET. *Methods Mol Biol,* **2004**, 284: 271-286.

151. Morise, H., Shimomura, O., Johnson, F.H., and Winant, J., Intermolecular energy transfer in the bioluminescent system of Aequorea. *Biochemistry,* **1974**, 13(12): 2656-2662.

152. Gomes, I., Jordan, B.A., Gupta, A., Rios, C., Trapaidze, N., and Devi, L.A., G protein coupled receptor dimerization: implications in modulating receptor function. *J Mol Med (Berl),* **2001**, 79(5-6): 226-242.

153. Eidne, K.A., Kroeger, K.M., and Hanyaloglu, A.C., Applications of novel resonance energy transfer techniques to study dynamic hormone receptor interactions in living cells. *Trends Endocrinol Metab,* **2002**, 13(10): 415-421.

154. Pfleger, K.D. and Eidne, K.A., New technologies: bioluminescence resonance energy transfer (BRET) for the detection of real time interactions involving G-protein coupled receptors. *Pituitary,* **2003**, 6(3): 141-151.

155. Kroeger, K.M., Hanyaloglu, A.C., and Eidne, K.A., Applications of BRET to study dynamic G-protein coupled receptor interactions in living cells. *Lett Pept Sci,* **2001**, 8(3-5): 155-162.

156. Walls, Z.F. and Gambhir, S.S., BRET-based method for detection of specific RNA species. *Bioconjugate Chem,* **2008**, 19(1): 178-184.

157. Dacres, H., Dumancic, M.M., Horne, I., and Trowell, S.C., Direct comparison of fluorescence- and bioluminescence-based resonance energy transfer methods for real-time monitoring of thrombin-catalysed proteolytic cleavage. *Biosens Bioelectron,* **2009**, 24(5): 1164-1170.

158. Kairdolf, B.A., Mancini, M.C., Smith, A.M., and Nie, S., Minimizing nonspecific cellular binding of quantum dots with hydroxyl-derivatized surface coatings. *Anal Chem,* **2008**, 80(8): 3029-3034.

159. Arai, R., Nakagawa, H., Tsumoto, K., Mahoney, W., Kumagai, I., Ueda, H., and Nagamune, T., Demonstration of a homogeneous noncompetitive immunoassay based on bioluminescence resonance energy transfer. *Anal Biochem,* **2001**, 289(1): 77-81.

160. Boute, N., Jockers, R., and Issad, T., The use of resonance energy transfer in high-throughput screening: BRET versus FRET. *Trends Pharmacol Sci,* **2002**, 23(8): 351-354.

161. Gammon, S.T., Villalobos, V.M., Roshal, M., Samrakandi, M., and Piwnica-Worms, D., Rational design of novel red-shifted BRET pairs: Platforms for real-time single-chain protease biosensors. *Biotechnol Prog,* **2009**, 25(2): 559-569.

162. Lizardi, P.M., Huang, X.H., Zhu, Z.R., Bray-Ward, P., Thomas, D.C., and Ward, D.C., Mutation detection and single-molecule counting using isothermal rolling-circle amplification. *Nat Genet,* **1998**, 19(3): 225-232.

163. Okamoto, H., Okada, S., Sugiyama, Y., Tanaka, T., Sugai, Y., Akahane, Y., Machida, A., Mishiro, S., Yoshizawa, H., Miyakawa, Y., and et al., Detection of hepatitis C virus RNA by a two-stage polymerase chain reaction with two pairs of primers deduced from the 5'-noncoding region. *Jpn J Exp Med,* **1990**, 60(4): 215-222.

164. Lanciotti, R.S., Kerst, A.J., Nasci, R.S., Godsey, M.S., Mitchell, C.J., Savage, H.M., Komar, N., Panella, N.A., Allen, B.C., Volpe, K.E., Davis, B.S., and Roehrig, J.T., Rapid detection of west nile virus from human clinical specimens, field-collected mosquitoes, and avian samples by a TaqMan reverse transcriptase-PCR assay. *J Clin Microbiol,* **2000**, 38(11): 4066-4071.

165. Payungporn, S., Chutinimitkul, S., Chaisingh, A., Damrongwantanapokin, S., Buranathai, C., Amonsin, A., Theamboonlers, A., and Poovorawan, Y., Single step multiplex real-time RT-PCR for H5N1 influenza A virus detection. *J Virol Methods,* **2006**, 131(2): 143-147.

166. Hashimoto, K., Ito, K., and Ishimori, Y., Sequence-specific gene detection with a gold electrode modified with DNA probes and an electrochemically active dye. *Anal Chem,* **1994**, 66(21): 3830-3833.

167. Wang, J., Cai, X., Rivas, G., Shiraishi, H., Farias, P.A., and Dontha, N., DNA electrochemical biosensor for the detection of short DNA sequences related to the human immunodeficiency virus. *Anal Chem,* **1996**, 68(15): 2629-2634.

168. Meric, B., Kerman, K., Ozkan, D., Kara, P., Erensoy, S., Akarca, U.S., Mascini, M., and Ozsoz, M., Electrochemical DNA biosensor for the detection of TT and Hepatitis B virus from PCR amplified real samples by using methylene blue. *Talanta,* **2002**, 56(5): 837-846.

169. Goodrich, T.T., Lee, H.J., and Corn, R.M., Direct detection of genomic DNA by enzymatically amplified SPR imaging measurements of RNA microarrays. *J Am Chem Soc,* **2004**, 126(13): 4086-4087.

170. Yao, C., Zhu, T., Tang, J., Wu, R., Chen, Q., Chen, M., Zhang, B., Huang, J., and Fu, W., Hybridization assay of hepatitis B virus by QCM peptide nucleic acid biosensor. *Biosens Bioelectron,* **2008**, 23(6): 879-885.

171. Alodhayb, A., Brown, N., Rahman, S.M.S., Harrigan, R., and Beaulieu, L.Y., Towards detecting the human immunodeficiency virus using microcantilever sensors. *Applied Physics Letters,* **2013**, 102(17).

172. Parida, M., Posadas, G., Inoue, S., Hasebe, F., and Morita, K., Real-time reverse transcription loop-mediated isothermal amplification for rapid detection of West Nile virus. *J Clin Microbiol,* **2004**, 42(1): 257-263.

173. Jinks, D.C., Minter, M., Tarver, D.A., Vanderford, M., Hejtmancik, J.F., and Mccabe, E.R.B., Molecular genetic diagnosis of sickle-cell disease using dried blood specimens on blotters used for newborn screening. *Hum Genet,* **1989**, 81(4): 363-366.

174. Witt, M. and Erickson, R.P., A rapid method for detection of Y-chromosomal DNA from dried blood specimens by the polymerase chain-reaction. *Hum Genet,* **1989**, 82(3): 271-274.

175. Martinez, A.W., Phillips, S.T., Butte, M.J., and Whitesides, G.M., Patterned paper as a platform for inexpensive, low-volume, portable bioassays. *Angew Chem Int Ed,* **2007**, 46(8): 1318-1320.

176. Carrilho, E., Phillips, S.T., Vella, S.J., Martinez, A.W., and Whitesides, G.M., Paper microzone plates. *Anal Chem,* **2009**, 81(15): 5990-5998.

177. Hutt-Fletcher, L.M., Epstein-Barr virus entry. *J Virol,* **2007**, 81(15): 7825-7832.

178. Khan, G., Coates, P.J., Kangro, H.O., and Slavin, G., Epstein Barr virus (EBV) encoded small RNAs: targets for detection by in situ hybridisation with oligonucleotide probes. *J Clin Pathol,* **1992**, 45(7): 616-620.

179. Wu, T.C., Mann, R.B., Epstein, J.I., MacMahon, E., Lee, W.A., Charache, P., Hayward, S.D., Kurman, R.J., Hayward, G.S., and Ambinder, R.F., Abundant expression of EBER1 small nuclear RNA in nasopharyngeal carcinoma. A morphologically distinctive target for detection of Epstein-Barr virus in formalin-fixed paraffin-embedded carcinoma specimens. *Am J Pathol,* **1991**, 138(6): 1461-1469.

180. Sheikh, T.I. and Qadri, I., Expression of EBV encoded viral RNA 1, 2 and anti-inflammatory cytokine (interleukin-10) in FFPE lymphoma specimens: a preliminary study for diagnostic implication in Pakistan. *Diagn Pathol,* **2011**, 6: 70.

181. Carrilho, E., Martinez, A.W., and Whitesides, G.M., Understanding wax printing: a simple micropatterning process for paper-based microfluidics. *Anal Chem,* **2009**, 81(16): 7091-7095.

182. Flint, S.J., Racaniello, V.R., and Krug, R., Principles of virology: molecular biology, pathogenesis, and control. 1st ed. 1999: *American Society Microbiology*. 820.

183. Baltimore, D., Expression of animal virus genomes. *Bacteriol Rev,* **1971**, 35(3): 235-241.

184. Chomczynski, P. and Sacchi, N., The single-step method of RNA isolation by acid guanidinium thiocyanate-phenol-chloroform extraction: twenty-something years on. *Nat Protoc,* **2006**, 1(2): 581-585.

185. Pelton, R., Bioactive paper provides a low-cost platform for diagnostics. *Trac-Trends Anal Chem,* **2009**, 28(8): 925-942.

186. Dye, C., Scheele, S., Dolin, P., Pathania, V., Raviglione, R.C., and Project, W.G.S.M., Global burden of tuberculosis - Estimated incidence, prevalence, and mortality by country. *Jama-J Am Med Assoc,* **1999**, 282(7): 677-686.

187. Keeler, E., Perkins, M.D., Small, P., Hanson, C., Reed, S., Cunningham, J., Aledort, J.E., Hillborne, L., Rafael, M.E., Girosi, F., and Dye, C., Reducing the global burden of tuberculosis: the contribution of improved diagnostics. *Nature,* **2006**, 444 Suppl 1: 49-57.

188. Perkins, M.D. and Small, P.M., Partnering for better microbial diagnostics. *Nat Biotechnol,* **2006**, 24(8): 919-921.

189. Small, P.M. and Pai, M., Tuberculosis diagnosis--time for a game change. *N Engl J Med,* **2010**, 363(11): 1070-1071.

190. Foulds, J. and O'Brien, R., New tools for the diagnosis of tuberculosis: the perspective of developing countries. *Int J Tuberc Lung Dis,* **1998**, 2(10): 778-783.

191. McNerney, R., Maeurer, M., Abubakar, I., Marais, B., McHugh, T.D., Ford, N., Weyer, K., Lawn, S., Grobusch, M.P., Memish, Z., Squire, S.B., Pantaleo, G., Chakaya, J., Casenghi, M., Migliori, G.B., Mwaba, P., Zijenah, L., Hoelscher, M., Cox, H., Swaminathan, S., Kim, P.S., Schito, M., Harari, A., Bates, M., Schwank, S., O'Grady, J., Pletschette, M., Ditui, L., Atun, R., and Zumla, A., Tuberculosis diagnostics and biomarkers: needs, challenges, recent advances, and opportunities. *J Infect Dis,* **2012**, 205 Suppl 2: S147-158.

192. Martin, A., Barrera, L., and Palomino, J.C., Biomarkers and diagnostics for tuberculosis. *Lancet,* **2010**, 376(9752): 1539-1540; author reply 1540.

193. Wallis, R.S., Pai, M., Menzies, D., Doherty, T.M., Walzl, G., Perkins, M.D., and Zumla, A., Tuberculosis 4 Biomarkers and diagnostics for tuberculosis: progress, needs, and translation into practice. *Lancet,* **2010**, 375(9729): 1920-1937.

194. Urdea, M., Penny, L.A., Olmsted, S.S., Giovanni, M.Y., Kaspar, P., Shepherd, A., Wilson, P., Dahl, C.A., Buchsbaum, S., Moeller, G., and

Hay Burgess, D.C., Requirements for high impact diagnostics in the developing world. *Nature,* **2006**, 444 Suppl 1: 73-79.

195. Ling, D.I., Flores, L.L., Riley, L.W., and Pai, M., Commercial nucleic-acid amplification tests for diagnosis of pulmonary tuberculosis in respiratory specimens: meta-analysis and meta-regression. *PLoS One,* **2008**, 3(2): e1536.

196. Neonakis, I.K., Spandidos, D.A., and Petinaki, E., Use of loop-mediated isothermal amplification of DNA for the rapid detection of Mycobacterium tuberculosis in clinical specimens. *Eur J Clin Microbiol Infect Dis,* **2011**, 30(8): 937-942.

197. Parsons, L.M., Somoskovi, A., Gutierrez, C., Lee, E., Paramasivan, C.N., Abimiku, A., Spector, S., Roscigno, G., and Nkengasong, J., Laboratory diagnosis of tuberculosis in resource-poor countries: challenges and opportunities. *Clin Microbiol Rev,* **2011**, 24(2): 314-350.

198. Niemz, A., Ferguson, T.M., and Boyle, D.S., Point-of-care nucleic acid testing for infectious diseases. *Trends Biotechnol,* **2011**, 29(5): 240-250.

199. Boehme, C.C., Nabeta, P., Henostroza, G., Raqib, R., Rahim, Z., Gerhardt, M., Sanga, E., Hoelscher, M., Notomi, T., Hase, T., and Perkins, M.D., Operational feasibility of using loop-mediated isothermal amplification for diagnosis of pulmonary tuberculosis in microscopy centers of developing countries. *J Clin Microbiol,* **2007**, 45(6): 1936-1940.

200. Chung, H.J., Castro, C.M., Im, H., Lee, H., and Weissleder, R., A magneto-DNA nanoparticle system for rapid detection and phenotyping of bacteria. *Nat Nanotechnol,* **2013**, 8(5): 369-375.

201. Nge, P.N., Rogers, C.I., and Woolley, A.T., Advances in microfluidic materials, functions, integration, and applications. *Chem Rev,* **2013**, 113(4): 2550-2583.

202. Whitesides, G.M., The origins and the future of microfluidics. *Nature,* **2006**, 442(7101): 368-373.

203. Martinez, A.W., Phillips, S.T., Wiley, B.J., Gupta, M., and Whitesides, G.M., FLASH: a rapid method for prototyping paper-based microfluidic devices. *Lab Chip,* **2008**, 8(12): 2146-2150.

204. Allen, P.B., Arshad, S.A., Li, B.L., Chen, X., and Ellington, A.D., DNA circuits as amplifiers for the detection of nucleic acids on a paperfluidic platform. *Lab Chip,* **2012**, 12(16): 2951-2958.

205. Ali, M.M., Aguirre, S.D., Xu, Y.Q., Filipe, C.D.M., Pelton, R., and Li, Y.F., Detection of DNA using bioactive paper strips. *Chem Commun (Camb),* **2009**(43): 6640-6642.

206. Araujo, A.C., Song, Y.J., Lundeberg, J., Stahl, P.L., and Brumer, H., Activated paper surfaces for the rapid hybridization of DNA through capillary transport. *Anal Chem,* **2012**, 84(7): 3311-3317.

207. Beerli, R.R. and Barbas, C.F., 3rd, Engineering polydactyl zinc-finger transcription factors. *Nat Biotechnol,* **2002**, 20(2): 135-141.

208. Wolfe, S.A., Nekludova, L., and Pabo, C.O., DNA recognition by Cys2His2 zinc finger proteins. *Annu Rev Biophys Biomol Struct,* **2000**, 29: 183-212.

209. Klug, A., The discovery of zinc fingers and their applications in gene regulation and genome manipulation. *Annu Rev Biochem,* **2010**, 79: 213-231.

210. Pavletich, N.P. and Pabo, C.O., zinc finger DNA recognition - crystal-structure of a Zif268-DNA complex at 2.1-A. *Science,* **1991**, 252(5007): 809-817.

211. Dhanasekaran, M., Negi, S., and Sugiura, Y., Designer zinc finger proteins: Tools for creating artificial DNA-binding functional proteins. *Acc Chem Res,* **2006**, 39(1): 45-52.

212. Mandell, J.G. and Barbas, C.F., Zinc finger tools: custom DNA-binding domains for transcription factors and nucleases. *Nucleic Acids Res,* **2006**, 34: W516-W523.

213. Segal, D.J., Beerli, R.R., Blancafort, P., Dreier, B., Effertz, K., Huber, A., Koksch, B., Lund, C.V., Magnenat, L., Valente, D., and Barbas, C.F., 3rd, Evaluation of a modular strategy for the construction of novel polydactyl zinc finger DNA-binding proteins. *Biochemistry,* **2003**, 42(7): 2137-2148.

214. Bogdanove, A.J. and Voytas, D.F., TAL effectors: customizable proteins for DNA targeting. *Science,* **2011**, 333(6051): 1843-1846.

215. Ikebukuro, K., Kumagai, T., Motoki, H., Osawa, Y., Matuo, T., Horiuchi, M., and Sode, K., Specific detection of PCR product from Legionella pneumophila strain Philadelphia1 using zinc finger protein Sp2. *Nucleic Acids Symp Ser (Oxf),* **2007**(51): 285-286.

216. Osawa, Y., Motoki, H., Matsuo, T., Horiuchi, M., Sode, K., and Ikebukuro, K., Zinc finger protein-based detection system of PCR products for pathogen diagnosis. *Nucleic Acids Symp Ser (Oxf),* **2008**(52): 23-24.

217. Osawa, Y., Ikebukuro, K., and Sode, K., Zn finger-based direct detection system for PCR products of Salmonella spp. and the Influenza A virus. *Biotechnol Lett,* **2009**, 31(5): 725-733.

218. Stains, C.I., Porter, J.R., Ooi, A.T., Segal, D.J., and Ghosh, I., DNA sequence-enabled reassembly of the green fluorescent protein. *J Am Chem Soc,* **2005**, 127(31): 10782-10783.

219. Ooi, A.T., Stains, C.I., Ghosh, I., and Segal, D.J., Sequence-enabled reassembly of beta-lactamase (SEER-LAC): a sensitive method for the detection of double-stranded DNA. *Biochemistry,* **2006**, 45(11): 3620-3625.

220. Bergval, I.L., Vijzelaar, R.N., Dalla Costa, E.R., Schuitema, A.R., Oskam, L., Kritski, A.L., Klatser, P.R., and Anthony, R.M., Development of multiplex assay for rapid characterization of Mycobacterium tuberculosis. *J Clin Microbiol,* **2008**, 46(2): 689-699.

221. Siritantikorn, S., Jintaworn, S., Noisakran, S., Suputtamongkol, Y., Paris, D.H., and Blacksell, S.D., Application of ImageJ program to the enumeration of Orientia tsutsugamushi organisms cultured in vitro. *Trans R Soc Trop Med Hyg,* **2012**, 106(10): 632-635.

222. Nie, Z., Deiss, F., Liu, X., Akbulut, O., and Whitesides, G.M., Integration of paper-based microfluidic devices with commercial electrochemical readers. *Lab Chip,* **2010**, 10(22): 3163-3169.

223. Wang, S., Ge, L., Song, X., Yan, M., Ge, S., Yu, J., and Zeng, F., Simple and covalent fabrication of a paper device and its application in sensitive chemiluminescence immunoassay. *Analyst,* **2012**, 137(16): 3821-3827.

224. Tomita, N., Mori, Y., Kanda, H., and Notomi, T., Loop-mediated isothermal amplification (LAMP) of gene sequences and simple visual detection of products. *Nat Protoc,* **2008**, 3(5): 877-882.

225. Iwamoto, T., Sonobe, T., and Hayashi, K., Loop-mediated isothermal amplification for direct detection of Mycobacterium tuberculosis complex, M. avium, and M. intracellulare in sputum samples. *J Clin Microbiol,* **2003**, 41(6): 2616-2622.

226. Petersohn, D. and Thiel, G., Role of zinc-finger proteins Sp1 and zif268/egr-1 in transcriptional regulation of the human synaptobrevin II gene. *Eur J Biochem,* **1996**, 239(3): 827-834.

227. Fujiwara, K. and Kitagawa, T., A new enzyme-linked-immunosorbent-assay (Elisa) for spermidine using glutaraldehyde coupling of the hapten

to carrier-coated microtiter plates. *J Biochem (Tokyo),* **1993**, 114(5): 708-713.

228. Pollock, N.R., Rolland, J.P., Kumar, S., Beattie, P.D., Jain, S., Noubary, F., Wong, V.L., Pohlmann, R.A., Ryan, U.S., and Whitesides, G.M., A paper-based multiplexed transaminase test for low-cost, point-of-care liver function testing. *Sci Transl Med,* **2012**, 4(152): 152ra129.

229. Lewis, G.G., DiTucci, M.J., and Phillips, S.T., Quantifying analytes in paper-based microfluidic devices without using external electronic readers. *Angew Chem Int Ed,* **2012**, 51(51): 12707-12710.

230. Liu, H. and Crooks, R.M., Paper-based electrochemical sensing platform with integral battery and electrochromic read-out. *Anal Chem,* **2012**, 84(5): 2528-2532.

231. Thom, N.K., Yeung, K., Pillion, M.B., and Phillips, S.T., "Fluidic batteries" as low-cost sources of power in paper-based microfluidic devices. *Lab Chip,* **2012**, 12(10): 1768-1770.

232. Yan, J., Ge, L., Song, X., Yan, M., Ge, S., and Yu, J., Paper-based electrochemiluminescent 3D immunodevice for lab-on-paper, specific, and sensitive point-of-care testing. *Chemistry,* **2012**, 18(16): 4938-4945.

233. Mori, Y. and Notomi, T., Loop-mediated isothermal amplification (LAMP): a rapid, accurate, and cost-effective diagnostic method for infectious diseases. *J Infect Chemother,* **2009**, 15(2): 62-69.

234. Ghosh, I., Stains, C.I., Ooi, A.T., and Segal, D.J., Direct detection of double-stranded DNA: molecular methods and applications for DNA diagnostics. *Mol Biosyst,* **2006**, 2(11): 551-560.

235. Li, X., Ballerini, D.R., and Shen, W., A perspective on paper-based microfluidics: current status and future trends. *Biomicrofluidics,* **2012**, 6(1): 11301-1130113.

236. Fu, E., Kauffman, P., Lutz, B., and Yager, P., Chemical signal amplification in two-dimensional paper networks. *Sensor Actuat B-Chem,* **2010**, 149(1): 325-328.

237. Lee, C.H., Hankus, M.E., Tian, L., Pellegrino, P.M., and Singamaneni, S., Highly sensitive surface enhanced Raman scattering substrates based on filter paper loaded with plasmonic nanostructures. *Anal Chem,* **2011**, 83(23): 8953-8958.

238. Wang, P., Ge, L., Ge, S., Yu, J., Yan, M., and Huang, J., A paper-based photoelectrochemical immunoassay for low-cost and multiplexed point-of-care testing. *Chem Commun (Camb),* **2013**, 49(32): 3294-3296.

239. Delaney, J.L., Hogan, C.F., Tian, J., and Shen, W., Electrogenerated chemiluminescence detection in paper-based microfluidic sensors. *Anal Chem,* **2011**, 83(4): 1300-1306.

240. Zang, D., Ge, L., Yan, M., Song, X., and Yu, J., Electrochemical immunoassay on a 3D microfluidic paper-based device. *Chem Commun (Camb),* **2012**, 48(39): 4683-4685.

241. Mazzeo, A.D., Kalb, W.B., Chan, L., Killian, M.G., Bloch, J.F., Mazzeo, B.A., and Whitesides, G.M., Paper-based, capacitive touch pads. *Adv Mater,* **2012**, 24(21): 2850-2856.